Molecular and Structural Aspects of Oocyte Maturation

Jurriaan J. Hölzenspies

Printed by F&N Boekservice, Eigen Beheer, Amsterdam
Printing of this thesis was financially supported by Bert and Trix Hölzenspies and the J.E. Jurriaanse Stichting

Cover design by Anette Versluis-Roozemond, Indielijn ontwerpbureau (http://www.indielijn.com)
Layout by Jurriaan J. Hölzenspies

Cover Illustrations:

Front – An immature porcine oocyte surrounded by several layers of cumulus cells during injection of GFP (green)

Back – Confocal images of maturing porcine oocytes labeled for DNA (blue) and the nuclear membrane (Lamin A; green) or microtubules (tubulin; red) showing progressively later stages from top to bottom as indicated.

ISBN: 978-90-393-5089-8

Molecular and Structural Aspects of Oocyte Maturation

Moleculaire en structurele aspecten van eicelmaturatie

(met een samenvatting in het Nederlands)

PROEFSCHRIFT

ter verkrijging van de graad van doctor aan de Universiteit Utrecht op gezag van de rector magnificus, prof.dr. J.C. Stoof, ingevolge het besluit van het college voor promoties in het openbaar te verdedigen op maandag 6 juli 2009 des middags te 12.45 uur

door

Jurriaan Jochem Hölzenspies
geboren op 25 november 1978, te Utrecht

Promotoren:	Prof.dr. W. Stoorvogel Prof.dr. B. Colenbrander
Co-promotoren:	Dr.ir. T. van Haeften Dr. B.A.J. Roelen

Voor mijn ouders,
Bert en Trix Hölzenspies

Table of Contents

Chapter 1

General introduction:

Development, growth, and maturation of mammalian oocytes

Development, growth, and maturation of mammalian oocytes

Folliculogenesis and early oocyte development

During early female mammalian embryogenesis, a small group of primordial germ cells that originate in the epiblast, migrate to the genital ridges via the hindgut. These cells undergo rapid mitotic divisions as they migrate and subsequently reach the developing gonads, at which point they are referred to as oogonia. These oogonia continue to multiply and remain attached to each other by cytoplasmic bridges until they undergo a final round of DNA synthesis. At this point multiplication ceases and oogonia enter prophase of the first meiotic division and become primary oocytes. Meiosis in primary oocytes progresses through several substages, defined by their chromatin configuration changes, known as leptotene, zygotene, and pachytene, before arresting at the diplotene stage of meiotic prophase I. Morphologically, this stage is identified by the presence of the oocyte nucleus, which is also known as germinal vesicle (GV). A single flattened layer of somatic cells, known as granulosa cells, surrounded by a basal lamina, is then formed around the primary oocyte, creating the primordial follicle. However, the majority of primary oocytes is not incorporated into primordial follicles and undergoes a series of degenerative processes known as atresia. In mammalian species, the primordial follicles are formed either before (human, cow, pig, sheep, guinea pig), or immediately after birth (mouse, rat, hamster). The primordial follicles can remain dormant for up to 50 years (in humans) until they are recruited into growth by paracrine signals in the ovary. The initial pool of primordial follicles is progressively depleted as follicles are recruited into further development [1-5].

A primordial follicle that is recruited into further follicular development first transforms into a primary follicle, in which the flattened cells in the granulosa layer become cuboidal and mitotic and in which the oocyte initiates transcription. When the granulosa cells grow beyond a single layer, the follicle is referred to as a secondary follicle, which is characterized by rapid multiplication of granulosa cells and the formation of a layer of theca cells around the basal lamina. The differentiation of the theca includes the formation of two distinct layers, a glandular theca interna surrounded by a fibrous layer that is highly vascularized, the theca externa. The granulosa cells increase production of FSH receptors at this stage, whereas cells of the theca interna start

expressing LH receptors, allowing blood-borne pituitary gonadotrophins to influence follicular development directly. This sensitivity to gonadotrophins is required for recruitment into gonadotrophin-dependent development. The oocytes within secondary follicles enter a growth phase, during which the cytoplasm is extensively reorganized: Various cell organelles, including mitochondria and ribosomes, accumulate and are redistributed, particularly towards cortical regions. Concurrently, large stores of protein, lipids, and mRNA are produced, cortical granule formation is initiated in the ooplasm, and a capsule of glycoproteins, the zona pellucida (ZP), starts to form between the oocyte and its surrounding granulosa cells. The granulosa cells become interconnected through formation of gap junctions. Granulosa cells within the corona radiata, which is the cell layer located immediately adjacent to the ZP, form transzonal projections, thin cytoplasmic extensions across the ZP that establish gap junctions with the oocyte. These follicular gap junctions allow exchange of small molecules (up to ~1 kDa), including metabolic precursors, nucleotides, and amino acids, between granulosa cells and between the granulosa cells and the oocyte [2;6].

As follicular development progresses into the tertiary (antral) stage, a fluid-filled cavity, the antrum, forms between the granulosa cell layers. Follicles at this stage of development rapidly increase their size as granulosa cells continue to proliferate and fluid is accumulated in the antrum. The transition

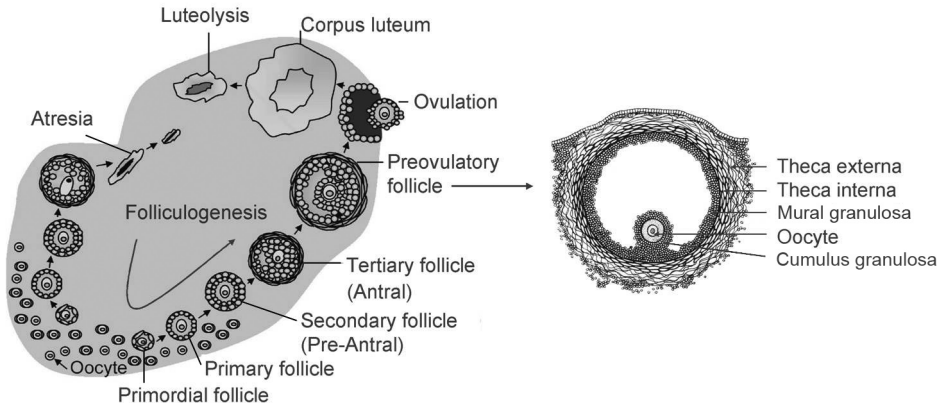

Figure 1: Schematic overview of folliculogenesis.
Recruitment and growth of follicles within the ovary ultimately culminates in either atresia or ovulation. The various stages leading up to these events are shown on the left, and a detailed depiction of the preovulatory follicle is shown on the right (adapted from Beker-van Woudenberg [10]).

from primordial to antral follicle takes several weeks (mouse, rat), up to several months (human, cow, pig). Upon reaching a certain size, depending on the species (a follicle diameter of 1, 2, and 4 mm in pigs, primates, and cows, respectively), follicles either become dependent on gonadotrophins for further growth, or go into atresia. Recruitment into gonadotrophin dependent development does not occur until puberty, when the levels of follicle stimulating hormone (FSH) and luteinizing hormone (LH) in the blood become sufficiently high to sustain further follicular development. Once recruited, follicles undergo a process known as selection, whereby one (human, cow) or several (pig, mouse) of these follicles obtain the ability to ovulate, i.e. become dominant (preovulatory). The remaining non-dominant follicles become atretic, presumably under the influence of signals from dominant follicles [7;8].

Upon formation of the antrum, the granulosa cells differentiate into two spatially and functionally distinct subtypes: Cumulus cells that constitute several cell layers tightly packed around the oocyte and mural granulosa cells that line the antrum. As the antral follicle continues to grow, the oocyte acquires the competence to resume and complete meiosis. Concurrently, the mural granulosa cells start to express LH receptors (LHRs), whereas expression of LHRs in cumulus cells is prevented by signals that emanate from the oocyte. As the expression of LHRs in the mural granulosa is established the follicle becomes capable of responding to the pre-ovulatory LH surge. The LH surge acts on the mural granulosa cells, thereby inducing changes in the antral follicle that ultimately lead to reinitiation of oocyte meiosis and expulsion of the oocyte from the follicle (ovulation). A marked change in follicular morphology is observed when the cumulus cells start to synthesize and secrete hyaluronic acid (HA) in response to the LH surge. Incorporation of HA into the extracellular matrix between the granulosa cells causes it to expand, as a result of which the follicular wall is weakened and the cumulus-oocyte complex (COC) is released into the fluid-filled antrum, and these HA-induced changes thus facilitate ovulation [2;6;9]. Figure 1 shows a schematic overview of the morphologically defined stages of folliculogenesis.

The ovarian cycle in the female is defined as the interval between successive ovulations and is subdivided into a follicular and a luteal phase. Prior to ovulation, a period when estrogen produced by the developing follicles is dominant constitutes the follicular phase. The follicular cells that remain in the ovary after ovulation form the corpus luteum, an ovarian structure that produces progesterone and heralds the aptly named luteal phase. The steroid hormones secreted by the corpus luteum are important for the development

and maintenance of a thickened endometrium. In most mammals, the corpus luteum is maintained until luteolytic factors, such as prostaglandin F2α, secreted by the endometrium induce its degeneration, a process known as luteolysis. Notably, maintenance of the corpus luteum in higher primates (including humans) is mediated by a relatively low level of LH that is sustained for the duration of the luteal phase and followed by spontaneous luteolysis. When pregnancy occurs, luteolysis is prevented by signals emanating from the trophoblast cells of the developing blastocyst(s). These signals inhibit the action of luteolytic factors in most mammals and provide endocrine support for the maintenance of the corpus luteum in higher primates. The external manifestation of the ovarian cycle is referred to as the estrous cycle in most mammals, and is characterized by a very limited period of receptivity to copulation around the time of ovulation ('heat'), the start of which marks the onset of the estrous cycle. In the absence of pregnancy, the endometrial tissues added during the luteal phase are reabsorbed in mammals with an estrous cycle. Higher primates on the other hand, have a menstrual cycle, the onset of which occurs between ovulations at the end of the luteal phase, and is marked by shedding of endometrial tissue via the vagina in a process known as menstruation [11].

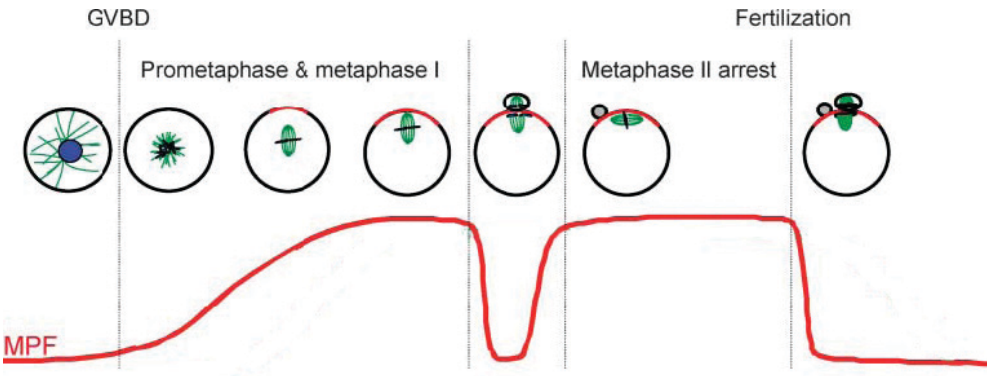

Figure 2: Schematic overview of meiotic maturation.
The various stages of oocyte maturation, starting at the germinal vesicle stage (top left), and ending at metaphase II arrest. Meiosis is not completed until fertilization occurs (top right). The activity of MPF during maturation is shown at the bottom. This figure is based on maturation in the mouse and was adapted from Brunet and Maro, 2005 [21].

Morphological aspects of oocyte maturation

During follicular development, prophase arrest in the oocyte is maintained by inhibitory signals that emanate from the surrounding follicular cells. The oocyte resumes meiosis when the inhibitory influence of the follicular cells is lifted in response to the pre-ovulatory LH surge, or upon removal of the oocyte from the follicle. The subsequent maturation process involves progression through the meiotic cell cycle (nuclear maturation), changes in the expression and localization of cytoplasmic proteins, and rearrangement of structural components (cytoplasmic maturation). Nuclear maturity is required for fertilization to occur and the completion of cytoplasmic maturation is required for several events that occur after fertilization and during subsequent embryonic development, including egg activation, formation of the pronuclei, and axis specification [12;13].

Nuclear maturation comprises a series of well-defined events, which allow identification of the maturation stage of an oocyte based on morphological identifiers (figure 2). Although chromatin configuration changes within the GV are known to occur after initiation of maturation, germinal vesicle breakdown (GVBD) is generally considered to mark the onset of nuclear maturation. Progression of nuclear maturation beyond GVBD is characterized by formation of the first metaphase spindle, extrusion of the polar body, and formation of the second metaphase spindle. In most mammals, nuclear maturation is completed when the second metaphase spindle has formed and the oocyte enters a second meiotic arrest, which is maintained until fertilization [14;15].

Progression through cytoplasmic maturation is much more difficult to discern. Although current knowledge of cytoplasmic maturation is incomplete, many cytoplasmic rearrangements are known to be important for the establishment of developmental competence, including changes in the distribution of endoplasmic reticulum (ER), Golgi, and cortical granules. The ER of immature oocytes consists of a network of small tubules that is more or less evenly distributed in the cytoplasm. During maturation, large (1-2 μm diameter) accumulations of ER are formed and exclusively observed in the cortex near the plasma membrane. Presently, ER (re-)distribution during mammalian oocyte maturation has only been investigated in detail in mouse and hamster oocytes [16;17], although images of ER in bovine oocytes suggest that other mammals may undergo a different redistribution of ER membranes [18]. In both mouse and bovine oocytes, Golgi membranes have been observed in large clusters

throughout the cytoplasm at the GV stage. These Golgi clusters are broken down into much smaller vesicle-like structures during maturation and this dispersed pattern is maintained in metaphase II (MII) oocytes [18;19]. Cortical granules (CGs) are small oocyte-specific organelles that redistribute from cytoplasmic clusters to a thin layer in the cortex, just underneath the plasma membrane. From this cortical position, the CGs can quickly be exocytosed in a massive event, known as the cortical reaction or polyspermy block, which is initiated when fertilization occurs. Once expelled into the perivitelline space, the proteins contained within the CGs mediate a hardening of the ZP that prevents spermatocytes from burrowing through [20].

Molecular aspects of oocyte maturation

Prophase arrest is maintained by the intra-oocyte activity of protein kinase A (PKA), which is activated by cyclic AMP (cAMP). The arrest is lifted when a drop in the concentration of cAMP in the oocyte occurs. A high concentration of cAMP in prophase-arrested oocytes can be maintained in several ways. Studies on mouse and Xenopus oocytes indicate that a G protein coupled receptor (GPCR) activates stimulatory G protein (Gs), which, in turn, stimulates conversion of ATP to cAMP by activating adenylate cyclase. Another possible mechanism of maintaining a high intra-oocyte level of cAMP is inhibition of phosphodiesterase activity, which converts cAMP to AMP. Moreover, cAMP produced in the granulosa cells could be transferred into the oocyte through the follicular gap junctions. Cumulus expansion coincides with a loss of gap junctions between the cumulus cells and the oocyte, and may thereby facilitate a reduction of cAMP in the oocyte that leads to meiosis resumption. The relative contributions of these mechanisms to the maintenance of prophase arrest in oocytes are species specific and still not completely understood [14;22].

The mechanism whereby the reception of the LH surge by the mural granulosa cells translates into a drop in intra-oocyte cAMP levels in mammals is unknown. It has become clear however, that inactivation of PKA in response to a reduction in cAMP concentration leads to changes in the activity of enzymes that regulate the phosphorylation state of M-phase promoting factor (MPF), which is switched from an inactive to an active state as a result. MPF is a central regulator of the cell cycle that comprises a catalytic subunit, cell division cycle 2 (CDC2; also known as cyclin dependent kinase 1), complexed with a regulatory subunit, cyclin B [15;22;23]. Interestingly, a recent study on por-

cine oocytes has indicated that a different regulator of CDC2 activity, Speedy (SPDY), a protein with no homology to cyclins, acts upstream of MPF. SPDY proteins are potent activators of CDC2 during early phases of oocyte maturation [24;25]. The activity of CDC2 is also controlled by phosphorylation of specific residues, although CDC2 is less sensitive to these regulatory phosphorylations when complexed with SPDY as compared to cyclin B [25]. Changes in the subcellular localization of CDC2 and its regulators may also contribute to regulation of CDC2 activity [26]. Sequestration of CDC2 to cytoplasmic domains may prevent CDC2 from phosphorylating specific substrates or limit access of regulatory proteins to phosphorylation sites on the CDC2 protein. Conversely, concentration of CDC2 at subcellular 'foci' of its target proteins could confer spatio-temporal specificity to CDC2 function. In both mitotic cells and oocytes, the activity of CDC2 regulates chromosome condensation, nuclear envelope breakdown, and formation of metaphase spindles, whereas transition from metaphase to anaphase requires inactivation of CDC2 [22;27]. The highly diverse regulatory mechanisms that control the activity of CDC2 are thus reflected in the diversity of cellular processes that are regulated by CDC2 during oocyte maturation. In somatic cells, controlled disassembly of the Golgi apparatus and ER exit sites at the G2/M transition is also regulated by CDC2 [28;29]. Although research on mouse and bovine oocytes suggests that similar processes may occur during oocyte maturation, a role of CDC2 in these processes has remained elusive in oocytes.

Spindle formation

Correct congression and segregation of chromosomes in mitotic and meiotic cells requires the formation of a bipolar spindle. The spindle is made up of spindle fibers, or microtubules, that consist of polymerized tubulin and form part of the cytoskeleton. Multiple microtubules can bind to a specialized protein complex, the kinetochore, which is formed at the centromere of each chromosome. Mitotic cells contain two specialized structures, the centrosomes, which migrate to opposite sides of the nucleus, during the G2/M transition. After nuclear envelope breakdown, microtubules emanate from the centrosomes in all directions, effectively probing the area around the centrosomes for available binding sites at the kinetochores of chromosomes, or specific sites in the cortex of the cell. Microtubules bound to cortical sites generate pushing and pulling forces that position the spindle to the center of the cell. These forces also occur in microtubules attached to kinetochores (kineto-

chore fibers), and thereby mediate alignment of chromosomes within a single plane at the center of the spindle, known as the metaphase plate [30].

Cells employ a series of checkpoints during the cell cycle to ensure that the processes required for cell division have been accurately completed and that both daughter cells receive one copy of each chromosome. Once the conditions of a checkpoint are met, transient signals mediate an irreversible transition to the next cell cycle stage [31]. One example is the spindle checkpoint, during which the separation of chromosomes is prevented until all chromosomes are aligned on the metaphase plate. The probing behaviour of microtubules, known as dynamic instability, is generated by alternate cycles of polymerization and depolymerization of tubulin [32]. Dynamic instability causes repeated capture and release of chromosomes, until the paired kinetochores within these chromosomes are captured by microtubules from opposite poles, causing tension to be generated within their centromeres. Tension

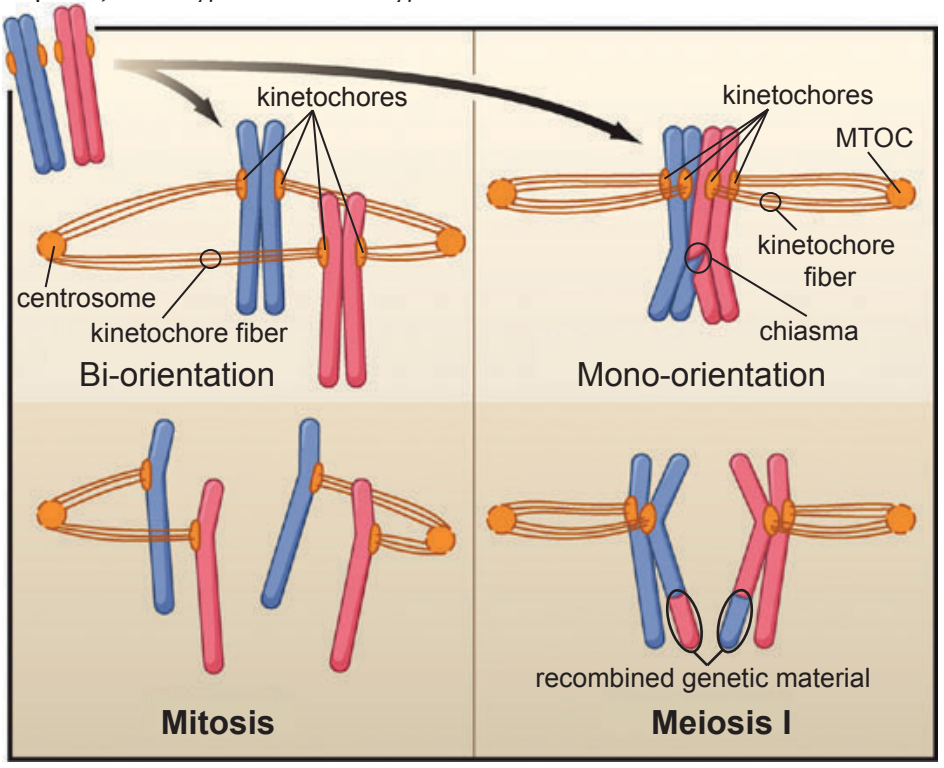

Figure 3: Kinetochore attachment in mitosis and meiosis.
Orientation of paternal (blue) and maternal (pink) chromosomes during metaphase (top) and anaphase (bottom) in mitosis and meiosis I (adapted from Watanabe et al. [33], with permission from Elsevier).

sensing mechanisms then cause stabilization of kinetochore-microtubule attachments, which leads to formation of kinetochore fibers that ensure proper alignment of chromosomes. Bipolar attachment of chromosomes at the metaphase plate is then maintained until all spindle checkpoint conditions have been satisfied [33]. Recent discoveries indicate that clathrin, a large molecule that is well known for its role in membrane trafficking, also causes stabilization of kinetochore fibers by crosslinking several microtubules attached to a single kinetochore. In support of these findings, it was demonstrated that clathrin-depleted somatic cells show an increased frequency of misalignment of chromosomes, which can lead to mis-segregation of chromosomes (aneuploidy) [34;35]. Many of these mitotic mechanisms also regulate the highly asymmetric divisions that occur during meiosis in oocytes. There are several marked differences however, and the currently known meiosis-specific mechanisms, relevant to this thesis, are presented in the following.

Oocytes do not contain centrosomes and studies in mouse oocytes showed that polymerization of microtubules occurs at multiple discrete sites within the cytoplasm, known as microtubule organizing centers (MTOCs). Formation of a bipolar spindle in these oocytes involves recruitment of MTOCs and microtubule stabilization near the condensed chromosomes, which are present in the cytoplasm after GVBD. Studies on several mammalian species, including mouse, cattle, pig, and human, have shown that the first meiotic spindle forms in a central position and subsequently migrates to the cortex. The oocyte spindle lacks astral microtubules and its asymmetric positioning involves a different cytoskeletal component, actin. Actin polymerizes into thin filaments that are abundantly present in the cortex, around the GV, and around the chromosomes just after GVBD, and these filaments are required for spindle migration towards and anchoring at the cortex. After extrusion of the first polar body, the second metaphase spindle forms in a cortical position [21;36].

Meiosis comprises an initial round of DNA replication followed by two consecutive divisions without an intermittent S-phase. The first meiotic division is ‘reductional’ in that instead of sister chromatids, homologous chromosomes are separated into daughter cells. During meiosis I, homologous chromosomes are attached to one another via chiasmata, specialized structures that facilitate recombination of genetic material. The chiasmata allow monopolar attachment of kinetochores within sister chromatids to generate tension and thus separation of homologous chromosomes to opposite poles, causing a reduction in chromosome number. Since orientation of chromosome pairs

on the first metaphase plate appears to be random, this leaves the oocyte with only one set of chromosomes, comprising a mixture of paternal and maternal chromosomes. The subsequent second meiotic division is very similar to mitosis, since kinetochore-attachment of sister chromatids is bipolar (figure 3) [33;37]. It is clear that meiosis resembles mitosis in many ways, although differential regulatory mechanisms are also abundant. However, the role of many important mitotic regulatory mechanisms, including the newly discovered role for clathrin in stabilizing the kinetochore fibers in mitotic spindles, is yet to be determined.

Manipulation of oocyte maturation

Chromosomal abnormalities in oocytes, resulting from errors during meiosis, occur with a remarkably high frequency in humans compared to other species and are a major cause of infertility and severe genetic disorders. Research on oocyte meiosis is therefore essential to gain a better understanding of the underlying causes of chromosomal aberrations, and may provide treatments for fertility problems, improvement of preimplantation genetic diagnosis, and improved in vitro fertilization [38]. However, the use of human oocytes in research is restrained by the limited availability of oocytes and ethical concerns [39]. Since the basic mechanisms of oocyte maturation are highly conserved between mammalian species, experimental evidence from a multitude of mammalian species may allow the development of a coherent model of the human female reproductive system. The use of several mammalian animal models in particular has become increasingly common in studies on oocyte development. An important example is the mouse, which has a short life cycle and can be relatively easily manipulated at the genetic level, thus providing a powerful means of interfering with fundamental processes in oocytes. The possibilities of genetic manipulation in the mouse range from conditional and/or tissue specific knockout of genes to introduction and expression of exogenous genes. Although these genetic tools can provide direct insight into gene function, several problems can occur, particularly when these tools are applied to genes involved in reproduction, due to complications such as differential effects between mouse strains, embryonic lethality, and transmission of epigenetic changes to offspring [40]. Pigs and cows have also taken a prominent position at the forefront of research on oocyte maturation and improved knowledge on the female reproductive system in these species provides additional potential benefits in veterinary medicine and food production. The

availability of techniques to manipulate oocytes from livestock is much more limited than in the mouse, however, and development of novel methods to apply these techniques to livestock animal models is necessary to confirm and expand on results obtained in the mouse.

In the last few decades, continued development of molecular tools has made manipulation of intracellular processes in somatic cells increasingly straightforward [41-44]. For several reasons, many of these tools are ineffective when applied to manipulation of oocyte maturation, since oocytes have to be competent to complete maturation and this competence is not reached until they are nearly fully grown. The transcriptional activity in these 'fully grown' oocytes is low and mostly limited to ribosomal genes that are transcribed in the nucleolus [45-50] and interference with transcription is therefore ineffective in manipulating oocyte maturation. Manipulation at the translational level is also challenging, because oocytes contain large stores of mRNA and protein [2;6]. Blocking translation often leads to a block of protein function in somatic cells due to high turnover rates of many proteins [51]. In oocytes however, even if translation of all mRNA encoding a specific protein is blocked, interference with the function of that protein is not guaranteed, as a large amount of protein may be available from intracellular stores.

The lack of functionality of different techniques in oocytes is exacerbated by practical problems, which occur at varying degrees in different species. Techniques that are commonly used to introduce substances that interfere with expression or function of proteins into somatic cells, such as transfection or incubation with membrane permeable inhibitors or activators of endogenous proteins, pose severe problems for use on oocytes. Aside from oocytes, these techniques would also affect the cumulus cells. Extensive interplay of signals from cumulus cells acting on the oocyte and vice versa, is known to be essential for oocyte development [6;7] and techniques that act only on cumulus cells or only on the oocyte are therefore important to elucidate the underlying mechanisms. Moreover, the zona pellucida, a thick protein matrix located between the oocyte and its cumulus cells that is involved in preventing polyspermy after fertilization [52;53], is prone to bind and/or cause aggregation of large molecules (personal observations).

To circumvent these practical difficulties, several different microinjection techniques have been developed to specifically interfere with the molecular mechanisms that govern oocyte maturation [54-59]. These techniques vary extensively in the amount of skill required, efficiency of injection, quantification of injected substance, and time required for initiation of interference. In

this thesis, microinjection was used to interfere with porcine oocyte maturation. Previously reported microinjection methods for porcine oocytes either have a very low efficiency [56], or lack a means of removing damaged and/or incorrectly injected oocytes [59]. Cumulus cells are required for in vitro porcine oocyte maturation [60] and damage to the these cells during injections causes clogging of injection needles with cell debris. The presence of cumulus cells also obscures a clear view of the oocyte and thereby hinders verification of injections. Thus, although microinjection has been proven a useful method to manipulate oocyte maturation, there is much room for improvement, particularly in its application to porcine oocytes.

Thesis overview

In this thesis, the molecular mechanisms that regulate structural events during oocyte maturation are investigated. The second chapter deals with the regulation of the activity and integrity of several cell organelles that mediate vesicular transport within the oocyte by the protein kinase CDC2. The data presented indicate a role for CDC2 in collapse of the Golgi apparatus into the ER and in regulating the activity of specialized subdomains of the ER, known as ER exit sites, where vesicle transport toward the Golgi originates. A novel and highly efficient method of microinjecting foreign substances that can be used to manipulate these intricate structural and molecular mechanisms, which are essential for competence acquisition in mammalian oocytes, is then introduced in the third chapter. Application of this microinjection technique to the manipulation of clathrin function during maturation is described in chapter four, demonstrating an essential role for clathrin in progression through meiosis. Finally, these findings are placed within the currently available framework of scientific knowledge that pertains to the mechanisms of cell division and their regulation during both mitosis and oocyte meiosis.

References

[1] Smitz JE, Cortvrindt RG. The earliest stages of folliculogenesis in vitro. Reproduction 2002; 123: 185-202.

[2] Fair T. Follicular oocyte growth and acquisition of developmental competence. Anim Reprod Sci 2003; 78: 203-216.

[3] Krysko DV, ez-Fraile A, Criel G, Svistunov AA, Vandenabeele P, D'Herde K. Life and death of female gametes during oogenesis and folliculogen-

esis. Apoptosis 2008; 13: 1065-1087.
[4] Guthrie HD, Garrett WM. Apoptosis during folliculogenesis in pigs. Reprod Suppl 2001; 58: 17-29.
[5] Telfer EE. In vitro development of pig preantral follicles. Reprod Suppl 2001; 58: 81-90.
[6] Eppig JJ. Oocyte control of ovarian follicular development and function in mammals. Reproduction 2001; 122: 829-838.
[7] van den Hurk R, Zhao J. Formation of mammalian oocytes and their growth, differentiation and maturation within ovarian follicles. Theriogenology 2005; 63: 1717-1751.
[8] Albertini DF, Combelles CM, Benecchi E, Carabatsos MJ. Cellular basis for paracrine regulation of ovarian follicle development. Reproduction 2001; 121: 647-653.
[9] Zhuo L, Kimata K. Cumulus oophorus extracellular matrix: its construction and regulation. Cell Struct Funct 2001; 26: 189-196.
[10] Beker-van Woudenberg ARCL. Fundamental aspects of bovine oocyte maturation. Utrecht University; 2004. Thesis.
[11] Johnson M.H., Everitt B.J. Essential Reproduction, 6 ed. Blackwell Science; 2007.
[12] Brevini TA, Cillo F, Antonini S, Gandolfi F. Cytoplasmic remodelling and the acquisition of developmental competence in pig oocytes. Anim Reprod Sci 2006; 98: 23-38.
[13] Combelles CM, Albertini DF. Microtubule patterning during meiotic maturation in mouse oocytes is determined by cell cycle-specific sorting and redistribution of gamma-tubulin. Dev Biol 2001; 239: 281-294.
[14] Mehlmann LM. Stops and starts in mammalian oocytes: recent advances in understanding the regulation of meiotic arrest and oocyte maturation. Reproduction 2005; 130: 791-799.
[15] Richard FJ. Regulation of meiotic maturation. J Anim Sci 2007; 85: E4-E6.
[16] Kline D. Attributes and dynamics of the endoplasmic reticulum in mammalian eggs. Curr Top Dev Biol 2000; 50: 125-154.
[17] Stricker SA. Structural reorganizations of the endoplasmic reticulum during egg maturation and fertilization. Semin Cell Dev Biol 2006; 17: 303-313.
[18] Payne C, Schatten G. Golgi dynamics during meiosis are distinct from mitosis and are coupled to endoplasmic reticulum dynamics until fertilization. Dev Biol 2003; 264: 50-63.

[19] Moreno RD, Schatten G, Ramalho-Santos J. Golgi apparatus dynamics during mouse oocyte in vitro maturation: effect of the membrane trafficking inhibitor brefeldin A. Biol Reprod 2002; 66: 1259-1266.
[20] Wessel GM, Brooks JM, Green E, Haley S, Voronina E, Wong J, Zaydfudim V, Conner S. The biology of cortical granules. Int Rev Cytol 2001; 209: 117-206.
[21] Brunet S, Maro B. Cytoskeleton and cell cycle control during meiotic maturation of the mouse oocyte: integrating time and space. Reproduction 2005; 130: 801-811.
[22] Dekel N. Cellular, biochemical and molecular mechanisms regulating oocyte maturation. Mol Cell Endocrinol 2005; 234: 19-25.
[23] Sun QY, Nagai T. Molecular mechanisms underlying pig oocyte maturation and fertilization. J Reprod Dev 2003; 49: 347-359.
[24] Kume S, Endo T, Nishimura Y, Kano K, Naito K. Porcine SPDYA2 (RINGO A2) stimulates CDC2 activity and accelerates meiotic maturation of porcine oocytes. Biol Reprod 2007; 76: 440-447.
[25] Karaiskou A, Perez LH, Ferby I, Ozon R, Jessus C, Nebreda AR. Differential regulation of Cdc2 and Cdk2 by RINGO and cyclins. J Biol Chem 2001; 276: 36028-36034.
[26] Beckhelling C, Perez-Mongiovi D, Houliston E. Localised MPF regulation in eggs. Biol Cell 2000; 92: 245-253.
[27] Liang CG, Su YQ, Fan HY, Schatten H, Sun QY. Mechanisms regulating oocyte meiotic resumption: roles of mitogen-activated protein kinase. Mol Endocrinol 2007; 21: 2037-2055.
[28] Kano F, Tanaka AR, Yamauchi S, Kondo H, Murata M. Cdc2 kinase-dependent disassembly of endoplasmic reticulum (ER) exit sites inhibits ER-to-Golgi vesicular transport during mitosis. Mol Biol Cell 2004; 15: 4289-4298.
[29] Lowe M, Gonatas NK, Warren G. The mitotic phosphorylation cycle of the cis-Golgi matrix protein GM130. J Cell Biol 2000; 149: 341-356.
[30] Grill SW, Hyman AA. Spindle positioning by cortical pulling forces. Dev Cell 2005; 8: 461-465.
[31] Tyson JJ, Novak B. Temporal organization of the cell cycle. Curr Biol 2008; 18: R759-R768.
[32] Pearson CG, Bloom K. Dynamic microtubules lead the way for spindle positioning. Nat Rev Mol Cell Biol 2004; 5: 481-492.
[33] Watanabe Y. A one-sided view of kinetochore attachment in meiosis. Cell 2006; 126: 1030-1032.

[34] Royle SJ, Lagnado L. Trimerisation is important for the function of clathrin at the mitotic spindle. J Cell Sci 2006; 119: 4071-4078.
[35] Royle SJ, Bright NA, Lagnado L. Clathrin is required for the function of the mitotic spindle. Nature 2005; 434: 1152-1157.
[36] Sun QY, Schatten H. Regulation of dynamic events by microfilaments during oocyte maturation and fertilization. Reproduction 2006; 131: 193-205.
[37] Yin S, Sun XF, Schatten H, Sun QY. Molecular insights into mechanisms regulating faithful chromosome separation in female meiosis. Cell Cycle 2008; 7: 2997-3005.
[38] Martin RH. Meiotic errors in human oogenesis and spermatogenesis. Reprod Biomed Online 2008; 16: 523-531.
[39] de Wert G, Mummery C. Human embryonic stem cells: research, ethics and policy. Hum Reprod 2003; 18: 672-682.
[40] Matthaei KI. Genetically manipulated mice: a powerful tool with unsuspected caveats. J Physiol 2007; 582: 481-488.
[41] Hendrie PC, Russell DW. Gene targeting with viral vectors. Mol Ther 2005; 12: 9-17.
[42] Colosimo A, Goncz KK, Holmes AR, Kunzelmann K, Novelli G, Malone RW, Bennett MJ, Gruenert DC. Transfer and expression of foreign genes in mammalian cells. Biotechniques 2000; 29: 314-2, 324.
[43] Potter H. Transfection by electroporation. Curr Protoc Immunol 2001; Chapter 10: Unit.
[44] Martin SE, Caplen NJ. Applications of RNA interference in mammalian systems. Annu Rev Genomics Hum Genet 2007; 8: 81-108.
[45] Fair T, Hyttel P, Greve T, Boland M. Nucleus structure and transcriptional activity in relation to oocyte diameter in cattle. Mol Reprod Dev 1996; 43: 503-512.
[46] Bouniol-Baly C, Hamraoui L, Guibert J, Beaujean N, Szollosi MS, Debey P. Differential transcriptional activity associated with chromatin configuration in fully grown mouse germinal vesicle oocytes. Biol Reprod 1999; 60: 580-587.
[47] Motlik J, Kopecny V, Travnik P, Pivko J. RNA synthesis in pig follicular oocytes. Autoradiographic and cytochemical study. Biol Cell 1984; 50: 229-235.
[48] Bjerregaard B, Maddox-Hyttel P. Regulation of ribosomal RNA gene expression in porcine oocytes. Anim Reprod Sci 2004; 82-83: 605-616.
[49] De La Fuente R, Eppig JJ. Transcriptional activity of the mouse oocyte

genome: companion granulosa cells modulate transcription and chromatin remodeling. Dev Biol 2001; 229: 224-236.
[50] Bevilacqua A, Kinnunen LH, Mangia F. Genetic manipulation of mammalian dictyate oocytes: factors affecting transient expression of microinjected DNA templates. Mol Reprod Dev 1992; 33: 124-130.
[51] Pan WH, Clawson GA. Antisense applications for biological control. J Cell Biochem 2006; 98: 14-35.
[52] Sun QY. Cellular and molecular mechanisms leading to cortical reaction and polyspermy block in mammalian eggs. Microsc Res Tech 2003; 61: 342-348.
[53] Wang WH, Day BN, Wu GM. How does polyspermy happen in mammalian oocytes? Microsc Res Tech 2003; 61: 335-341.
[54] Jaffe LA, Norris RP, Freudzon M, Ratzan WJ, Mehlmann LM. Microinjection of follicle-enclosed mouse oocytes. Methods Mol Biol 2009; 518: 157-173.
[55] Kline D. Quantitative microinjection of mouse oocytes and eggs. Methods Mol Biol 2009; 518: 135-156.
[56] Ohashi S, Naito K, Liu J, Sheng Y, Yamanouchi K, Tojo H. Expression of Exogenous Proteins in Porcine Maturing Oocytes after mRNA Injection: Kinetic Analysis and Oocyte Selection Using EGFP mRNA. The Journal of Reproduction and Development 2001; 47: 351-357.
[57] Chen J, Hudson E, Chi MM, Chang AS, Moley KH, Hardie DG, Downs SM. AMPK regulation of mouse oocyte meiotic resumption in vitro. Dev Biol 2006; 291: 227-238.
[58] Xiong B, Yu LZ, Wang Q, Ai JS, Yin S, Liu JH, OuYang YC, Hou Y, Chen DY, Zou H, Sun QY. Regulation of intracellular MEK1/2 translocation in mouse oocytes: cytoplasmic dynein/dynactin-mediated poleward transport and cyclin B degradation-dependent release from spindle poles. Cell Cycle 2007; 6: 1521-1527.
[59] Dai YF, Lee C, Hutchings A, Sun YM, Moor R. Selective requirement for Cdc25C protein synthesis during meiotic progression in porcine oocytes. Biology of Reproduction 2000; 62: 519-532.
[60] Schoevers EJ, Colenbrander B, Roelen BA. Developmental stage of the oocyte during antral follicle growth and cumulus investment determines in vitro embryo development of sow oocytes. Theriogenology 2007; 67: 1108-1122.

Chapter 2

CDC2/SPDY transiently associates with endoplasmic reticulum exit sites during oocyte maturation

Jurriaan J. Hölzenspies[1,2], Willem Stoorvogel[2], Ben Colenbrander[1], Bernard A. J. Roelen[1], Dagmar R. Gutknecht[3], Theo van Haeften[2]

[1]Department of Farm Animal Health, Faculty of Veterinary Medicine, Utrecht University, Utrecht, the Netherlands
[2]Department of Biochemistry & Cell Biology, Faculty of Veterinary Medicine, Utrecht University, Utrecht, the Netherlands
[3]Department of Reproductive Medicine, University Medical Centre, Utrecht, the Netherlands

Adapted from BMC Developmental Biology 2009, 9:8

CDC2/SPDY transiently associates with endoplasmic reticulum exit sites during oocyte maturation

Abstract

Mammalian oocytes acquire competence to be fertilized during meiotic maturation. The protein kinase CDC2 plays a pivotal role in several key maturation events, in part through controlled changes in CDC2 localization. Although CDC2 is involved in initiation of maturation, a detailed analysis of CDC2 localization at the onset of maturation is lacking. In this study, the subcellular distribution of CDC2 and its regulatory proteins cyclin B and SPDY in combination with several organelle markers at the onset of pig oocyte maturation has been investigated. Our results demonstrate that CDC2 transiently associates with a single domain, identified as a cluster of endoplasmic reticulum (ER) exit sites (ERES) by the presence of SEC23, in the cortex of maturing porcine oocytes prior to germinal vesicle break down. Inhibition of meiosis resumption by forskolin treatment prevented translocation of CDC2 to this ERES cluster. Phosphorylated GM130 (P-GM130), which is a marker for fragmented Golgi, localized to ERES in almost all immature oocytes and was not affected by forskolin treatment. After removal of forskolin from the culture media, the transient translocation of CDC2 to ERES was accompanied by a transient dispersion of P-GM130 into the ER suggesting a role for CDC2 in redistributing Golgi components that have collapsed into ERES further into the ER during meiosis. Finally, we show that SPDY, rather than cyclin B, colocalizes with CDC2 at ERES, suggesting a role for the CDC2/SPDY complex in regulating the secretory pathway during oocyte maturation. Our data demonstrate the presence of a novel structure in the cortex of porcine oocytes that comprises ERES and transiently accumulates CDC2 prior to germinal vesicle breakdown. In addition, we show that SPDY, but not cyclin B, localizes to this ERES cluster together with CDC2.

Introduction

Fully grown immature mammalian oocytes are arrested at the diplotene stage of meiotic prophase I. Oocyte maturation is initiated in vivo when the mural granulosa cells respond to the preovulatory luteinizing hormone

surge, or in vitro when oocytes are isolated from follicles [1]. Germinal vesicle breakdown (GVBD) marks the onset of nuclear maturation, which progresses into formation of the first metaphase spindle, followed by extrusion of the first polar body and formation of the second metaphase spindle. At metaphase II, oocytes enter a second period of meiotic arrest, which is maintained until fertilization. Meiosis resumption is often characterized by the occurrence of GVBD, since this is the first clear morphological event that takes place after release from meiotic inhibition. However, extensive rearrangements of components within the ooplasm, known as cytoplasmic maturation [2], already start to occur prior to GVBD [3].

Cytoplasmic maturation includes dynamic changes in the distribution and integrity of the Golgi apparatus and endoplasmic reticulum (ER) [4-6]. In somatic cells, the Golgi apparatus is fragmented at the onset of mitosis and starts to reform at telophase [7]. Two distinct views on the mechanism of Golgi partitioning during mitotis have been proposed [7;8]. One view holds that association of Golgi fragments with the metaphase spindle allows equal partitioning of Golgi components into the two daughter cells [9-11]. The second view is based on the idea of a dynamic Golgi apparatus, in which Golgi proteins continuously cycle through the ER. Coat protein II (COPII)-coated vesicles that traffic from ER to Golgi originate at subdomains of the ER, known as ER exit sites (ERES). Vesicle formation at ERES is inhibited during mitosis as a consequence of which cycling Golgi proteins become trapped in the ER [12]. Golgi components are then equally distributed into daughter cells together with the ER and the Golgi is reformed from vesicles that form at ERES when the ER export block is lifted at telophase [13;14]. Although the general distribution of ER during oocyte maturation has been studied extensively [15], a function for ERES during oocyte maturation remains to be elucidated. Evidence for a role of either of these two mechanisms in the control of Golgi dynamics during oocyte meiosis is lacking. It is clear that cytoplasmic processes constitute an integral part of both mitosis and meiosis, and we therefore use the term 'meiosis resumption' to indicate the moment when the first rearrangement of components occurs within the oocyte in response to release from the inhibitory influence of the follicular environment.

In most cells, cell division cycle 2 (CDC2, also referred to as cyclin-dependent kinase 1) complexes with cyclin B to form M-phase promoting factor (MPF), a well known central regulator of both mitotic and meiotic events. MPF regulates chromosome condensation, nuclear envelope breakdown, and formation of metaphase spindles in both somatic cells and oocytes, whereas

transition from metaphase to anaphase requires inactivation of MPF [16]. In mitotic cells, disassembly of Golgi and ERES are regulated by CDC2 through phosphorylation of GM130 and p47, respectively [17;18]. Despite the similarities in CDC2 functions during mitosis and meiosis, it is unclear whether the activity of CDC2 exerts a similarly stringent control over the integrity of the Golgi apparatus and ERES in oocytes as it does in mitotic cells.

The activity of CDC2 during the meiotic divisions of porcine oocytes is known to be controlled by at least two regulatory proteins, i.e. cyclin B and speedy (SPDY) [19;20]. SPDY proteins have no homology to cyclins, but are potent activators of CDC2 during early phases of oocyte maturation [21]. CDC2 activity can alternatively be controlled through phosphorylation of specific residues. Compared to the CDC2/cyclin B complex, the activity of CDC2 when complexed with SPDY is less sensitive to phosphorylation [19]. Finally, CDC2 activity may be regulated by changing the subcellular distribution of CDC2 and/or its regulators [22]: Sequestration of CDC2 to subcellular domains may prevent CDC2 from phosphorylating specific substrates or limit access of regulatory proteins to CDC2. Conversely, concentration of CDC2 at subcellular 'foci', such as the Golgi or ERES, could confer spatio-temporal specificity to CDC2 function.

To establish the role of the subcellular (re-)distribution of CDC2, and its regulatory proteins cyclin B and SPDY, in the regulation of early oocyte maturation, we examined their localization and the distribution of cell organelles containing potential CDC2 target proteins during pig oocyte maturation. The localization of these organelles was investigated using antibodies raised against the ERES marker SEC23, the Golgi marker GM130, and phosphorylated GM130 (P-GM130), a marker for fragmented Golgi. Our results demonstrate that CDC2 transiently associates with a P-GM130-labeled structure in the cortex of maturing porcine oocytes prior to GVBD. Using the ERES marker SEC23, we show that this structure consists of a cluster of ERES. Furthermore, our data on the distribution of CDC2 and its regulatory protein SPDY in oocytes suggest a role for the CDC2/SPDY complex in regulation of secretion during oocyte maturation.

Materials and Methods

Reagents and antibodies

All chemicals were purchased from Sigma Chemical Co. (St. Louis,

MO, USA), unless otherwise indicated. The following antibodies and reagents were used (concentration or dilution and catalog number in brackets): mouse monoclonal anti-CDC2 (1 μg/ml; sc-54) and goat polyclonal anti-SEC23 (2 μg/ml; sc-12107) from Santa Cruz Biotechnologies (Santa Cruz, CA, USA); rabbit polyclonal anti-Calnexin (1:250; SPA-860) from Stressgen Biotechnologies (San Diego, CA, USA); mouse monoclonal anti-PSTAIR (1 μg/ml; ab10345, which is directed against EGVPSTAIREISLLKE, a conserved region in cyclin-dependent kinases (CDKs) [23;24]) and rabbit polyclonal anti-gamma-tubulin (1:1000; ab11321) from Abcam (Cambridge, UK); mouse monoclonal anti-NUP153 (4 μg/ml; MMS-102P) from Covance (Berkeley, CA, USA); mouse monoclonal anti-GM130 (1 μg/ml; G65120) and mouse monoclonal anti-cyclin B1 (5 μg/ml; 554179) from BD Biosciences (San Jose, CA, USA); rabbit polyclonal anti-SPDY (2.2 μg/ml; NB100-2521, directed against a conserved region that is present in both isoforms) from Novus Biologicals (Littleton, CO, USA); Mitotracker Deep Red (200 nM; M22426), goat anti-mouse IgG alexa488, goat anti-rabbit IgG alexa568, and rabbit anti-goat IgG alexa488 (20 μg/ml; A11029, A11036, and A11078, respectively) from Molecular Probes (Eugene, OR, USA); donkey anti-mouse IgG Cy3 (6.25 μg/ml; 715-165-151) from Jackson ImmunoResearch Laboratories Inc. (West Grove, PA, USA); rabbit polyclonal anti-P-GM130 (1:100; detects GM130 phosphorylated on serine 25 [25]) was a generous gift from Dr. Martin Lowe (University of Manchester, UK).

Collection, culture, and assessment of porcine cumulus oocyte complexes

Cumulus-oocyte complexes (COCs) were collected from sow (Sus scrofa) ovaries, obtained from a slaughterhouse, by aspiration of 3-6 mm follicles [26] and subsequently selected using well established morphological criteria [27]. In vitro maturation (IVM) was performed as previously described [26], with the exception that media were not covered with oil. Briefly, COCs were collected in HEPES buffered M199 and washed in M199 (Gibco BRL) supplemented with 2.2 mg/ml $NaHCO_3$, 0.1% (w/v) polyvinylpyrrolidone (PVP), 100 μM cysteamine, 75 μg/ml potassium penicillin G and 50 μg/ml streptomycin sulphate (oocyte maturation medium; OMM) [27-29], and equilibrated in a CO_2 incubator (38.5°C; 5% CO_2) for at least 2 h before use. Selected COCs were cultured at 38.5°C under 5% CO_2 for 22 h in OMM supplemented with 0.05 IU/ml recombinant human FSH (rhFSH; a kind gift from Organon, Oss, the Netherlands). When COCs were cultured beyond 22 h, the medium was replaced with OMM without FSH (24 h and 44 h culture conditions). Based

on overall morphology and DNA staining pattern that was assessed by confocal laser scanning microscopy (see below), in vitro matured COCs were subdivided into three categories: germinal vesicle (GV), meiosis I (MI; indicated by the presence of a metaphase plate, anaphase I and telophase I stages were included in this group), and meiosis II (MII; as indicated by the presence of a metaphase plate and the first polar body). Oocytes that could not be scored or showed an aberrant morphology and did not fit any of the above criteria were excluded from statistical analyses.

Inhibition of meiosis resumption by forskolin treatment

COCs were kept in DMSO (control; 1:500) or 100 μM forskolin (50 mM forskolin in DMSO diluted 1:500) [30] during isolation and selection. Next, oocytes were denuded in DMSO or forskolin, fixed, and stained for CDC2 and DNA. In forskolin chase experiments, COCs treated with forskolin during isolation and selection were washed and cultured in OMM without forskolin for 0.5, 1, 2, or 18 h, and subsequently denuded and fixed. Finally, all groups were labeled for CDC2, P-GM130, and DNA, and the presence of structures was assessed using confocal laser scanning microscopy (as described below).

Immunofluorescence staining for confocal laser scanning microscopy

After culture, COCs were washed in 80 mM PIPES, 5 mM EGTA, 2 mM $MgCl_2$, pH 6.8, supplemented with 0.3% (w/v) PVP (PEM-PVP) at 37°C. To minimize mechanical stress that accompanies denudation procedures, but maintain sufficient antibody penetration after fixation, oocytes were partially denuded by gentle pipetting in PEM-PVP supplemented with either 0.01% (w/v) pronase (for < 22 h cultured oocytes), or 0.1% (w/v) hyaluronidase (for ≥ 22 h cultured oocytes). After washing in PEM-PVP at 37°C, oocytes were fixed in freshly prepared PEM-PVP containing 4% (v/v) paraformaldehyde (PF; Electron Microscopy Sciences, Hatfield, PA, USA) at room temperature (RT) for 1 h. Fixed oocytes were stored in PEM-PVP containing 1% (v/v) PF at 4°C for up to one week. For immunolabeling, oocytes were washed twice in PBS (0.1 M; pH 7.4) containing 0.3% (w/v) PVP (PBS-PVP) and once in PBS containing 0.1% (w/v) saponin (PBS-S) for 5 min. Aspecific binding sites were blocked using 1% (w/v) BSA and either 2% (v/v) normal goat serum, or 2% (v/v) normal horse serum (when goat polyclonal anti-SEC23 was used), both from Vector Lab (Burlingame, CA, USA), in PBS-S (blocking buffer) supplemented with 100 mM glycine for 2 h at RT or overnight at 4°C. Subsequent

immunolabeling steps were performed sequentially in blocking buffer for 1 h at RT and followed by three rinses in PBS-S for 10 min each. Primary and secondary antibody dilutions were centrifuged at 100,000 g for 1 h before use. As negative controls, all experiments included 5-10 oocytes that were incubated with purified mouse IgG combined with rabbit IgG or normal goat serum matching the host species of primary antibodies used as appropriate. Control IgG concentrations and serum dilutions were identical to primary antibodies in the same experiment. DNA was labeled with 10 μM TO-PRO-3 iodide (Molecular Probes) in PBS-S for 20 min. After a final three washes in PBS-S, oocytes were mounted in a 0.12 mm 8 well Secure-Seal Spacer (Molecular Probes) on a coverslip, covered in Vectashield (Vector Lab), and sealed with a microscope slide (Superfrost Plus; Menzel, Braunschweig, Germany).

Image acquisition and analysis

Images were obtained through a 40x oil immersion objective (N.A. 1.3) using a BioRad Radiance 2100MP confocal system (Zeiss/BioRad, Hertfordshire, UK), equipped with 488, 543, and 637 nm lasers, or a Leica TCS SP2 confocal system (Leica Microsystems GmbH, Wetzlar, Germany), equipped with 488, 568, and 633 nm lasers. Dual and triple channel images were obtained by sequential scanning. ImageJ (NIH; http://rsb.info.nih.gov/ij/) image analysis software was used for qualitative analysis of images. Laser power and acquisition settings were adjusted to produce submaximal pixel values in the oocyte and settings used to image control IgG stainings were matched to the highest settings used to image primary antibody staining in the same experiment. Consecutive confocal sections were taken at 4 μm intervals. Scoring of the structures described in this paper was performed by sequential scanning through oocytes from top to bottom in live view mode and noting the presence or absence of a structure. When a structure was present, sections through both structure and DNA were taken, whereas only DNA-containing sections were taken in oocytes that did not contain a structure. Images were selected based on the presence of DNA and a structure within 6 consecutive sections to clearly show both maturation stage and presence of a structure in a single image. Background subtraction and contrast/brightness enhancement (up to ~20% enhancement using the maximum slider in imageJ) were performed on stacks of images, followed by maximum intensity Z-projection of consecutive sections to include both the structure and the region of the oocyte that contained chromatin. Contrast/brightness enhancement of IgG controls was identical to images from the same experiment.

SDS-PAGE and Western blot

Oocytes were completely denuded by vortexing for 15 min in PBS-PVP containing protease inhibitor (Roche Molecular Biochemicals, Almere, the Netherlands). Denuded oocytes were separated from cumulus cells by two consecutive washes. Leftover cumulus cells were collected by centrifugation of the cumulus-containing suspension for 15 min at 16,000g, and oocytes were collected by centrifugation for 5 min at 16,000g. After removal of the supernatant, the cumulus cells and oocytes were snap-frozen in liquid nitrogen and stored at -20°C. Positive controls consisted of HeLa cells that were grown to near confluence and collected by centrifugation in PBS containing protease inhibitor (Roche). Cells were resuspended in 62.5 mM Tris-HCl, 2% SDS, and 10% glycerol (SDS sample buffer) to a concentration of $5x10^6$ cells/ml and snap-frozen in liquid nitrogen. After addition of SDS sample buffer to oocyte and granulosa cell samples, all samples were incubated at 100°C for 5 min. Proteins were separated on 10% polyacrylamide gels (30 µl/slot) by SDS-PAGE and transferred to Polyvinylidene Fluoride membranes (Hybond-P; GE Healthcare Amersham Biosciences Europe Gmbh, Freiburg, Germany), which were subsequently blocked in PBS containing 0.1% Tween-20 (PBST) supplemented with 5% (w/v) non-fat milk powder (Protifar; Nutricia, Zoetermeer, the Netherlands), and incubated in antibody dilutions in PBST containing 0.5% (w/v) Protifar. Primary antibodies were probed using horseradish peroxidase-conjugated goat anti-mouse antibodies (Jackson ImmunoResearch Laboratories Inc., Westgrove, PA, USA) and detected by Supersignal west pico chemiluminescent substrate (Pierce Biotechnology, Rockford, IL, USA).

Statistical analysis

Data are presented as weighted mean percentage ± weighted SEM of oocytes, unless otherwise indicated. Statistical analysis was performed on the original dichotomous data in SPSS 12.0 (SPSS Inc., Chicago, IL, USA) using chi-square tests unless otherwise indicated.

Results

CDC2 accumulates in a single cortical structure in GV stage oocytes

To determine the subcellular distribution of CDC2, oocytes were fixed after 0 or 24 h of in vitro maturation (IVM), immuno-labeled and analyzed by

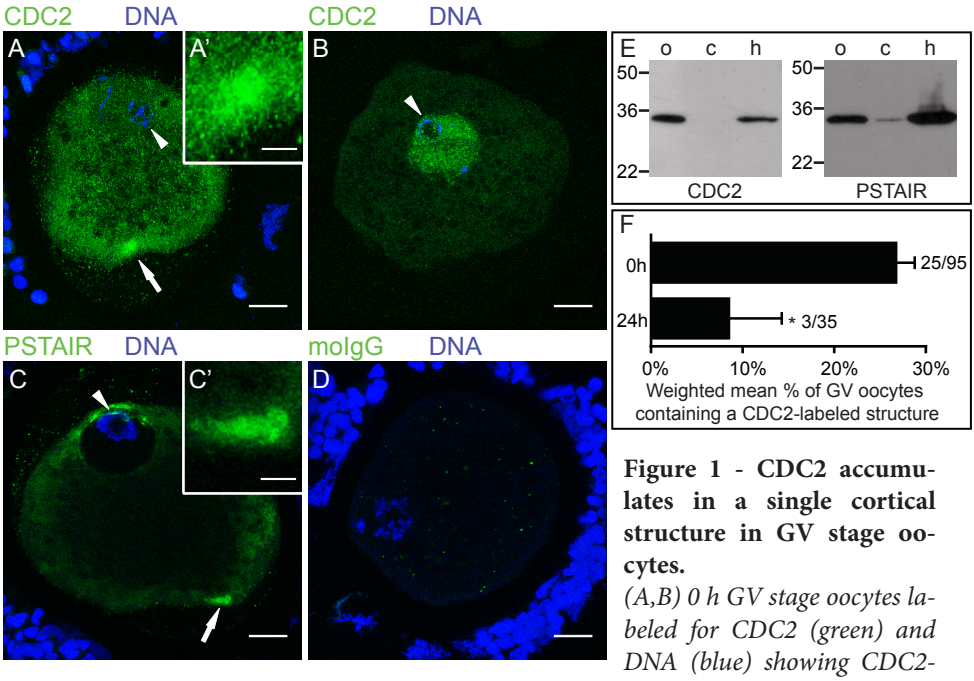

Figure 1 - CDC2 accumulates in a single cortical structure in GV stage oocytes.

*(A,B) 0 h GV stage oocytes labeled for CDC2 (green) and DNA (blue) showing CDC2-accumulation in the cortex of the oocyte (A) and in the GV (B). (C) 0 h GV stage oocyte showing PSTAIR labeling (green) and DNA (blue). PSTAIR also accumulates in a cortical domain. Arrows indicate the area that is shown enlarged in the insets (A',C'), and arrowheads denote the GV. (D) 0 h GV stage oocyte from the same experiment as the oocyte in A, labeled with mouse IgG (moIgG; green) and DNA marker (blue). The image was produced using the same confocal settings and enhancements as in A. All images are Z-projections of 3 consecutive confocal sections. Scale bars represent 20 µm in A-D, and 5 µm in A' and C'. (E) Western blot of CDC2 and PSTAIR on ~250 oocytes (o) and cumulus cells (c) collected during the denuding procedure of these oocytes showing a specific band at ~34 kDa. A HeLa cell lysate (h) was used as positive control. Molecular weight (kDa) is indicated on the left of each set of lanes. (F) Weighted mean percentage ± weighted SEM of GV stage oocytes that contained a CDC2-labeled cortical domain at 0 and 24 hours of maturation in 3 independent experiments. Absolute numbers are indicated to the right of the bars (number of positive oocytes/total number of oocytes) and * denotes significant difference ($P < 0.05$).*

confocal laser scanning microscopy. At 0 h, we observed a single large CDC2-containing cytoplasmic structure in the cortex of ~25% of GV oocytes (Fig. 1A). High magnification images showed that this CDC2-positive structure was composed of clustered smaller units (Fig. 1A'). Additionally, ~35% of oocytes displayed CDC2 staining in the GV (Fig. 1B), a pattern that rarely coincided with staining in a cortical structure. Staining with an anti-PSTAIR antibody

Table 1 - Listing of markers used to establish the identity of cortical structures in immature oocytes.

Name	Type	Target	Reference	Present in a cortical structure
CDC2	mouse monoclonal antibody	Cell division cycle 2, catalytic subunit of MPF	[22]	+
PSTAIR	mouse monoclonal antibody	Cyclin binding domain in all Cdks	[23]	+
SEC23	goat polyclonal antibody	SEC23, component of the coat protein II complex	[18]	+
P-GM130	rabbit polyclonal antibody	GM130 phosphorylated on serine 25	[25]	+
Calnexin	rabbit polyclonal antibody	Calnexin, transmembrane protein	[33]	-
Gamma-tubulin	rabbit polyclonal antibody	Gamma-tubulin, cytoskeletal component	[32]	-
Mitotracker*	Fixable live cell dye	Oxidation within mitochondria	[34]	-
NUP153	mouse monoclonal antibody	Nucleoporin 153 kDa	[35]	-
GM130	mouse monoclonal antibody	Structural Golgi protein	[25]	-
Cyclin B	mouse monoclonal antibody	Cyclin B, regulatory subunit of MPF	[22]	-
SPDY	rabbit polyclonal antibody	SPDY, regulatory protein of CDC2	[19]	+

* *Stained by 30 min incubation in maturation medium prior to fixation.*

(Fig. 1C,C'), which recognizes the cyclin-binding domain that is conserved in all CDKs, including CDC2 [23], showed a morphologically identical structure. As could be expected from a broader specificity, PSTAIR-reactive antibodies also labeled other intracellular areas, e.g. cytoplasmic areas near the GV at the plasma membrane of the oocyte (Fig. 1C). Labeling with control

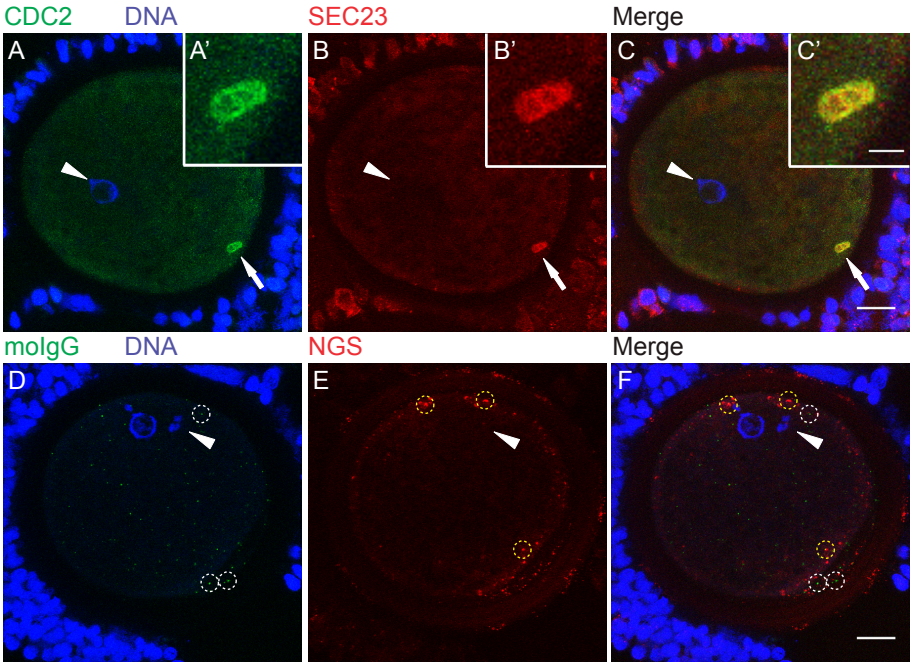

Figure 2 - CDC2 associates with ER exit sites.
(A-C) 0 h GV stage oocyte labeled for CDC2 (A, green), DNA (A, blue), and SEC23 (B, red). Colocalization (yellow) of CDC2 and SEC23 in a cortical domain in the ooplasm is evident in the merged image (C). (D-F) 0 h GV stage oocyte from the same experiment as A-C, labeled with mouse IgG (moIgG, D, green), DNA-marker (D, blue), and normal goat serum (NGS, E, red). Aspecific dots of moIgG staining (examples are marked with white circles in D,F) and NGS (examples are marked with yellow circles in E,F) do not colocalize in the merged image (F). Confocal sections from an acquisition depth equivalent to A-C are shown, and enhancements of D-F were identical to A-C. Images are Z-projections of 6 consecutive sections; scale bars represent 20 μm in C and F, and 5 μm in C'. Arrows indicate the region of the oocyte that is shown enlarged in the insets (A'-C'). Arrowheads denote the position of the GV.

IgG from pre-immune serum revealed sporadic non-specific small puncta (Fig. 1D). Specificity of the CDC2 and PSTAIR directed antibodies was further supported by immunoblotting, which revealed a single specific band at the expected 34 kDa molecular weight in oocyte and HeLa cell lysates. Little if any CDC2 and PSTAIR could be detected in the cumulus cells isolated from cumulus-oocyte complexes, which is probably due to low mitotic activity of these cells (Fig. 1E).

The rate of oocyte maturation in our experimental system was consistent with those previously reported in IVM studies using similar maturation

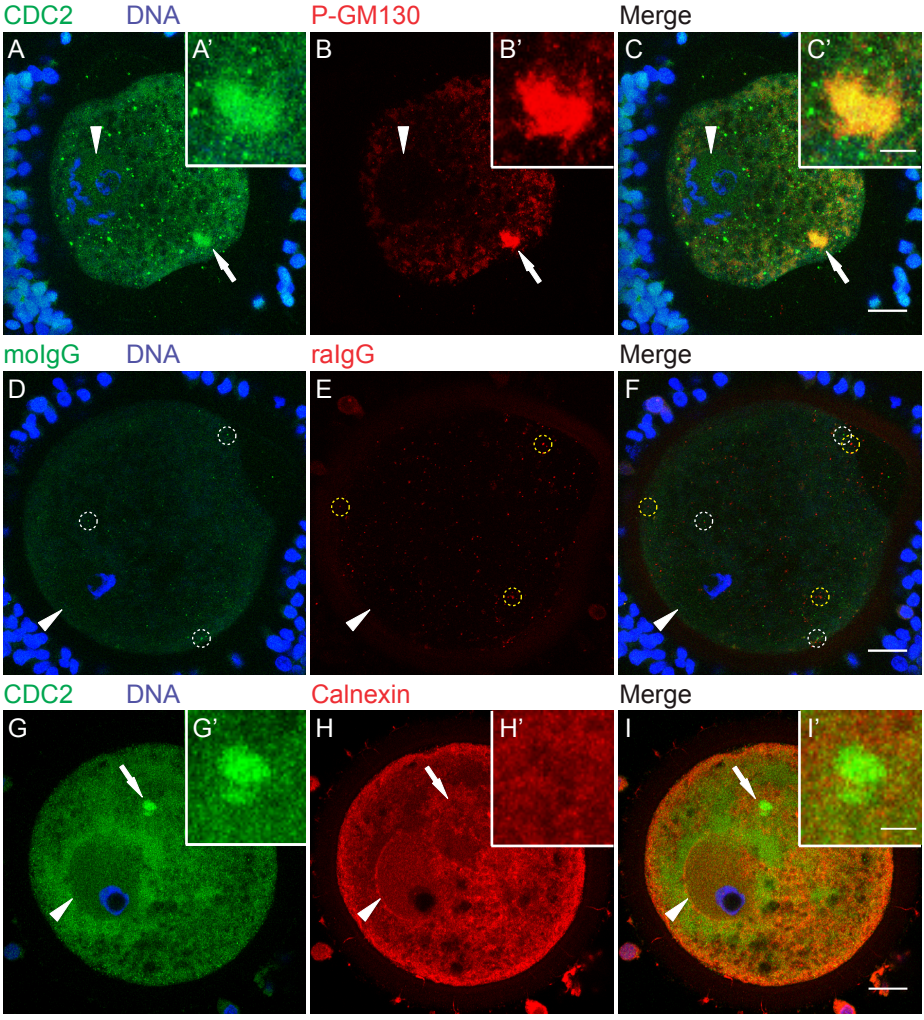

Figure 3 – The fragmented Golgi marker P-GM130 colocalizes with CDC2 at ERES in immature oocytes.

(A-C) 0 h GV stage oocyte labeled for CDC2 (A, green), DNA (A, blue), and phosphorylated GM130 (B, red). Colocalization (yellow) of CDC2 and phosphorylated GM130 in a cortical compartment in the ooplasm is evident in the merged image (C). (D-F) 0 h GV stage oocyte from the same experiment as A-C, labeled with moIgG (D, green), DNA-marker (D, blue), and rabbit IgG (raIgG, E, red). None of the aspecific dots (examples are marked with white circles in D,F and yellow circles in E,F) colocalize in the merged image (F). This control image was subjected to the same enhancements as A-C, and selected to show confocal sections from an equivalent acquisition depth. (G-I) 0 h GV stage oocyte labeled for CDC2 (G, green), DNA (G, blue), and the ER-marker calnexin (H, red). No colocalization (yellow) of CDC2 and calnexin was observed in the merged image (I).

Images are Z-projections of 6 consecutive sections (A-F), or 3 consecutive sections (G-I); scale bars represent 20 μm in C, F, and I, and 5 μm in C' and I'. Arrows indicate the region of the oocyte that is shown enlarged in the insets (A'-C' and G'-I'). Arrowheads denote the position of the GV.

conditions [31]: All oocytes were in GV stage directly after isolation (0 h; n = 103); after 24 h of culture (n = 67), 39 ± 5% of oocytes were still in GV, while 61 ± 5% had progressed to MI or MII; after 44 h of maturation (n = 56), 88 ± 4% of oocytes were in MII stage. The association of CDC2 with the cortical structure depended on the state of oocyte maturation, since the percentage of GV oocytes containing a CDC2-labeled structure was significantly reduced from 26 ± 2% at 0 h to 9 ± 6% at 24 h of IVM (Fig. 1F), while this CDC2-labeled structure was not observed in any oocytes that had progressed to MI or MII. Taken together, these data demonstrate that CDC2 associates with a single cortical structure prior to GVBD and suggest that this association is transient.

CDC2 associates with ER exit sites

To identify the nature of these CDC2-labeled structures, immature (0 h) oocytes were double-labeled for CDC2 and several other markers: SEC23, GM130, P-GM130, calnexin, gamma-tubulin, NUP153, and mitotracker (see Table 1). SEC23 is a component of the COPII complex, which is involved in the formation of transport vesicles at ERES. COPII-coated vesicles transfer cargo from ER to Golgi and dissociate their coat after fission from ERES. In 0 h GV oocytes, half of the CDC2-labeled structures were positive for SEC23 (Fig. 2A-C; IgG controls are shown in D-F), identifying them as ERES. GM130 is a Golgi matrix protein. At the onset of mitosis, GM130 is phosphorylated by CDC2 resulting in fragmentation of the Golgi apparatus and redistribution of the GM130 protein [25]. Almost all (95 ± 3%) CDC2-positive structures in 0 h GV oocytes also labeled for P-GM130 (Fig. 3A-C; IgG controls are shown in D-F). Calnexin is an ER-resident transmembrane protein, that localizes to the rough ER, but not to ERES [33;36]. Accordingly, we observed calnexin in a reticular pattern and at the nuclear envelope in 0 h GV oocytes (Fig. 3H,I). Consistent with its absence at ERES, calnexin was not found at CDC2-labeled cortical structures in any of the GV oocytes examined (Fig. 3G,I). Finally, gamma-tubulin (Fig. 4A-C), which localizes to microtubule organizing centers, mitotracker (Fig. 4D-I), a marker for mitochondria, and

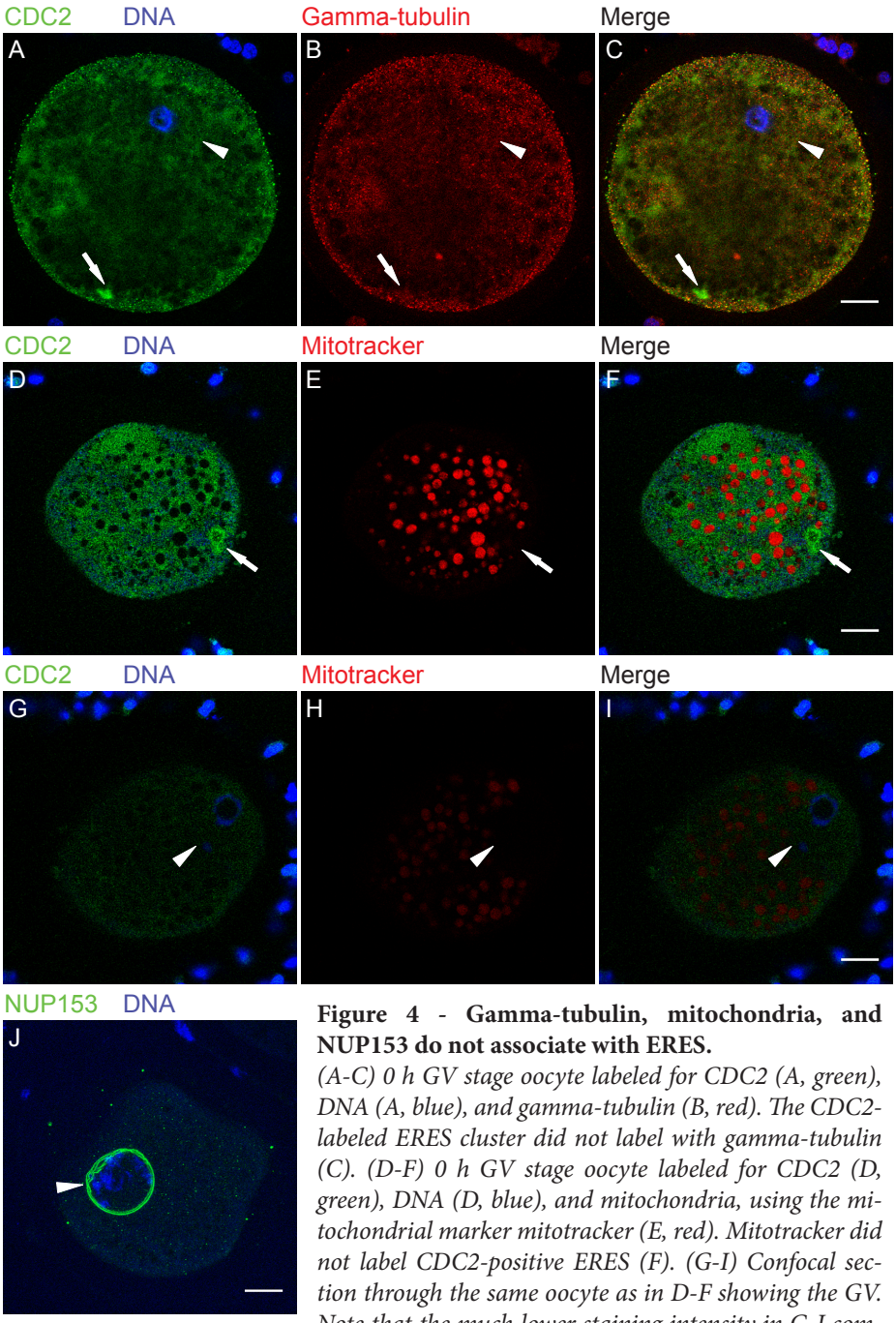

Figure 4 - Gamma-tubulin, mitochondria, and NUP153 do not associate with ERES.

(A-C) 0 h GV stage oocyte labeled for CDC2 (A, green), DNA (A, blue), and gamma-tubulin (B, red). The CDC2-labeled ERES cluster did not label with gamma-tubulin (C). (D-F) 0 h GV stage oocyte labeled for CDC2 (D, green), DNA (D, blue), and mitochondria, using the mitochondrial marker mitotracker (E, red). Mitotracker did not label CDC2-positive ERES (F). (G-I) Confocal section through the same oocyte as in D-F showing the GV. Note that the much lower staining intensity in G-I compared to D-F is solely the result of a ~65 µm change in depth of imaging, since acquisi-

tion settings and image enhancement were identical between these images. (J) 0 h GV stage oocyte labeled for NUP153 (green) and DNA (blue). None of the oocytes examined (0/15) showed a cortical domain. The 3 separate double lines around the GV are the result of small size and shape changes between the 3 consecutive sections used to produce the image. Images are either Z-projections of 3 consecutive sections (A-C,J), or single sections (D-I); scale bars represent 20 μm in C, F, I, and J. Arrows indicate CDC2-labeled ERES, and arrowheads denote the position of the GV.

NUP153 (Fig. 4J), one of the nuclear pore complex proteins that localizes to the nuclear membrane and to annulate lamellae, were not observed at CDC2-labeled structures. These results indicate that CDC2 accumulates in a specialized compartment in the smooth ER that comprises ERES.

Inhibition of meiosis resumption prevents association of CDC2 with P-GM130-labeled ERES

In our lab, collecting, selecting, and denuding oocytes requires approximately 2.5 h. Although oocytes in our experimental 0 h condition are still at the GV stage, they may already have resumed meiosis during this experimental interval. To prevent premature meiosis resumption during oocyte isolation, cumulus-oocyte complexes were collected in the presence of 100 μM forskolin [30]. Forskolin stimulates the activity of adenylate cyclase, thus raising the intracellular cAMP concentration. Under these conditions, oocytes are maintained in prophase I arrest [37]. The presence of forskolin during oocyte isolation and denuding significantly reduced the occurrence of CDC2-labeling at the ERES cluster in GV stage oocytes (Fig. 5A), supporting the idea that CDC2 is recruited to ERES early after meiosis resumption. Since maintenance of meiotic arrest by forskolin is reversible [38], oocytes were isolated in the presence of forskolin, and examined at several time points after removal of forskolin from the culture media (forskolin chase). The percentage of GV oocytes containing CDC2-labeled ERES increased within 2 h of chase (Fig. 5B,D), followed by a decline to ~10% after 18 h of chase. In 0 h forskolin treated oocytes, the occurrence of P-GM130-labeled ERES equaled that in 0 h controls. A gradual decline in the percentage of GV oocytes containing P-GM130-labeled ERES was observed after forskolin removal (Fig. 5C,E). Combined, these results indicate that P-GM130 accumulates at ERES prior to meiosis resumption, and that CDC2 transiently associates with ERES just after the oocyte is released from the inhibitory influence of the follicle.

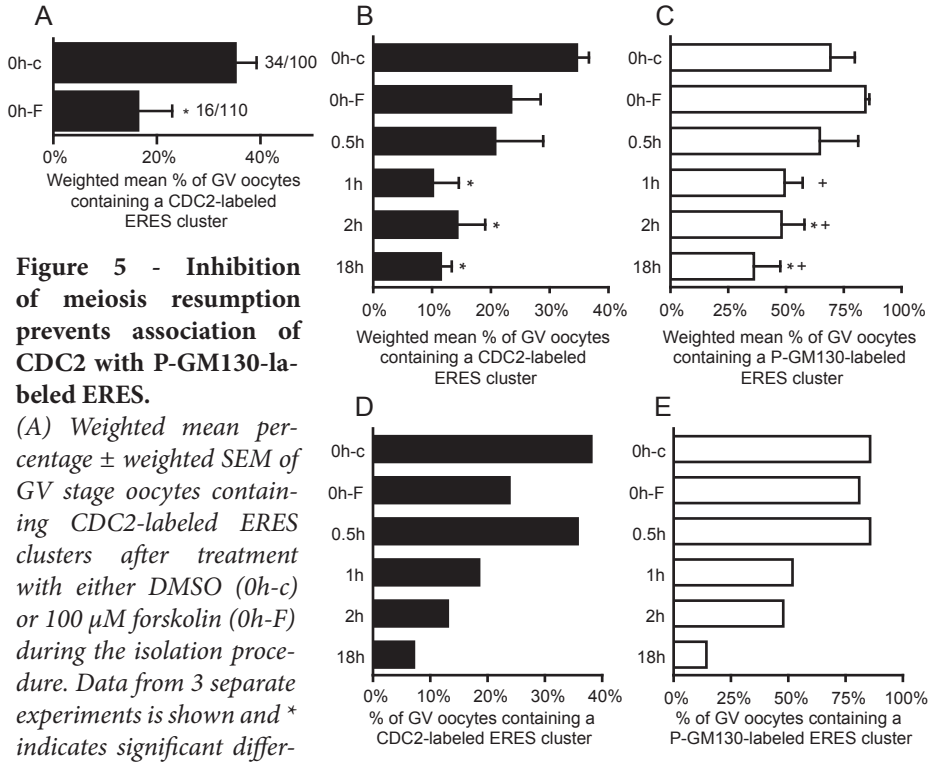

Figure 5 - Inhibition of meiosis resumption prevents association of CDC2 with P-GM130-labeled ERES.

*(A) Weighted mean percentage ± weighted SEM of GV stage oocytes containing CDC2-labeled ERES clusters after treatment with either DMSO (0h-c) or 100 μM forskolin (0h-F) during the isolation procedure. Data from 3 separate experiments is shown and * indicates significant difference (P<0.05). Absolute numbers are shown next to the bars (number of positive oocytes/total number of oocytes). (B,C) Forskolin chase bar graphs (n = 3; 20-30 oocytes per group), showing the weighted mean percentage ± weighted SEM of GV stage oocytes containing a cluster of ERES, labeled for CDC2 (B) and/or P-GM130 (C). In one of the experiments shown, an equal percentage of CDC2-labeled ERES was observed in 0h-F and 0h-c groups. As a result, the difference between 0h-c and 0h-F is significant in A, but not in B. The original dichotomous data (presence/absence of an ERES cluster) was analyzed in SPSS using binary logistic regression. All groups were compared to 0h-c and 0h-F conditions for a total of 10 comparisons per label. The familywise significance level was set to 0.05, and was adjusted for pairwise comparisons using the Holm-Bonferroni procedure. Significant differences compared to 0h-c or 0h-F are indicated by * or +, respectively. (D,E) Representative example of a forskolin chase experiment from the series of experiments shown in B,C, showing the percentage of GV stage oocytes containing a cluster of ERES, labeled for CDC2 (D) and/or P-GM130 (E). Note that the increase in the occurrence of CDC2-labeled ERES at 0.5h after release from forskolin-maintained inhibition of maturation (D) is obscured in the chart showing combined data from three experiments (B), because it occurred at varying time points. Conditions on the y-axis are: 0 h DMSO control (0h-c), 0 h forskolin (0h-F), and 0.5, 1, 2, and 18 h of maturation after forskolin removal (0.5h/1h/2h/18h).*

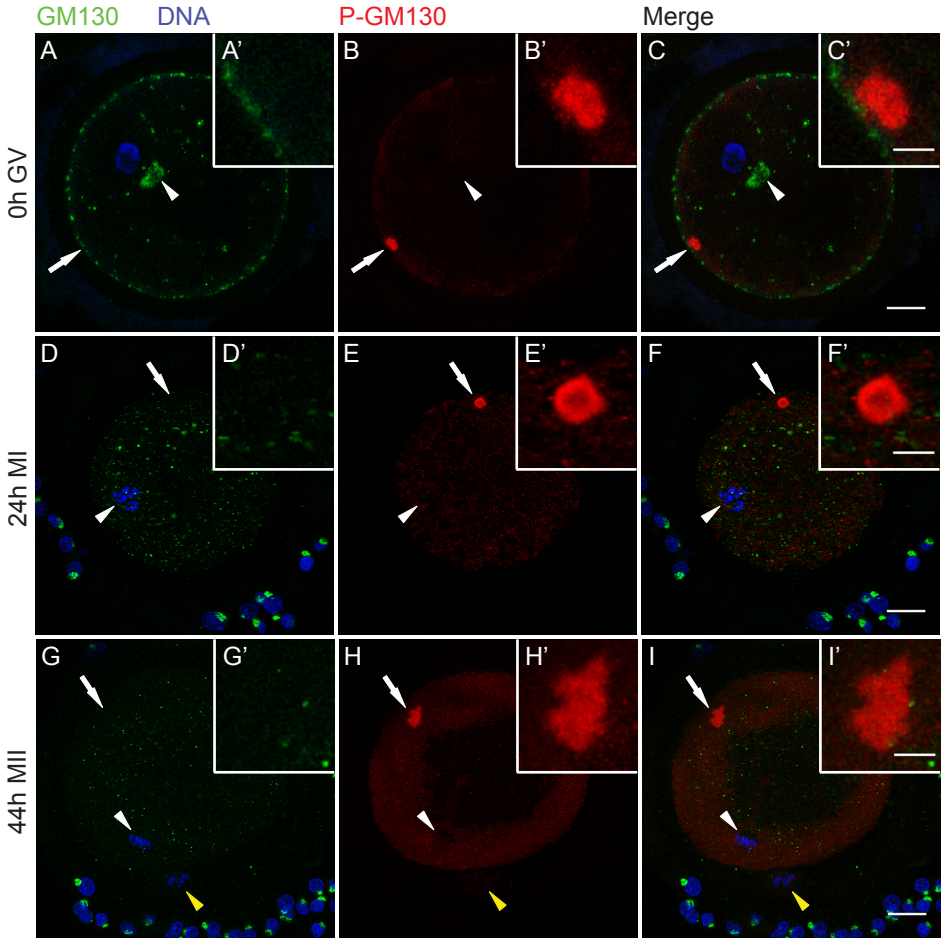

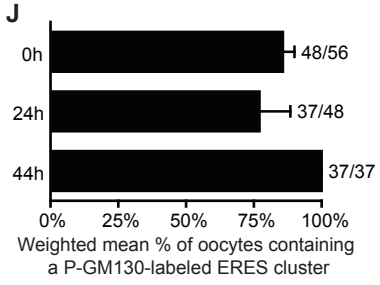

Figure 6 - Phosphorylated GM130 is stored at ERES during maturation.

Oocytes were stained for GM130 (green), P-GM130 (red), and DNA (blue) at different maturation stages. (A-C) 0 h GV stage oocyte containing a perinuclear Golgi apparatus (arrowhead). (D-F) 24 h matured MI oocyte containing a metaphase plate (arrowhead). (G-I) 44 h matured MII oocyte showing the second metaphase plate (arrowhead) and a polar body (yellow arrowhead). Arrows indicate the area that is shown enlarged in the insets. Z-projections of 3 (A-F) or 6 (G-I) consecutive sections are shown; scale bars represent 20 μm in C, F and I, and 5 μm in C' F' and I'. Arrows indicate the region of the oocyte that is shown enlarged in the insets (A'-I'). (J) Weighted mean percentage ± weighted SEM of oocytes that contain a P-GM130-labeled cortical domain at the indicated maturation times. Results from 2 independent experiments are shown.

Phosphorylated GM130 is stored at ERES during maturation

Given the role of CDC2 in phosphorylating the Golgi protein GM130, labeling for both GM130 and P-GM130 should provide information on the role of CDC2-labeled cortical domains in Golgi-protein redistribution during meiosis. To establish the distribution of GM130 and its phosphorylated form P-GM130 during oocyte maturation, oocytes were double-labeled for GM130 and P-GM130 after 0, 24, and 44 h of IVM. GM130 staining revealed an intact Golgi apparatus and several GM130-labeled areas in the periphery of 0 h GV oocytes, whereas GM130 was not detected in CDC2-labeled ERES (Fig. 6A). As maturation progressed, GM130 staining in the oocyte was observed in progressively smaller and more dispersed fragments, whereas intact GM130-labeled Golgi complexes were observed in the cumulus cells (Fig. 6A,D,G). Staining for GM130 and P-GM130 did not overlap (Fig. 6C,F,I). At the GV stage, P-GM130 localized to a cortical domain (Fig. 6B,C). P-GM130 labeling persisted in the cortical domain in MI and MII stage oocytes, and increased in the ER as maturation progressed (Fig. 6E,H,J). No P-GM130 staining was detected in the polar body (Fig. 6H,I). These data indicate that during oocyte maturation, GM130 is stored in the ER in its phosphorylated form.

CDC2 associates with SPDY at ERES

The activity of CDC2 during cell division has been studied most extensively as MPF, a complex of CDC2 and cyclin B. Recently, evidence has been obtained that CDC2 activity in porcine oocytes can alternatively be controlled by SPDY, a protein with no homology to cyclin B [19]. Here, we used a combination of staining approaches to identify the regulatory component of CDC2 during early phases of maturation. Interestingly, we found that SPDY was present in CDC2-positive ERES in 0 h GV oocytes (Fig. 7A-C). Since simultaneous labeling of oocytes for cyclin B and CDC2 was not possible due to the same host species of cyclin B and CDC2 antibodies, we used an alternative approach in which we identified ERES by the presence of P-GM130. Oocytes (0 h, GV) double-labeled for P-GM130 and cyclin B showed no cyclin B in P-GM130-labeled ERES (0/21). Instead, about half of the oocytes (10/21) showed clear cyclin B labeling in the GV (Fig. 7D-F). Consistent with these observations, anti-PSTAIR antibodies, which do not detect CDC2 when bound to cyclin B [23], labeled P-GM130-containing ERES (11/18), whereas PSTAIR was not observed in the GV of any of the oocytes examined (0/18; Fig. 7G-I). These results indicate that CDC2 at ERES associates with SPDY,

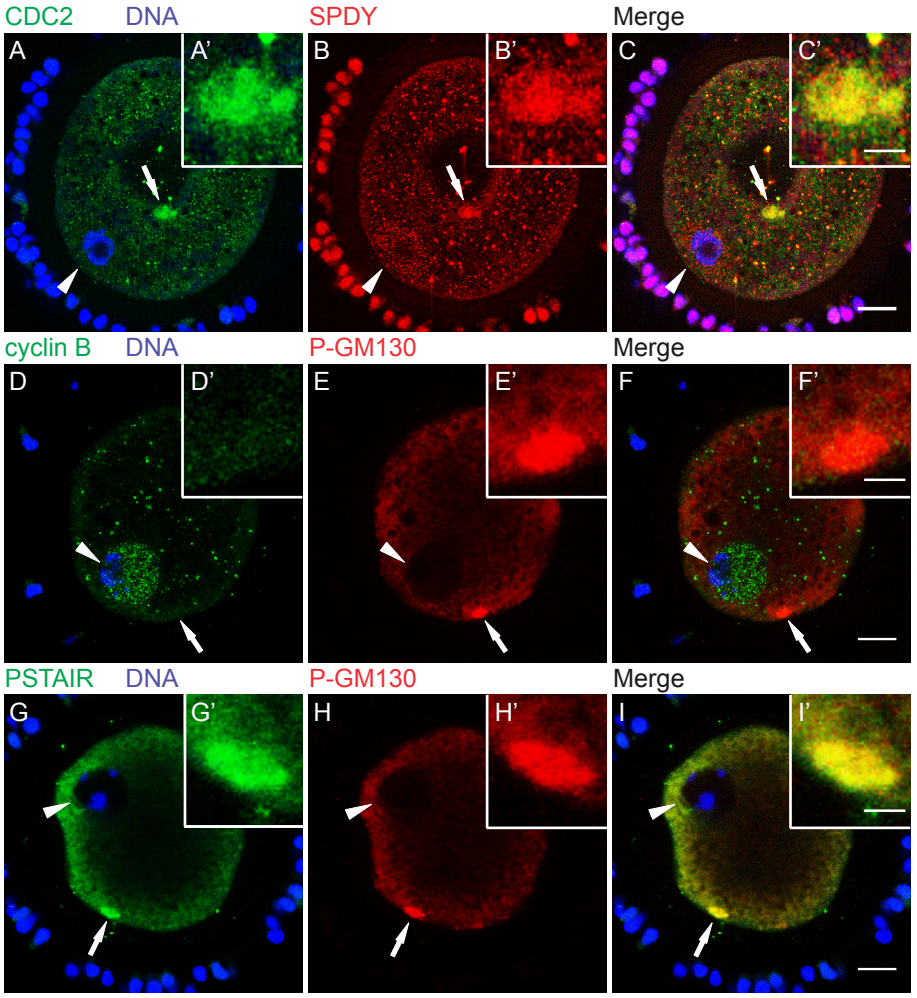

Figure 7 - CDC2 associates with SPDY at ERES.
(A-C) 0 h GV stage oocyte labeled for CDC2 (A, green), DNA (A, blue), and SPDY (B, red). Both CDC2 and SPDY localize to the same cortical domain (C). Note that the center of this oocyte is dented (the area that contains the arrow) causing the structure to appear in the middle of the oocyte, whereas it is located in the cortex. (D-F) 0 h GV stage oocyte stained for Cyclin B (D, green), DNA (D, blue), and P-GM130 (E, red). Cyclin B did not localize to the P-GM130-labeled cortical domain (F). (G-I) 0 h GV stage oocyte labeled for PSTAIR (G, green), DNA (G, blue), and P-GM130 (H, red). Spatial overlap of PSTAIR and phosphorylated GM130 staining (yellow) in a cortical domain is evident in the merged image (I). Images are Z-projections of 2 (A-C) or 3 (D-I) consecutive sections; scale bars represent 20 μm in C, F, and I, and 5 μm in C', F', and I'. Arrows indicate the region of the oocyte that is shown enlarged in the insets (A'-I'). Arrowheads denote the position of the GV.

but not cyclin B, at the onset of oocyte maturation.

Discussion

Here, we show that the cell-cycle regulating protein CDC2 transiently associates with a cluster of ERES at the onset of oocyte maturation, and propose that this association is involved in Golgi retention. Detailed microscopical analysis of large numbers of oocytes showed that during the initial phases of in vitro maturation, CDC2 localized to a large (~7 μm diameter) structure, that was exclusively observed in the cortex, in about a quarter of GV oocytes (Fig. 1A,F). The ERES marker SEC23 colocalized with CDC2 in about half of these cortical domains (Fig 2A-C), demonstrating that at least some of these CDC2-positive compartments consist of active ERES. A morphologically identical domain labeled for the CDC2 target protein P-GM130 was observed in ~80% of 0 h GV stage oocytes (Fig. 6J), and almost all CDC2-labeled cortical domains also labeled for P-GM130. In addition to this morphological likeness, only one P-GM130-labeled domain was observed per oocyte and this domain was always found in a cortical position. These identical features of SEC23, CDC2, and/or P-GM130-labeled domains indicate that all of these domains were composed of ERES, albeit mostly inactive ERES, since the majority was devoid of SEC23 labeling.

Membrane trafficking, and thus association of SEC23 with ERES, is inhibited during mitosis in somatic cells [12-14], which may in part be due to disassembly of ERES [18]. Upon disassembly, ERES-resident proteins disperse into the ER where they remain until the ERES are reformed at the start of interphase [18]. Our results support this view, since P-GM130 disperses from the ERES-containing domain into the ER prior to GVBD (Fig. 5C,E and fig. 6B,E,H). However, P-GM130 localization at the cortical domain was observed in >80% of oocytes at MI and MII (Fig. 6J). No difference in either morphology or position within the oocyte could be observed throughout maturation using P-GM130 as a marker for this domain (Fig. 6). Therefore, it can be inferred that the P-GM130-labeled domain is composed of ERES throughout maturation. When compared to ERES described in most somatic cells and bovine oocytes [6;18], the cortical domain in porcine oocytes is exceptionally large. Since SEC23 was not found outside the cortical domain (Fig. 2B), we conclude that most if not all ERES are clustered together in the cortex at this stage. The presence of this single cluster of ERES has not been reported before and appears to be a unique feature of oocytes.

During pre-GVBD IVM, the percentage of GV oocytes containing CDC2-labeled ERES decreased significantly (Fig. 1D). When the onset of maturation was prevented by isolating COCs in the presence of the adenylate cyclase-stimulating drug forskolin, the occurrence of CDC2-labeled ERES was significantly decreased (Fig. 5A), demonstrating that CDC2 translocation to and accumulation at ERES is initiated upon release from meiotic inhibition. This CDC2 translocation may therefore constitute the first sign of meiosis resumption. CDC2 accumulation at ERES was transient since the occurrence of CDC2-labeled ERES increased within 2 h after release from forskolin-maintained meiotic arrest, and subsequently declined to a much lower level after 18 h of maturation (Fig. 5B,D). CDC2-labeled ERES could not be detected in oocytes that had undergone GVBD, indicating that CDC2 accumulation, and hence CDC2 activity, at ERES is specific for pre-GVBD stages. Transient localization of CDC2 at ERES would also explain the discrepancy between the occurrence of the CDC2- (~25 %; Fig. 1F) and the P-GM130-labeled (~80 %; Fig. 5C and 6J) ERES cluster in immature oocytes. These results corroborate the proposition that stage dependent translocation of CDC2 underlies specific spatial and temporal control of CDC2 activity within oocytes [39-41].

It is evident from studies on somatic cells that CDC2 is involved in fragmentation and partitioning of the Golgi during early phases of mitosis [25]. Golgi fragmentation is initiated by CDC2-dependent phosphorylation of the membrane-resident Golgi protein GM130 [17], followed by vesiculation of the collapsing cisternae [42]. In our experiments, the presence of forskolin during oocyte isolation did not change the occurrence of P-GM130-labeled ERES at 0 h (Fig. 5C,E), indicating that P-GM130 accumulation at ERES precedes meiosis resumption. The percentage of GV oocytes with a P-GM130-containing ERES cluster declined from 80% in forskolin-inhibited 0 h matured oocytes to 35% at 18 h of maturation after forskolin removal (Fig. 5C). When oocytes were matured for longer intervals, i.e. 24 or 44 h, the percentage of oocytes showing a P-GM130-containing ERES cluster equaled that of the 0 h controls (Fig. 6J), whereas CDC2 did not localize at ERES clusters in MI (24 h) and MII (44 h) oocytes. These data indicate that the transient presence of CDC2 is closely followed by a transient absence of P-GM130 at ERES, prior to GVBD. Given the role of CDC2 in controlling ERES disassembly at the onset of mitosis [18], we propose that CDC2 controls dispersion of P-GM130 from ERES into the reticular ER.

Two models on Golgi partitioning during cell division are currently prevalent in literature. One model claims that Golgi inheritance occurs in-

dependently from the ER by association of Golgi-derived vesicles with the developing spindle, which facilitates subsequent equal partitioning of these Golgi fragments during telophase [7]. In the other model, known as the ER-dependent model, Golgi proteins redistribute into the ER during metaphase and Golgi stacks are reformed in daughter cells upon reinitiation of ER export [8]. In our experimental model, most oocytes contained a P-GM130-labeled ERES cluster immediately after isolation and at MI and MII (Fig. 6J), whereas P-GM130 was completely absent in the region surrounding the metaphase plates at both MI and MII (Fig. 6E,H). Staining of the non-phosphorylated form of GM130 in the oocyte showed an increasingly dispersed pattern as maturation progressed (Fig. 6A,D,G), and P-GM130 staining in the ER increased relative to staining in ERES (Fig. 6B,E,H), suggesting that phosphorylation of GM130 and redistribution of P-GM130 into the ER continues after meiosis resumption. Phosphorylation of Golgi-resident GM130 presumably triggers efficient translocation of this protein into the ER, because the distributions of GM130 and P-GM130 were mutually exclusive in porcine oocytes (Fig. 6C,F,I). Taken together, these results indicate that Golgi inheritance in oocytes occurs through redistribution of Golgi components into the ER, and thus support an ER-dependent model in oocytes.

Our data indicate that CDC2 at ERES was not complexed with cyclin B (Fig. 7D-I). Instead, we observed SPDY at CDC2-labeled ERES (Fig. 7A-C), suggesting that SPDY regulates CDC2 activity at ERES. Although we cannot conclude directly from our data that SPDY associates with CDC2 at ERES, additional evidence that SPDY may be a key regulatory protein of CDC2 upstream of MPF in porcine oocytes is provided by the observation that (1) CDC2/cyclin B activity can only be detected in a histone H1 kinase assay after 18-24 h of maturation [43-46] and that (2) injection of SPDY mRNA into oocytes accelerates oocyte maturation by stimulating MPF [21].

Our identification of a specialized cortical ERES-containing domain prompted us to compare it to similar structures described for other species. Morphologically, this cortical domain resembles Organized Smooth ER (OSER), which consists of stacked membrane arrays [47]. In our study, the ER-resident protein calnexin could not be detected in the CDC2-containing domain (Fig. 3G-I), indicating that this domain does not consist of reticular ER. In Xenopus laevis oocytes, cyclin B was found to localize to annulate lamellae, which may constitute one of the forms of OSER in immature oocytes [35]. Our studies show that neither the annulate lamellae marker NUP153 (Table 1, fig. 4J), nor cyclin B (Fig. 7A-C), localize to the cortical domain in immature

porcine oocytes, suggesting that this domain does not consist of OSER or annulate lamellae. Primordial oocytes of several species contain an aggregate of organelles, the Balbiani body, which resembles the CDC2-labeled domain in size and in that there is only one of these bodies per oocyte. The Balbiani body contains components of several organelles including mitochondria, Golgi, and ER, and dissipates after the primordial stage [48]. P-GM130-labeled cortical domains were devoid of markers for intact Golgi (Fig. 6 A,D,G) and mitochondrial markers (Table 1, fig. 4D-I), showing that the cortical domain and the Balbiani body are unrelated structures.

Based on observations in mitotic cells and our data from porcine oocytes, we hypothesize that prior to meiosis resumption, GM130 at the Golgi is phosphorylated by CDC2 [17;25] and subsequently transferred to ERES. Upon initiation of oocyte maturation, CDC2 activity at ERES may result in dissociation of SEC23-containing coats and consequent cessation of vesiculation [18;49]. Other protein complexes that control ERES function may also be phosphorylated [50], allowing dispersion of P-GM130 into the reticular ER, as observed for the ERES transmembrane marker Yip1A-GFP in CHO cells [18]. This mechanism could prevent recycling of GM130 back to the fragmenting Golgi and in this way facilitate complete Golgi breakdown. As pre-GVBD maturation proceeds, CDC2 is transported away from ERES (Fig. 1F), which may result in the renewed recruitment of P-GM130 to ERES (Fig. 6J). Since reformation of Golgi complexes at ERES has been observed in somatic cells [12-14], storage of P-GM130 in a cluster of ERES may allow for highly efficient and local reformation of the Golgi apparatus once the metaphase block of ER export is lifted after fertilization.

Conclusions

In this study, we have observed a novel domain in the cortex of porcine oocytes that comprises a cluster of ERES. We found that the well-known meiotic regulator CDC2 transiently localizes to this domain during pre-GVBD maturation, immediately after the oocyte is released from the inhibitory influence of the follicular environment. Our data further suggest that CDC2, in conjunction with its regulatory protein SPDY, plays a role in regulating storage of structural Golgi elements at this ERES cluster. The early role of the CDC2/SPDY complex described here adds to the available evidence [21] that points to a role for CDC2/SPDY upstream of MPF during oocyte maturation. Finally, these findings demonstrate that pre-GVBD maturation comprises not

only a set of changes in chromatin configuration [51], but also controlled and highly local events within the cytoplasm of the oocyte, that may be important in regulating the secretory system during the meiotic divisions.

References

[1] Handel MA, Eppig JJ. Sexual dimorphism in the regulation of mammalian meiosis. Curr Top Dev Biol 1998; 37: 333-358.

[2] Brevini TA, Cillo F, Antonini S, Gandolfi F. Cytoplasmic remodelling and the acquisition of developmental competence in pig oocytes. Anim Reprod Sci 2006; 98: 23-38.

[3] Sun QY, Wu GM, Lai L, Park KW, Cabot R, Cheong HT, Day BN, Prather RS, Schatten H. Translocation of active mitochondria during pig oocyte maturation, fertilization and early embryo development in vitro. Reproduction 2001; 122: 155-163.

[4] Mehlmann LM, Terasaki M, Jaffe LA, Kline D. Reorganization of the endoplasmic reticulum during meiotic maturation of the mouse oocyte. Dev Biol 1995; 170: 607-615.

[5] Moreno RD, Schatten G, Ramalho-Santos J. Golgi apparatus dynamics during mouse oocyte in vitro maturation: effect of the membrane trafficking inhibitor brefeldin A. Biol Reprod 2002; 66: 1259-1266.

[6] Payne C, Schatten G. Golgi dynamics during meiosis are distinct from mitosis and are coupled to endoplasmic reticulum dynamics until fertilization. Dev Biol 2003; 264: 50-63.

[7] Shorter J, Warren G. Golgi architecture and inheritance. Annu Rev Cell Dev Biol 2002; 18: 379-420.

[8] Colanzi A, Suetterlin C, Malhotra V. Cell-cycle-specific Golgi fragmentation: how and why? Curr Opin Cell Biol 2003; 15: 462-467.

[9] Shima DT, Cabrera-Poch N, Pepperkok R, Warren G. An ordered inheritance strategy for the Golgi apparatus: visualization of mitotic disassembly reveals a role for the mitotic spindle. J Cell Biol 1998; 141: 955-966.

[10] Jokitalo E, Cabrera-Poch N, Warren G, Shima DT. Golgi clusters and vesicles mediate mitotic inheritance independently of the endoplasmic reticulum. J Cell Biol 2001; 154: 317-330.

[11] Seemann J, Pypaert M, Taguchi T, Malsam J, Warren G. Partitioning of the matrix fraction of the Golgi apparatus during mitosis in animal cells. Science 2002; 295: 848-851.

[12] Altan-Bonnet N, Sougrat R, Liu W, Snapp EL, Ward T, Lippincott-Schwartz J. Golgi inheritance in mammalian cells is mediated through endoplasmic reticulum export activities. Mol Biol Cell 2006; 17: 990-1005.
[13] Prescott AR, Farmaki T, Thomson C, James J, Paccaud JP, Tang BL, Hong W, Quinn M, Ponnambalam S, Lucocq J. Evidence for prebudding arrest of ER export in animal cell mitosis and its role in generating Golgi partitioning intermediates. Traffic 2001; 2: 321-335.
[14] Zaal KJ, Smith CL, Polishchuk RS, Altan N, Cole NB, Ellenberg J, Hirschberg K, Presley JF, Roberts TH, Siggia E, Phair RD, Lippincott-Schwartz J. Golgi membranes are absorbed into and reemerge from the ER during mitosis. Cell 1999; 99: 589-601.
[15] Kline D. Attributes and dynamics of the endoplasmic reticulum in mammalian eggs. Curr Top Dev Biol 2000; 50: 125-154.
[16] Dekel N. Cellular, biochemical and molecular mechanisms regulating oocyte maturation. Mol Cell Endocrinol 2005; 234: 19-25.
[17] Lowe M, Rabouille C, Nakamura N, Watson R, Jackman M, Jamsa E, Rahman D, Pappin DJ, Warren G. Cdc2 kinase directly phosphorylates the cis-Golgi matrix protein GM130 and is required for Golgi fragmentation in mitosis. Cell 1998; 94: 783-793.
[18] Kano F, Tanaka AR, Yamauchi S, Kondo H, Murata M. Cdc2 kinase-dependent disassembly of endoplasmic reticulum (ER) exit sites inhibits ER-to-Golgi vesicular transport during mitosis. Mol Biol Cell 2004; 15: 4289-4298.
[19] Karaiskou A, Perez LH, Ferby I, Ozon R, Jessus C, Nebreda AR. Differential regulation of Cdc2 and Cdk2 by RINGO and cyclins. J Biol Chem 2001; 276: 36028-36034.
[20] Naito K, Hawkins C, Yamashita M, Nagahama Y, Aoki F, Kohmoto K, Toyoda Y, Moor RM. Association of p34cdc2 and cyclin B1 during meiotic maturation in porcine oocytes. Dev Biol 1995; 168: 627-634.
[21] Kume S, Endo T, Nishimura Y, Kano K, Naito K. Porcine SPDYA2 (RINGO A2) stimulates CDC2 activity and accelerates meiotic maturation of porcine oocytes. Biol Reprod 2007; 76: 440-447.
[22] Beckhelling C, Perez-Mongiovi D, Houliston E. Localised MPF regulation in eggs. Biol Cell 2000; 92: 245-253.
[23] Yamashita M, Yoshikuni M, Hirai T, Fukada S, Nagahama Y. A Monoclonal Antibody Against the PSTAIR Sequence of p34 cdc2 Catalytic Subunit of Maturation-Promoting Factor and Key Regulator of the Cell

Cycle. Dev Growth Differ 1991; 33: 617-624.
[24] Marcote MJ, Knighton DR, Basi G, Sowadski JM, Brambilla P, Draetta G, Taylor SS. A three-dimensional model of the Cdc2 protein kinase: localization of cyclin- and Suc1-binding regions and phosphorylation sites. Mol Cell Biol 1993; 13: 5122-5131.
[25] Lowe M, Gonatas NK, Warren G. The mitotic phosphorylation cycle of the cis-Golgi matrix protein GM130. J Cell Biol 2000; 149: 341-356.
[26] Schoevers EJ, Colenbrander B, Roelen BA. Developmental stage of the oocyte during antral follicle growth and cumulus investment determines in vitro embryo development of sow oocytes. Theriogenology 2007; 67: 1108-1122.
[27] Abeydeera LR, Wang WH, Prather RS, Day BN. Maturation in vitro of pig oocytes in protein-free culture media: fertilization and subsequent embryo development in vitro. Biol Reprod 1998; 58: 1316-1320.
[28] Yamauchi N, Nagai T. Male pronuclear formation in denuded porcine oocytes after in vitro maturation in the presence of cysteamine. Biol Reprod 1999; 61: 828-833.
[29] Grupen CG, Nagashima H, Nottle MB. Cysteamine enhances in vitro development of porcine oocytes matured and fertilized in vitro. Biol Reprod 1995; 53: 173-178.
[30] Fan HY, Li MY, Tong C, Chen DY, Xia GL, Song XF, Schatten H, Sun QY. Inhibitory effects of cAMP and protein kinase C on meiotic maturation and MAP kinase phosphorylation in porcine oocytes. Mol Reprod Dev 2002; 63: 480-487.
[31] Schoevers EJ, Bevers MM, Roelen BA, Colenbrander B. Nuclear and cytoplasmic maturation of sow oocytes are not synchronized by specific meiotic inhibition with roscovitine during in vitro maturation. Theriogenology 2005; 63: 1111-1130.
[32] Lee J, Miyano T, Moor RM. Spindle formation and dynamics of gamma-tubulin and nuclear mitotic apparatus protein distribution during meiosis in pig and mouse oocytes. Biol Reprod 2000; 62: 1184-1192.
[33] Hobman TC, Zhao B, Chan H, Farquhar MG. Immunoisolation and characterization of a subdomain of the endoplasmic reticulum that concentrates proteins involved in COPII vesicle biogenesis. Mol Biol Cell 1998; 9: 1265-1278.
[34] Poot M, Zhang YZ, Kramer JA, Wells KS, Jones LJ, Hanzel DK, Lugade AG, Singer VL, Haugland RP. Analysis of mitochondrial morphology and function with novel fixable fluorescent stains. J Histochem Cy-

tochem 1996; 44: 1363-1372.
[35] Beckhelling C, Chang P, Chevalier S, Ford C, Houliston E. Pre-M phase-promoting factor associates with annulate lamellae in Xenopus oocytes and egg extracts. Mol Biol Cell 2003; 14: 1125-1137.
[36] Mezzacasa A, Helenius A. The transitional ER defines a boundary for quality control in the secretion of tsO45 VSV glycoprotein. Traffic 2002; 3: 833-849.
[37] Han SJ, Conti M. New pathways from PKA to the Cdc2/cyclin B complex in oocytes: Wee1B as a potential PKA substrate. Cell Cycle 2006; 5: 227-231.
[38] Racowsky C. Effect of forskolin on maintenance of meiotic arrest and stimulation of cumulus expansion, progesterone and cyclic AMP production by pig oocyte-cumulus complexes. J Reprod Fertil 1985; 74: 9-21.
[39] Marangos P, Carroll J. The dynamics of cyclin B1 distribution during meiosis I in mouse oocytes. Reproduction 2004; 128: 153-162.
[40] Terasaki M, Okumura E, Hinkle B, Kishimoto T. Localization and dynamics of Cdc2-cyclin B during meiotic reinitiation in starfish oocytes. Mol Biol Cell 2003; 14: 4685-4694.
[41] Mitra J, Schultz RM. Regulation of the acquisition of meiotic competence in the mouse: changes in the subcellular localization of cdc2, cyclin B1, cdc25C and wee1, and in the concentration of these proteins and their transcripts. J Cell Sci 1996; 109 (Pt 9): 2407-2415.
[42] Misteli T, Warren G. Mitotic disassembly of the Golgi apparatus in vivo. J Cell Sci 1995; 108: 2715-2727.
[43] Wehrend A, Meinecke B. Kinetics of meiotic progression, M-phase promoting factor (MPF) and mitogen-activated protein kinase (MAP kinase) activities during in vitro maturation of porcine and bovine oocytes: species specific differences in the length of the meiotic stages. Anim Reprod Sci 2001; 66: 175-184.
[44] Kuroda T, Naito K, Sugiura K, Yamashita M, Takakura I, Tojo H. Analysis of the roles of cyclin B1 and cyclin B2 in porcine oocyte maturation by inhibiting synthesis with antisense RNA injection. Biol Reprod 2004; 70: 154-159.
[45] Shimada M, Zeng WX, Terada T. Inhibition of phosphatidylinositol 3-kinase or mitogen-activated protein kinase kinase leads to suppression of p34(cdc2) kinase activity and meiotic progression beyond the meiosis I stage in porcine oocytes surrounded with cumulus cells. Biol

Reprod 2001; 65: 442-448.
[46] Anger M, Klima J, Kubelka M, Prochazka R, Motlik J, Schultz RM. Timing of Plk1 and MPF activation during porcine oocyte maturation. Mol Reprod Dev 2004; 69: 11-16.
[47] Snapp EL, Hegde RS, Francolini M, Lombardo F, Colombo S, Pedrazzini E, Borgese N, Lippincott-Schwartz J. Formation of stacked ER cisternae by low affinity protein interactions. J Cell Biol 2003; 163: 257-269.
[48] Kloc M, Bilinski S, Etkin LD. The Balbiani body and germ cell determinants: 150 years later. Curr Top Dev Biol 2004; 59: 1-36.
[49] Stephens DJ. De novo formation, fusion and fission of mammalian COPII-coated endoplasmic reticulum exit sites. EMBO Rep 2003; 4: 210-217.
[50] Mancias JD, Goldberg J. Exiting the endoplasmic reticulum. Traffic 2005; 6: 278-285.
[51] Sun XS, Liu Y, Yue KZ, Ma SF, Tan JH. Changes in germinal vesicle (GV) chromatin configurations during growth and maturation of porcine oocytes. Mol Reprod Dev 2004; 69: 228-234.

Chapter 3

A method for (co-)injection of quantifiable amounts of fluorescent molecules into mammalian oocytes

Jurriaan J. Hölzenspies[1,2], Willem Stoorvogel[2], Ben Colenbrander[1], Bernard A. J. Roelen[1], Theo van Haeften[2]

[1]Department of Farm Animal Health, Faculty of Veterinary Medicine, Utrecht University, Utrecht, the Netherlands
[2]Department of Biochemistry & Cell Biology, Faculty of Veterinary Medicine, Utrecht University, Utrecht, the Netherlands

In preparation

A method for (co-)injection of quantifiable amounts of fluorescent molecules into mammalian oocytes

Abstract

Mammalian oocytes are difficult to manipulate at the molecular level due to their low transcriptional activity and the presence of large stores of mRNA and protein. Although microinjection has become an important tool to interfere with intracellular processes in oocytes, injection success, final concentrations of injected substances, and viability after injection are difficult to assess with current techniques. To address these problems, we have devised a novel method that utilizes a pressure-based microinjection system to introduce fluorescent substances into oocytes and epifluorescence microscopy to evaluate injected oocytes. Our validation of this method shows that it is an efficient means of manipulating oocytes using consistent concentrations of injected substances, without resulting in adverse effects on oocyte maturation. As an example of its application, we demonstrate that this method is useful for evaluating the kinetics of small molecule transfer through gap junctions between oocytes and their surrounding cumulus cells.

Introduction

Fully grown immature mammalian oocytes are arrested at meiotic prophase I. When maturation is initiated, oocytes undergo germinal vesicle breakdown (GVBD), after which the first metaphase spindle, the first polar body, and the second metaphase spindle are formed sequentially. Maturation is completed when oocytes enter a second period of meiotic arrest at metaphase II, which is maintained until fertilization [1].

To identify and characterize the molecular players that regulate and drive these processes is a difficult task because the molecular tools that are readily available for studies on somatic cells are often not suited for studying mammalian oocytes. Mammalian oocytes are characterized by a lack of transcription after GVBD [2-6] and oocytes are thus not easily manipulated by cDNA transfection. Moreover, knock-out animals have not been generated for many relevant proteins and this is especially true for larger mammalian species, including the pig.

Microinjection has been used for RNA interference in oocytes [7-9]. Since many proteins have long half-lives and are abundantly present in oocytes, approaches that aim to interfere at the translational level will often be ineffective in manipulating protein function during maturation, and are more suitable for interfering with protein expression during pre-implantation development. Nevertheless, co-injection of GFP mRNA with other mRNA or antisense RNA has proven to be an effective method to select injected oocytes for viability and/or active translation [10-12]. However, this method does not allow selection of oocytes until stable expression is established after 6 – 18 h of maturation [13]. Successfully injected oocytes are therefore cultured in the presence of oocytes that ultimately degenerate as a result of injection. Apoptotic signals from degenerating cumulus oocyte complexes (COCs) that have been damaged as a consequence of the injection procedure may induce apoptosis in other COCs [14], which could lead to further reduction in the number of viable oocytes and thus reduced efficiency of the procedure. Microscopic identification of damaged COCs is compromised by several layers of tightly packed cumulus cells that obscure the view of the underlying oocyte and are required for efficient in vitro maturation of porcine oocytes [15]. Moreover, injection of controlled amounts of mRNA leads to extensive variation in expression levels [13], which can cause experimental variation. Although mRNA injection is a powerful method that has already provided several interesting insights into oocyte maturation [10-12], the drawbacks indicate that alternative approaches for molecular interference are required. Microinjection methods have also been applied to introduce antibodies, peptides, and mutant proteins, allowing direct interference with protein function [16-19]. Although such methods are valuable tools, their power is often limited by the lack of good selection criteria for successful and reproducible injection and viability.

In this study, we have developed a pressure-based microinjection protocol that allows immediate confirmation of successful injection, assessment of viability, and matching of final concentrations of injected molecules between oocytes. We injected a highly stable GFP variant into immature oocytes and found that GFP fluorescence was retained in a high percentage of injected oocytes, even after 44 h of culture followed by fixation, indicating the value of this method for controlled oocyte manipulation. Another possible application for microinjection is to assess gap junctional communication between oocytes and their surrounding cumulus cells [20;21]. To measure gap junction permeability, these studies relied on the introduction of small fluorescent molecules into oocytes and categorical scoring to asses transfer to cumulus

cells, yet this transfer was not quantified real-time. We employed our microinjection method to introduce a mixture of two spectrally separated fluorescent molecules, with a substantial difference in molecular weight that either prevented or allowed transfer through cumulus-oocyte gap junctions. Timed fluorescence ratio measurements of these dyes in injected oocytes was then used to determine the kinetics of transfer through gap junctions.

Materials and Methods

Oocyte isolation, selection, and culture

All chemicals were purchased from Sigma Chemical Co. (St. Louis, MO, USA), unless otherwise indicated. Cumulus-oocyte complexes (COCs) were collected from slaughterhouse sow (Sus scrofa) ovaries, by aspirating 3-6 mm follicles, and washed in TL-HEPES-PVP (114 mM NaCl, 3.2 mM KCl, 2 mM $NaHCO_3$, 0.4 mM $NaH_2PO_4 \bullet H_2O$, 0.25 mM sodium pyruvate, 10 mM sodium lactate, 0.5 mM $MgCl_2 \bullet 6H_2O$, 2 mM $CaCl_2 \bullet 2H_2O$, 10 mM HEPES, 0.1% (w/v) polyvinylpyrrolidone, pH 7.4). In vitro maturation was performed as described previously [22].

Microinjection and image acquisition

All steps prior to in vitro maturation were performed in the presence of 1 mM dibutyryl cAMP (dbcAMP) to maintain prophase arrest. COCs were partially denuded by repeated pipetting until the cumulus investment was reduced to 3-6 layers, washed in microinjection medium (HEPES-buffered M199; Gibco BRL, Grand Island, NY, USA), and transferred to 5 µl drops of microinjection medium (5 oocytes/drop; Fig. 1A) under oil (Oil for embryo culture; Irvine Scientific, Santa Ana, CA, USA). Microinjection was performed at 37 °C on an IX71 inverted microscope (Olympus, Zoeterwoude, the Netherlands) equipped with two transferman NK2 micromanipulators (Eppendorf, Hamburg, Germany) and a Thermo Plate (MATS-U55R30; Tokai Hit, Shizuoka-ken, Japan). Oocytes were immobilized on a suction pipette (MPH-LG-30; Humagen Fertility Diagnostics, Charlottesville, VA, USA) and injected using a beveled rigid borosilicate micropipette with a 30° angle and 3.5 µm tip diameter (custom tips; Eppendorf). Control oocytes that were not injected were kept under identical conditions in the same injection dish. GFP (SuperGlo GFP; Qbiogene Inc., Montreal, QC, Canada) was dialyzed against

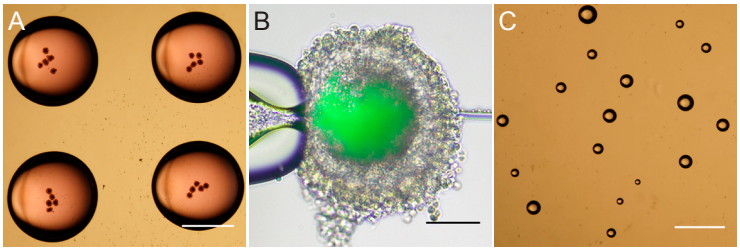

Figure 1 – Microinjection conditions
(A) Groups of 5 oocytes were transferred to 5 µl drops of microinjection medium containing 1 mM dbcAMP under oil and microinjection was performed within these drops. Bar, 2 mm (B) Merge of fluorescent (FITC) and phase contrast images of a COC within 1 min after injection of a GFP-tagged protein into the oocyte. Bar, 50 µm. Note that the GFP signal has spread evenly throughout the oocyte. (C) DIC image of small GFP-containing droplets that were pipetted onto a coverslip under oil and used to generate fluorescence standard curves. Bar, 1 mm.

microinjection buffer, concentrated to 1 mg/ml, and stored at -80 °C until injection. Tetramethylrhodamine (TRITC)-labeled 3 kDa Dextran (Dextran-TRITC; Molecular Probes, Eugene, OR, USA), Calcein (Molecular Probes), and fluorescein (FITC)-labeled 18-mer oligonucleotides with a random sequence (18-mer-FITC; 5' CCC TCA CCT CTT ACC TCA 3'-FITC; Gene Tools LLC, Philomath, OR, USA) were diluted in microinjection buffer to 1 mM, 100 mM, and 1 mM, respectively, and stored at -20 °C until injection. Microinjection solutions were centrifuged for 10 min at 16,000 g, and ~1 µl, was back-loaded into micropipettes, which were connected to a Femtojet pressure injection system (Eppendorf). Fluorescence intensity in oocytes was monitored during injections to ensure equal fluorescence intensities between injected oocytes (Fig. 1B).

Drops of a 1:10 dilution of the injection solution were produced using a thinly pulled glass pipette and pipetted onto a coverslip coated with Sigmacote that was kept in a microinjection dish at 37 °C under oil (Fig. 1C). The images used to measure total fluorescence were obtained using a FITC or TRITC filter (Olympus) with a stabilized 100 W Hg^{2+} lamp at 100x magnification on a DP20 camera (Olympus) using 50 (FITC) or 100 (GFP and TRITC) ms exposure. Images were recorded either after all injections were completed (for GFP), or at several different timepoints after injection (for dextran-TRITC mixtures). Image analysis was performed in ImageJ (NIH; http://rsb.info.nih.gov/ij/). Regions of interest (ROIs) of droplets, oocytes, and cumulus cells were drawn by thresholding epifluorescence images of the FITC channel for GFP and the TRITC channel for mixtures containing dextran-TRITC and background sub-

traction was performed by subtracting the average pixel intensity in the cumulus from the average pixel intensity in the oocyte. The resulting background subtracted average pixel intensity in the oocyte was then multiplied with the number of pixels in de oocyte ROI to calculate the integrated density, which was used as a measure of total fluorescence. For DNA labeling, oocytes were washed and denuded in 80 mM PIPES, 5 mM EGTA, 2 mM $MgCl_2$, pH 6.9, supplemented with 0.3% (w/v) PVP (PEM-PVP) at 37°C, followed by fixation in the same buffer containing 4% (v/v) paraformaldehyde (fixative; Electron Microscopy Sciences, Hatfield, PA, USA) at room temperature for 1 h. Following two washes in PBS (0.1 M; pH 7.4) containing 0.3% (w/v) PVP (PBS-PVP), oocytes were incubated in PBS-PVP supplemented with 100 mM glycine for 15 min and permeabilized by a 10 min incubation in PBS containing 0.1% (w/v) saponin. DNA labeling and preparation of microscope slides were then performed as previously described [22]. Confocal images were acquired using a Nikon eclipse TE300 (Nikon Corp., Tokyo, Japan), equipped with a BioRad Radiance 2100MP confocal system (Zeiss/BioRad, Hertfordshire, UK), and a 40x oil immersion objective (N.A. 1.3). All data are given as mean ± SD and statistical analysis was performed in Microsoft Excel.

Flow Cytometry

GFP and a protein construct tagged with the same type of GFP (Hölzenspies et al., to be published elsewhere) were coupled to paramagnetic epoxy beads (Dynal Biotech, Lake Success, NY) according to the manufacturer's instructions. Both GFP and the GFP-tagged protein construct were incubated with 10^7 beads in 50 µl PBS at a concentration of 1.25 µM for 24 h under rotation at room temperature. Control beads (mock) were incubated in PBS only. When indicated, the same method used to fix oocytes was applied to beads. Beads were analyzed using a FACSCalibur flow cytometer (BD Biosciences, San Jose, CA) and FCS Express software.

Results

Validation of fluorescence measurement

For somatic cells, the injected volume of a stable fluorescent substance correlates closely with total cellular fluorescence [23]. Given that immature mammalian oocytes are spherical with only minor variations in diameter (112

A

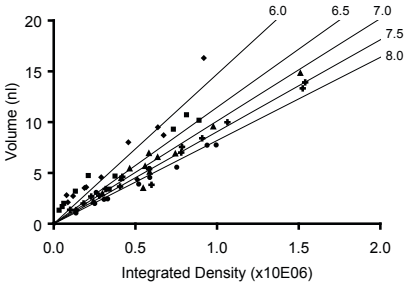

B

pH	Symbol	α	R^2	N
6.0	♦	14.722	0.9463	13
6.5	■	11.452	0.9694	11
7.0	▲	10.095	0.9768	14
7.5	+	9.052	0.9798	16
8.0	●	8.189	0.9913	12

Figure 2 – GFP fluorescence intensity is injection volume and pH dependent

Microdroplets of 1:10 dilutions of 1 mg/ml GFP-tagged protein in microinjection buffers at the indicated pH values were analyzed by fluorescence measurement at the same magnification and microscope settings as were used for oocytes. (A) The integrated density (= total area x mean pixel intensity) was charted against the measured volume of each droplet. For each pH value, linear regression was used to generate lines following the formula y = αx, with the intercept set at 0. (B) Table showing characteristics (the slope α, the determination coefficient R2, and the number of observations N) of the linear correlation between volume and integrated density at different pH values.

± 5 µm in this study), the intracellular concentration of the injected fluorescent substance should correlate directly with the total fluorescence of injected oocytes. We employed a previously described method [23], using parallel GFP fluorescence intensity measurements on microdrops of injection fluid, to determine the injected volume and concentration of GFP in injected oocytes. Total GFP fluorescence in the microdrops, as measured by fluorescence microscopy, increased linearly with their volume (Fig 2A), and could thus serve as a measure to determine the total amount of injected GFP in oocytes. Fluorescence measurement of microdrops of GFP diluted in freshly prepared buffers with different pH values was used to determine pH dependence of GFP fluorescence. Linear regression of these data yielded a strong correlation of fluorescence intensity with droplet size at all pH values, and revealed that the intensity of GFP fluorescence increased with increasing pH (Fig. 2B). It is therefore essential to prepare a calibration curve in microdrops at a pH value similar to that of the cytoplasm of live oocytes (pH 7.4; [24]).

Selection of oocytes based on sustained fluorescence

Epifluorescent images were taken immediately after the injection and used to match fluorescence intensity between oocytes. At this point, oocytes with fluorescence intensities at or near average (average integrated density = 5.05 ± 1.18 (SD) x 10^5) were taken into culture (126/175; 72 %), and all other oocytes were discarded (Fig. 3A,B). Our injection method was further

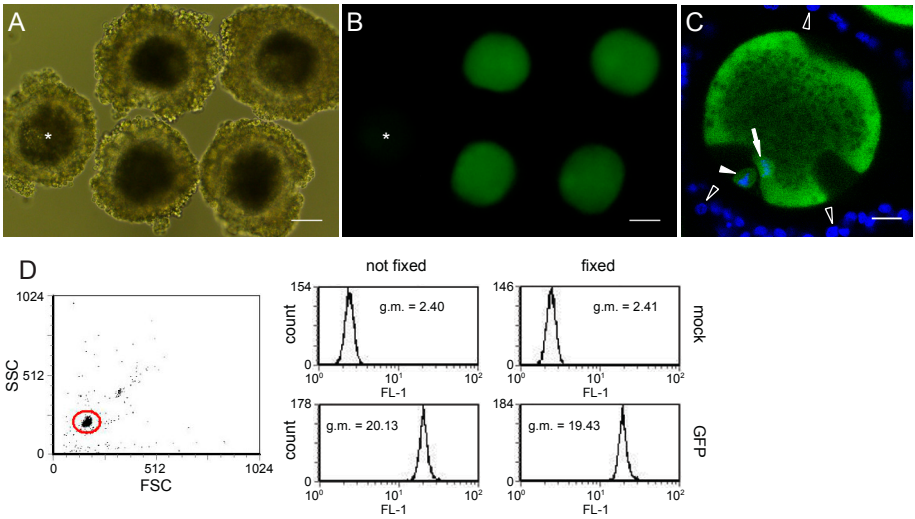

Figure 3 – Selection of GFP-injected oocytes and GFP fluorescence after fixation
DIC (A) and epifluorescence (B) images of COCs just after injection of GFP into the oocyte. As an example, the oocyte marked with an asterisk was considered unsuccessfully injected and removed from the experiment. Bar, 50 µm. (C) GFP-injected oocytes were matured to metaphase II, partially denuded, fixed, labeled for DNA (blue), and analyzed for GFP fluorescence (green). A single confocal section is shown. Note that GFP was not detected in remaining cumulus cells (open arrowheads). The arrow indicates the metaphase plate and the arrowhead indicates the polar body. Bar, 20 µm. (D) To evaluate the effect of fixation on GFP fluorescence, GFP was covalently coupled to beads and analyzed by flow cytometry. A total of 5000 single beads were gated (red circle) for each condition as exemplified in the left graph. GFP-coated beads and mock beads were either fixed or left untreated prior to analysis as indicated. The geometric mean (g.m.) of GFP fluorescence (FL-1) was not affected by fixation.

evaluated by comparing the percentage of matured non-injected control versus GFP-injected oocytes after 44 h of culture. Any oocytes that degenerated during in vitro maturation were removed and experiments in which non-injected control oocytes showed a maturation rate < 60 % were excluded from analysis. In six separate successful experiments with 15-30 oocytes per group, respectively 77 ± 9 % (100/130) and 75 ± 4 % (89/118) of non-injected and GFP-injected oocytes had matured to metaphase II. Analysis of these results using chi-square tests indicated that the microinjection procedure did not affect maturation ($P > 0.05$). Mature GFP-injected oocytes retained their GFP fluorescence even after fixation and DNA labeling (Fig. 3C). To independently determine potential fixation effects on the intensity of GFP fluorescence, GFP-tagged protein constructs were covalently coupled to beads (non-conjugated

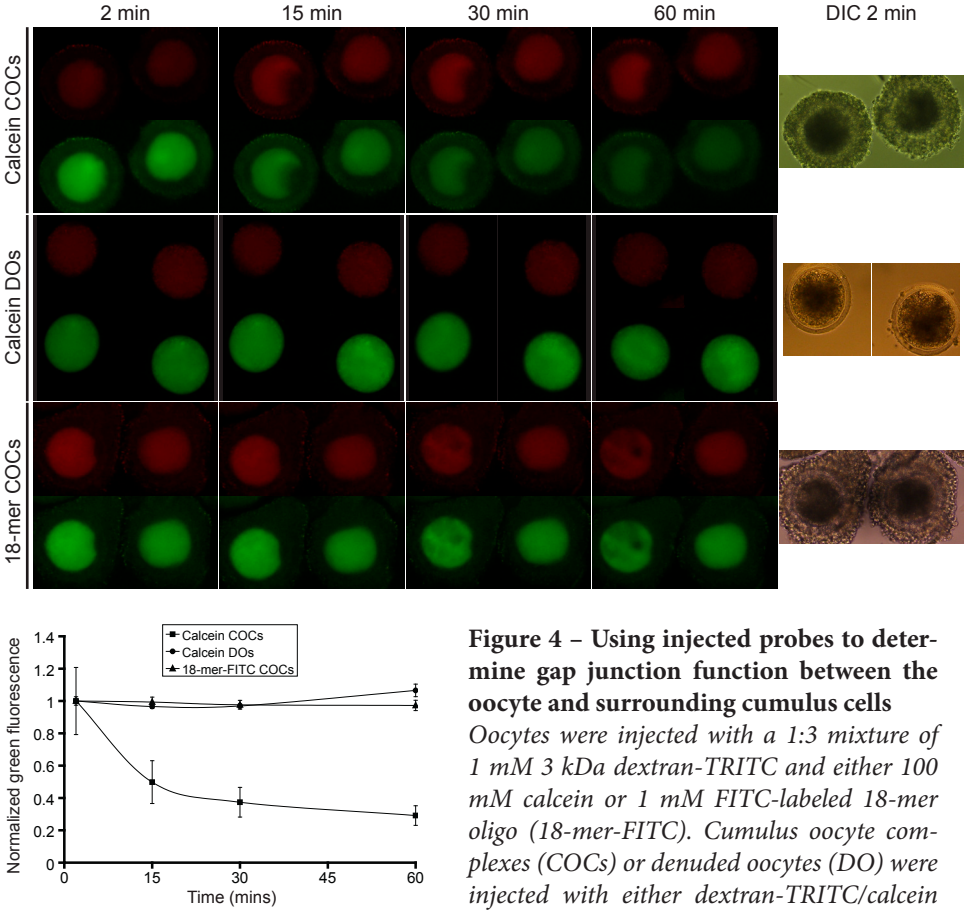

Figure 4 – Using injected probes to determine gap junction function between the oocyte and surrounding cumulus cells
Oocytes were injected with a 1:3 mixture of 1 mM 3 kDa dextran-TRITC and either 100 mM calcein or 1 mM FITC-labeled 18-mer oligo (18-mer-FITC). Cumulus oocyte complexes (COCs) or denuded oocytes (DO) were injected with either dextran-TRITC/calcein or dextran-TRITC/18-mer-FITC mixtures as indicated. The oocytes were imaged at 2, 15, 30, and 60 min after injection (as indicated) using 50 ms exposure in the FITC channel (green; calcein and 18-mer-FITC) and 100 ms exposure in the TRITC channel (red; dextran-TRITC). In addition, oocytes were photographed using DIC immediately after injection (far right column). The graph at the bottom shows the signals for 18-mer-FITC or calcein relative to dextran-TRITC, normalized to values at 2 min. Each point represents average values ± SD of 2-4 oocytes.

GFP did not bind to the beads), incubated for 1 h in the presence or absence of fixative and assayed for fluorescence by flow cytometry (Fig. 3D). Beads carrying GFP-tagged protein construct showed a clear fluorescent signal in comparison to non-conjugated beads. The fluorescence intensity was unchanged by fixation, supporting the usefulness of GFP-tagged constructs for determining final concentrations in injected oocytes even after fixation. It should be noted, however, that there is always a possibility that incomplete fixation al-

lows leakage of non-fixed proteins from permeabilized cells.

Measurement of gap junction kinetics by injecting a mixture of gap junction permeant and non-permeant spectrally separated fluorescent molecules

To further validate our method, we tested its usefulness to determine the rate at which small molecules are transferred through the gap junctions between oocytes and cumulus cells. Oocytes were injected with a mixture of calcein and 3 kDa dextran-TRITC. These probes were observed separately by epifluorescence microscopy using FITC and TRITC filters, respectively. Calcein was previously shown to transfer through cumulus-oocyte gap junctions [25;26]. In contrast, 3 kDa dextran should not be transferred as these gap junctions have a molecular weight cutoff of ~1 kDa [27] and was used to determine the variation in relative concentration between injected oocytes (average integrated density = 3.34 ± 0.78 (SD) x 10^5). The ratio of total fluorescence intensity of these molecules in oocytes within COCs was then followed with time to determine gap junction kinetics over a 1 h period. As a negative control, we used denuded oocytes that lack neighboring cumulus cells.

Figure 4 shows fluorescent images recorded through FITC (green) and TRITC (red) filters of two example oocytes at 2, 15, 30, and 60 min after injection as indicated. Cumulus cells surrounding the oocytes are clearly visible in the differential interference constrast (DIC) images on the far right. Quantification of the signals (graph in Fig. 4) revealed that dextran (TRITC) fluorescence was maintained at a constant concentration in all injected oocytes. In contrast, the calcein (FITC) signal was rapidly lost from oocytes contained within COCs. The initial signal appeared to be reduced with first order kinetics to ~ 30% of its original value and using 30 % as a basal level had a halving time of ~10 min. This loss of calcein fluorescence was not observed in denuded oocytes, further supporting the role of gap junctions in calcein transfer to the cumulus cells. We also injected a mixture of dextran-TRITC with 18-mer-FITC, of which the transfer through gap junctions at the oocyte-cumulus cell interface was unknown. Unlike calcein, 18-mer-FITC was not transferred via gap junctions.

Discussion

Here, we describe a novel pressure-based microinjection method to introduce fluorescent molecules into fully grown immature porcine oocytes and

to assess the amount of injected substance by measuring total fluorescence intensity within oocytes after injection. The efficiency and possible applications of this method were first examined by injecting GFP, which is commonly used to tag proteins and study their distribution in living cells. We found that successfully injected oocytes could be selected based on their fluorescence immediately after injection, and that quantification of total fluorescence intensity could be used to assess the concentration of injected molecules in oocytes. Our results indicate that this method provides a highly efficient means of introducing consistent amounts of exogenous fluorescently labeled proteins into oocytes.

We found that the fluorescence intensity of the GFP variant used in this study is pH dependent, which becomes important when using injection buffers with pH values other than ~7.5. For example, our injection method was initially optimized for introduction of fluorescent tubulin (data not shown). To prevent premature polymerization of tubulin, the pH of the injection buffer we used was 6.9 [28], whereas the intracellular pH of porcine oocytes is approximately 7.4 [24].

Determination of total fluorescence of oocytes (co-)injected with GFP is a valuable method to examine variation in injection volume. Oocytes selected after GFP injection were viable and competent to complete maturation, since these oocytes matured with the same efficiency as non-injected controls and retained their GFP fluorescence even after maturation and fixation (Fig. 3C). Our results demonstrate that the fixation procedure did not reduce GFP fluorescence intensity, indicating that a decrease in fluorescence intensity could only be caused by breakdown of GFP during in vitro maturation.

Interference with protein function in mammalian oocytes can be extremely difficult, since large quantities of mRNA and protein are stored in the oocyte to accommodate cellular metabolism, meiosis, and several post-fertilization mitotic divisions. A previously described mRNA microinjection method has proven to be effective in manipulating oocyte maturation [10-12]. However, only ~30 % of injected oocytes showed stable expression after 18 h of maturation and although the injected volume was carefully controlled and kept identical between oocytes, expression levels varied extensively [13]. Our pressure-based microinjection method had a much higher efficiency (~75 %), which may be attributable to the selection of oocytes immediately after injection, as signals from oocytes that have been damaged during the injection procedure may induce apoptosis in other oocytes [14]. In addition, we found that careful examination of fluorescence during injection can be used

to ensure that oocytes contain consistent amounts of an injected fluorescent substance.

We observed that the membrane impermeable dye calcein is rapidly transferred out of calcein/dextran-TRITC-injected oocytes when connections with the cumulus cells remained intact, but not when these connections were severed by denudation, thus validating the technique for studying gap junction kinetics. In contrast to calcein, 18-mer-FITC, an oligonucleotide with a morpholino backbone similar in size to small interfering RNAs (siRNA), failed to transfer through the gap junctions within the same time frame (Fig. 4). In somatic cells, however, transfer of siRNAs through connexin 43 homotypic gap junctions has been demonstrated previously [29]. The oocyte-cumulus cell interface contains junctions between connexin 37 in the oocyte and connexin 43 in the transzonal projections that emanate from the cumulus cells [27] and transfer of siRNA through these heterotypic gap junctions has not been investigated previously. Although further research is required to settle the issue, our results suggest that the heterotypic gap junctions at the oocyte-cumulus cell interface do not allow rapid passage of siRNAs. Nevertheless, our data clearly indicate that the method of injection and fluorescence measurement presented here is an efficient way to examine the characteristics of gap junctions between oocytes and surrounding cumulus cells.

In this study, we have demonstrated that a combination of pressure-based microinjection with epifluorescence microscopy provides a highly efficient method of introducing consistent amounts of foreign substances into immature porcine oocytes. Our results further indicate that this method can be used to interfere with oocyte maturation and to investigate the characteristics of gap junctions between oocytes and their surrounding cumulus cells.

References

[1] Handel MA, Eppig JJ. Sexual dimorphism in the regulation of mammalian meiosis. Curr Top Dev Biol 1998; 37: 333-358.

[2] Fair T, Hyttel P, Greve T, Boland M. Nucleus structure and transcriptional activity in relation to oocyte diameter in cattle. Mol Reprod Dev 1996; 43: 503-512.

[3] Bouniol-Baly C, Hamraoui L, Guibert J, Beaujean N, Szollosi MS, Debey P. Differential transcriptional activity associated with chromatin configuration in fully grown mouse germinal vesicle oocytes. Biol Reprod 1999; 60: 580-587.

[4] Motlik J, Kopecny V, Travnik P, Pivko J. RNA synthesis in pig follicular oocytes. Autoradiographic and cytochemical study. Biol Cell 1984; 50: 229-235.
[5] Bjerregaard B, Maddox-Hyttel P. Regulation of ribosomal RNA gene expression in porcine oocytes. Anim Reprod Sci 2004; 82-83: 605-616.
[6] Bevilacqua A, Kinnunen LH, Mangia F. Genetic manipulation of mammalian dictyate oocytes: factors affecting transient expression of microinjected DNA templates. Mol Reprod Dev 1992; 33: 124-130.
[7] Paradis F, Vigneault C, Robert C, Sirard MA. RNA interference as a tool to study gene function in bovine oocytes. Mol Reprod Dev 2005; 70: 111-121.
[8] Mehlmann LM. Oocyte-specific expression of Gpr3 is required for the maintenance of meiotic arrest in mouse oocytes. Dev Biol 2005; 288: 397-404.
[9] Wianny F, Zernicka-Goetz M. Specific interference with gene function by double-stranded RNA in early mouse development. Nat Cell Biol 2000; 2: 70-75.
[10] Ohashi S, Naito K, Sugiura K, Iwamori N, Goto S, Naruoka H, Tojo H. Analyses of mitogen-activated protein kinase function in the maturation of porcine oocytes. Biology of Reproduction 2003; 68: 604-609.
[11] Kume S, Endo T, Nishimura Y, Kano K, Naito K. Porcine SPDYA2 (RINGO A2) stimulates CDC2 activity and accelerates meiotic maturation of porcine oocytes. Biol Reprod 2007; 76: 440-447.
[12] Kuroda T, Naito K, Sugiura K, Yamashita M, Takakura I, Tojo H. Analysis of the roles of cyclin B1 and cyclin B2 in porcine oocyte maturation by inhibiting synthesis with antisense RNA injection. Biol Reprod 2004; 70: 154-159.
[13] Ohashi S, Naito K, Liu J, Sheng Y, Yamanouchi K, Tojo H. Expression of Exogenous Proteins in Porcine Maturing Oocytes after mRNA Injection: Kinetic Analysis and Oocyte Selection Using EGFP mRNA. The Journal of Reproduction and Development 2001; 47: 351-357.
[14] Krysko DV, ez-Fraile A, Criel G, Svistunov AA, Vandenabeele P, D'Herde K. Life and death of female gametes during oogenesis and folliculogenesis. Apoptosis 2008; 13: 1065-1087.
[15] Schoevers EJ, Colenbrander B, Roelen BA. Developmental stage of the oocyte during antral follicle growth and cumulus investment determines in vitro embryo development of sow oocytes. Theriogenology 2007; 67: 1108-1122.

[16] Morikawa M, Seki M, Kume S, Endo T, Nishimura Y, Kano K, Naito K. Meiotic resumption of porcine immature oocytes is prevented by ooplasmic Gsalpha functions. J Reprod Dev 2007; 53: 1151-1157.
[17] Hoshino Y, Sato E. Protein kinase B (PKB/Akt) is required for the completion of meiosis in mouse oocytes. Dev Biol 2008; 314: 215-223.
[18] Chen J, Hudson E, Chi MM, Chang AS, Moley KH, Hardie DG, Downs SM. AMPK regulation of mouse oocyte meiotic resumption in vitro. Dev Biol 2006; 291: 227-238.
[19] Inoue M, Naito K, Nakayama T, Sato E. Mitogen-activated protein kinase translocates into the germinal vesicle and induces germinal vesicle breakdown in porcine oocytes. Biol Reprod 1998; 58: 130-136.
[20] Ali A, Paradis F, Vigneault C, Sirard MA. The potential role of gap junction communication between cumulus cells and bovine oocytes during in vitro maturation. Mol Reprod Dev 2005; 71: 358-367.
[21] Isobe N, Terada T. Effect of the factor inhibiting germinal vesicle breakdown on the disruption of gap junctions and cumulus expansion of pig cumulus-oocyte complexes cultured in vitro. Reproduction 2001; 121: 249-257.
[22] Hölzenspies JJ, Stoorvogel W, Colenbrander B, Roelen BA, Gutknecht DR, van Haeften T. CDC2/SPDY transiently associates with endoplasmic reticulum exit sites during oocyte maturation. BMC Dev Biol 2009; 9: 8.
[23] Lee GM. Measurement of volume injected into individual cells by quantitative fluorescence microscopy. J Cell Sci 1989; 94(Pt 3): 443-447.
[24] Ruddock NT, Machaty Z, Milanick M, Prather RS. Mechanism of intracellular pH increase during parthenogenetic activation of In vitro matured porcine oocytes. Biol Reprod 2000; 63: 488-492.
[25] Thomas RE, Armstrong DT, Gilchrist RB. Bovine cumulus cell-oocyte gap junctional communication during in vitro maturation in response to manipulation of cell-specific cyclic adenosine 3',5'-monophosophate levels. Biol Reprod 2004; 70: 548-556.
[26] Sasseville M, Gagnon MC, Guillemette C, Sullivan R, Gilchrist RB, Richard FJ. Regulation of gap junctions in porcine cumulus-oocyte complexes: Contributions of granulosa cell contact, gonadotropins and lipid rafts. Mol Endocrinol 2009.
[27] Kidder GM, Mhawi AA. Gap junctions and ovarian folliculogenesis. Reproduction 2002; 123: 613-620.
[28] Peloquin J, Komarova Y, Borisy G. Conjugation of fluorophores to tubu-

lin. Nat Methods 2005; 2: 299-303.

[29] Valiunas V, Polosina YY, Miller H, Potapova IA, Valiuniene L, Doronin S, Mathias RT, Robinson RB, Rosen MR, Cohen IS, Brink PR. Connexin-specific cell-to-cell transfer of short interfering RNA by gap junctions. J Physiol 2005; 568: 459-468.

Chapter 4

Clathrin is essential for meiotic spindle function in porcine oocytes

Jurriaan J. Hölzenspies[1,2], Bernard A. J. Roelen[1], Ben Colenbrander[1], Roland A. Romijn[3], Wieger Hemrika[3], Willem Stoorvogel[2], Theo van Haeften[2]

[1]Department of Farm Animal Health, Faculty of Veterinary Medicine, Utrecht University, Utrecht, the Netherlands
[2]Department of Biochemistry & Cell Biology, Faculty of Veterinary Medicine, Utrecht University, Utrecht, the Netherlands
[3]U-Protein Express BV, Utrecht, the Netherlands

Submitted for publication

Clathrin is essential for meiotic spindle function in porcine oocytes

Abstract

Mammalian oocytes acquire competence for fertilization during meiotic maturation, a process that includes completion of the first meiotic division and formation of the second metaphase spindle. Clathrin is a large protein complex that has originally been defined for its role in intracellular membrane traffic, but was recently shown to have a second independent function, involving the stabilization of kinetochore fibers in mitotic spindles of dividing somatic cells. To study whether clathrin also functions at meiotic spindles in oocytes we microinjected green fluorescent protein-tagged C-terminal and N-terminal clathrin protein constructs into isolated porcine oocytes prior to in vitro maturation. In oocytes, both constructs associated with meiotic spindles similar to endogenous clathrin, but induced misalignment and clumping of chromosomes, formation of satellite spindles, and failure of polar body extrusion. These results demonstrate a crucial role for clathrin in the function of the first and second meiotic spindle in maturing oocytes.

Introduction

During development, mammalian oocytes are arrested at prophase I, and resume meiosis when maturation is initiated in response to the LH surge. Oocyte maturation is characterized by several key events, including disintegration of the nuclear envelope, also referred to as germinal vesicle (GV) breakdown, formation of the first metaphase spindle, extrusion of the first polar body, and formation of the second metaphase spindle. In most mammals, oocytes enter a second period of meiotic arrest at metaphase II, which is maintained until fertilization [1;2]. Nondisjunction of chromosomes during the meiotic divisions of oocytes is a major source of genetic disorders in humans [3], and it is thus important to understand the machinery that controls proper chromosome segregation. In mitotic cells, the kinetochore fibers of the metaphase spindle are associated with and stabilized by a large cytosolic protein, clathrin [4;5].

Clathrin is a ubiquitously expressed protein and has a prominent role

in intracellular membrane transport pathways that rely on clathrin coated vesicles [4;6-8]. Clathrin forms a large three-legged hexameric protein complex called triskelion, which is composed of three heterodimers of a ~190 kDa heavy chain (CHC) and a ~25 kDa light chain (CLC). Triskelions can polymerize into a polyhedral coat that drives the formation of clathrin-coated vesicles, which bud off from several membranes, including the plasma membrane and the trans-Golgi network [6;8]. The second function of clathrin is to prevent misalignment and mis-segregation of chromosomes, presumably by bridging microtubules independently of its role in membrane transport [4;5]. Clathrin-depleted somatic cells show diverse mitotic defects, including activation of the spindle check point and disruption of cytokinesis, culminating in aberrant chromosome segregation and incomplete cell division. Although clathrin has also been observed to associate with the second meiotic spindle in mouse oocytes [9], a role for clathrin in spindle function in maturing oocytes has not been established.

In the present study, we have investigated the role of clathrin in the meiotic progression of maturing porcine oocytes. Clathrin function at metaphase spindles requires both the N- and C-terminal domains of CHC [4;5;10]. To

Table 1. Primers for full length, C-terminal, and N-terminal clathrin heavy chain.

Primers for PCR	**Forward**	**Reverse**
Full length clathrin + untranslated regions	5'-GGA GGA GAC CAT ACC CCC CGA CAG-3'	5'-AAC AGA TTG AAT ATT AAG CAG T-3'
Cloning primers	***Bsa I site*** (5'-GGTCTC$(N)_6$-3') ***BamHI site*** (5'-GGATCC-3')	***Not I site*** (5'-GCGGCCGC-3')
Full length clathrin	5'-GGG GTC TCG GAT CCG CCC AGA TTC TGC CAA TTC GTT TTC AGG-3'	5'-GCG GCC GCC ATG CTG TAC CCA AAG CCA GGC TG-3'
C-terminal clathrin	5'-GGA TCC AAA TTT GAT GTC AAT ACT TCA GCA GTG CAG GTC-3'	5'-GCG GCC GCC ATG CTG TAC CCA AAG CCA GGC TG-3'
N-terminal clathrin	5'-GGG GTC TCG GAT CCG CCC AGA TTC TGC CAA TTC GTT TTC AGG-3'	5'-GCG GCC GCG TAT ACA CTA AGT GCC AAT GTC GGG TCC-3'

interfere with clathrin function, we microinjected green fluorescent protein (GFP)-tagged constructs that constituted either the N- or the C-terminal domain of porcine CHC. Our data provide novel insights into the involvement of clathrin in mammalian oocyte maturation and demonstrate an essential role for clathrin in meiotic spindle function.

Materials and Methods

Recombinant clathrin constructs

Porcine clathrin heavy chain was PCR-amplified from porcine brain cDNA using the Expand Long Template PCR System (ELT-PCR; Roche Applied Science, Indianapolis, IN, USA) according to the manufacturer's instructions with primers designed based on homology between the known human (NM_004859), bovine (NM_174023), and mouse (NM_001003908) CHC sequences (table 1, primers for PCR), and sequenced (Baseclear, Leiden, the Netherlands; EMBL accession number FM210346, accession date March 3, 2009). The PCR product was then diluted 1:1000 and amplified again using Pfu DNA polymerase (Fermentas, Burlington, Ontario, Canada) to obtain coding cDNA for residues 1-479 (N-CHC) and residues 1073-1675 (C-CHC) and to introduce in-frame BamHI – NotI restriction sites for C-terminal clathrin and BsaI – NotI for N-terminal clatrin (table 1, cloning primers). Both constructs were cloned into pCR4-TOPO (Invitrogen, Paisley, UK) and positive clones were sequenced (Baseclear). N- and C-terminal CHC constructs were then ligated into pUPE (U-Protein Express BV, Utrecht, The Netherlands) containing the Superglo GFP sequence followed by a His-tag at the N-terminus of the C-terminal construct and at the C-terminus of the N-terminal construct. Recombinant CHC constructs were expressed in HEK293E cells. HEK293E cells from a 1 l suspension culture were pelleted by centrifugation and resuspended in 0.5 M Tris-HCl, pH 7.5 containing protease inhibitor (Roche), lysed by repeated freeze-thawing and further homogenized in a Potter-Elvehjem homogenizer. Nuclei, organelles and large protein complexes were removed by sequential centrifugation steps at 1000 g for 20 min, 20,000 g for 20 min, and finally 200,000 g for 1.5h. Protein constructs were purified from the resulting supernatant by Ni^{2+}-affinity chromatography (Ni Sepharose FF, GE Healthcare Europe GmbH, Diegem, Belgium). Efficient elution from the Ni Sepharose column was achieved using 25 mM Tris-HCl (pH 8.5), 500 mM NaCl, 500 mM imidazole for C-terminal, and 25 mM Tris-HCl (pH 7.5), 100 mM EDTA

for N-terminal clathrin protein constructs. Eluted proteins were subsequently subjected to gel-filtration (Superdex 200 pg 16/600; GE Healthcare) and concentrated in microinjection buffer (120 mM KCl, 20 mM HEPES-KOH, pH 6.9; adjusted from [11]) using Vivaspin tubes with a 10 kDa molecular weight cut-off (GE Healthcare). The yields of N- and C-terminal CHC constructs were ~1 mg/ml protein in 2 and 0.8 ml of microinjection buffer, respectively. GFP (Superglo GFP; Qbiogene, Montreal, Canada) was dialyzed in the same microinjection buffer and used as negative control. Supplemental figure 1 shows control GFP and purified N- and C-terminal clathrin protein constructs separated by SDS-PAGE on a 10 % polyacrylamide gel stained with coomassie.

Oocyte isolation, selection, microinjection and culture

All chemicals were purchased from Sigma Chemical Co. (St. Louis, MO, USA), unless otherwise indicated. Cumulus-oocyte complexes (COCs) were collected by aspiration from 3-6 mm follicles from sow (Sus scrofa) ovaries, which were acquired from a slaughterhouse. The collected COCs were allowed to settle and washed several times in a buffer containing 114 mM NaCl, 3.2 mM KCl, 2 mM $NaHCO_3$, 0.4 mM $NaH_2PO_4 \bullet H_2O$, 0.25 mM sodium pyruvate, 10 mM sodium lactate, 0.5 mM $MgCl_2 \bullet 6H_2O$, 2 mM $CaCl_2 \bullet 2H_2O$, 10 mM HEPES, 0.1% (w/v) polyvinylpyrrolidone (PVP), 1 mM dibutyryl cAMP (dbcAMP), pH 7.4. Oocytes were maintained in prophase arrest during collection and microinjection by the presence of dbcAMP. Prior to injection, oocytes were partially denuded by gentle pipetting until 3-6 layers of cumulus remained, and washed in HEPES-buffered M199 from Gibco BRL (Grand Island, NY, USA) supplemented with 1 mM dbcAMP. For injection, groups of 5 oocytes were placed in 5 µl drops of this medium under oil at 37°C on an IX71 inverted microscope (Olympus, the Netherlands) equipped with a heated stage. A suction pipette was used to immobilize oocytes and beveled rigid borosilicate micropipettes with a 30° angle and a 3.5 µm tip diameter (custom tips; Eppendorf, Hamburg, Germany) were used to perform injections. Injection solutions were centrifuged for 10 min at 16,000 g just prior to use and ~1 µl was backloaded into the micropipettes, which were subsequently connected to a Femtojet pressure injection system (Eppendorf). Immediately after injection, total GFP fluorescence was evaluated at 100x magnification using a fluorescence microscope equipped with a FITC filter and a DP20 camera (Olympus) using 100 ms exposure. Any oocytes showing much higher or lower fluorescence intensity than average (typically 20-30% of injected oocytes) were immediately removed from the experiment (see for example Fig. 2B). In

vitro maturation was performed as described previously [12].

Immunofluorescence and imaging

COCs were washed and denuded by gentle pipetting in 80 mM PIPES, 5 mM EGTA, 2 mM $MgCl_2$, 0.3% (w/v) PVP, pH 6.9 at 37°C, and then fixed in the same buffer containing 4% (v/v) paraformaldehyde (Electron Microscopy Sciences, Hatfield, PA, USA) at room temperature for 1 h. After fixation, oocytes were washed twice in 0.1 M phosphate buffer (pH 7.4) containing 0.3% (w/v) PVP, and permeabilized in 0.1 M phosphate buffer supplemented with 0.1% (w/v) saponin (Riedel de Haen AG, Seelze, Germany). Permeabilized oocytes were blocked in 0.1 M phosphate buffer containing 0.1% (w/v) saponin, 1% (w/v) BSA and 2% (v/v) normal goat serum (Vector Lab, Burlingame, CA, USA) supplemented with 100 mM glycine for 2 h at RT. After this blocking step, oocytes were subjected to sequential 1 h incubations with primary and secondary antibodies, which had been diluted in blocking solution without glycine and centrifuged at 100,000 g for 1 h before use. To label microtubules, a mixture of rabbit polyclonal antibodies directed against α-tubulin (1:400; Abcam, Cambridge, UK) and β-tubulin (1:400; Sigma) was used. Clathrin was labelled with CON.1, which is directed against a conserved region (AA 23-44) of CLC [13], and X22, which is directed against a conserved region (AA 1109-1128) near the C-terminus of CHC [14;15]. CON.1 and X22 were produced from hybridoma cultures in our lab (kindly provided by Dr. F.M. Brodsky). Irrelevant primary antibodies of the same isotype and at identical concentrations (Sigma) were used as negative controls. Secondary antibodies were goat anti-mouse IgG alexa488 and goat anti-rabbit IgG alexa568 (Molecular Probes, Eugene, OR, USA), and DNA was labeled for 20 min with 10 μM TO-PRO-3 iodide (Molecular Probes). Each labeling step was followed by three washes in 0.1 M phosphate buffer supplemented with 0.1% (w/v) saponin. Finally, oocytes were sealed in Vectashield (Vector Lab) on Superfrost Plus microscope slides (Menzel, Braunschweig, Germany) in 0.12 mm Secure-Seal Spacers (Molecular Probes).

Confocal images were obtained using a Nikon eclipse TE300 microscope (Nikon Corp., Tokyo, Japan) equipped with a 40x oil immersion objective (N.A. 1.3) and a BioRad Radiance 2100MP confocal system (Zeiss/Bio-Rad, Hertfordshire, UK). Multichannel images were recorded by sequential excitation using 488, 543, and 637 nm lasers. Images were acquired using settings adjusted for submaximal confocal settings (at least 50% of extracellular pixel values below threshold value and 0.1 – 0.5% of pixel values inside the

oocyte above maximal pixel value), and analyzed using ImageJ (NIH; http://rsb.info.nih.gov/ij/). Submaximal confocal settings were also used to measure spindle recruitment since variations in spindle location and orientation cause large differences in diffraction due to the large size and high lipid content of oocytes. GFP fluorescence intensity on meiotic spindles was determined relative to cortical regions. Images shown are maximum intensity Z-projections of 6 consecutive confocal sections (unless otherwise indicated) taken at 2 μm intervals and subjected to limited contrast/brightness enhancements up to ~20%. Control images were produced with the highest settings and enhancements used to create images of specific antibody stainings from the same experiment. Supplemental movies were produced using ImageJ and the VolumeJ plugin [16] as described in the supplemental data.

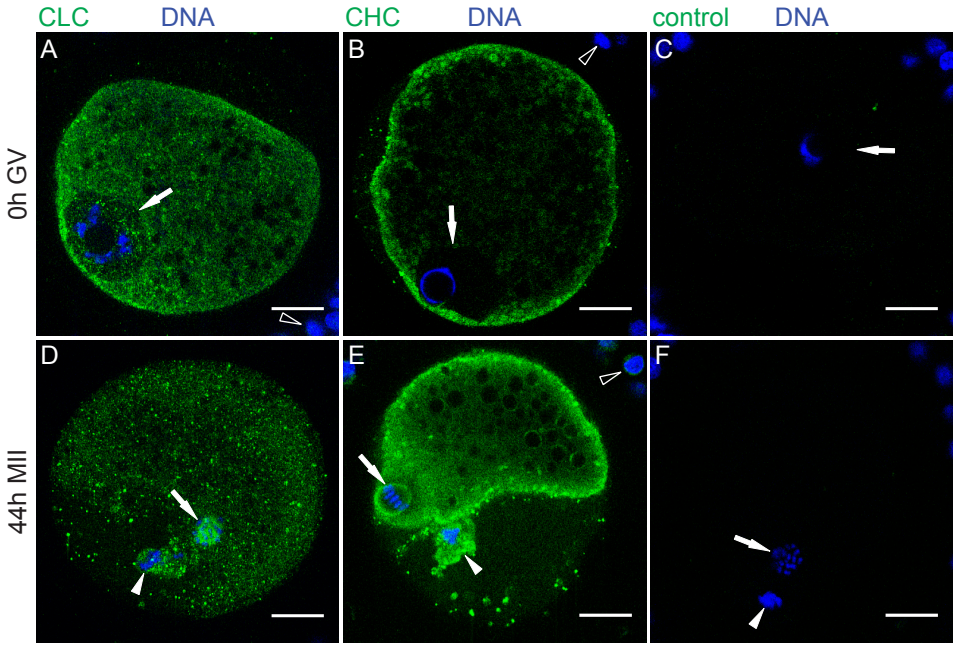

Figure 1 – Distribution of endogenous clathrin during oocyte maturation
(A,B) 0 h GV stage oocytes labeled for DNA (blue) and CLC (A; green), CHC (B; green), or irrelevant control antibody (C; green). Arrows indicate the GV. (D,E) 44 h MII stage oocytes labeled for DNA (blue) and CLC (D; green), CHC (E; green), or irrelevant control antibody (F; green). Arrows and arrowheads indicate the MII spindle and the polar body respectively. Open arrowheads indicate cumulus cells in all images. Scale bars, 20 μm.

Statistical analysis

The ratio of oocytes at each aberrant stage versus oocytes at the reference stage (normal MII) shown in figure 5 was compared between NIC/N-CHC-GFP/GFP-C-CHC and GFP conditions using multinomial logistic regression models. Several models were employed to investigate the interaction between maturation stage, which was used as an ordinal variable, and condition. Based on a minimized Akaike information criterion (AIC) value, a model that incorporated both N-CHC-GFP and GFP-C-CHC conditions and their respective controls, and used experiment number to control for random effects was chosen for final analysis. Student's t-tests and chi-square tests were performed in Microsoft Excel and multinomial regression was performed in the R environment [17] using the "lmer" function of the lme4 package [18]. P values were considered significant at $P < 0.05$ (Bonferroni corrected). Mean percentages and SEM were weighted by the number of oocytes in each experiment.

Results

Distribution of endogenous clathrin during oocyte maturation

To investigate the distribution of endogenous clathrin, porcine oocytes were fixed either directly after isolation or after 44 h of in vitro maturation, immuno-labeled for either light chain or heavy chain clathrin, and analyzed using confocal laser scanning microscopy. Freshly isolated oocytes were exclusively at the GV stage, whereas 44 h matured oocytes accumulated at the MII stage. In both immature GV and MII stage oocytes, CLC and CHC were found diffusely throughout the cytoplasm but also in association with punctate structures that were predominantly observed at the oocyte cortex, possibly corresponding to clathrin coated vesicles (Fig. 1). In MII stage oocytes, both CLC and CHC were also observed on the metaphase spindle and in the polar body (Fig. 1D,E). Control oocytes in which the primary antibodies were replaced with identical concentrations of negative control mouse IgG showed only a few scattered puncta at the same confocal settings (Fig. 1C,F), demonstrating the specificity of clathrin labeling. Notably, the staining intensity of CLC and CHC was considerably higher in oocytes than in the surrounding cumulus cells, both at the onset of maturation (Fig. 1A,B) and at MII arrest (Fig. 1D,E).

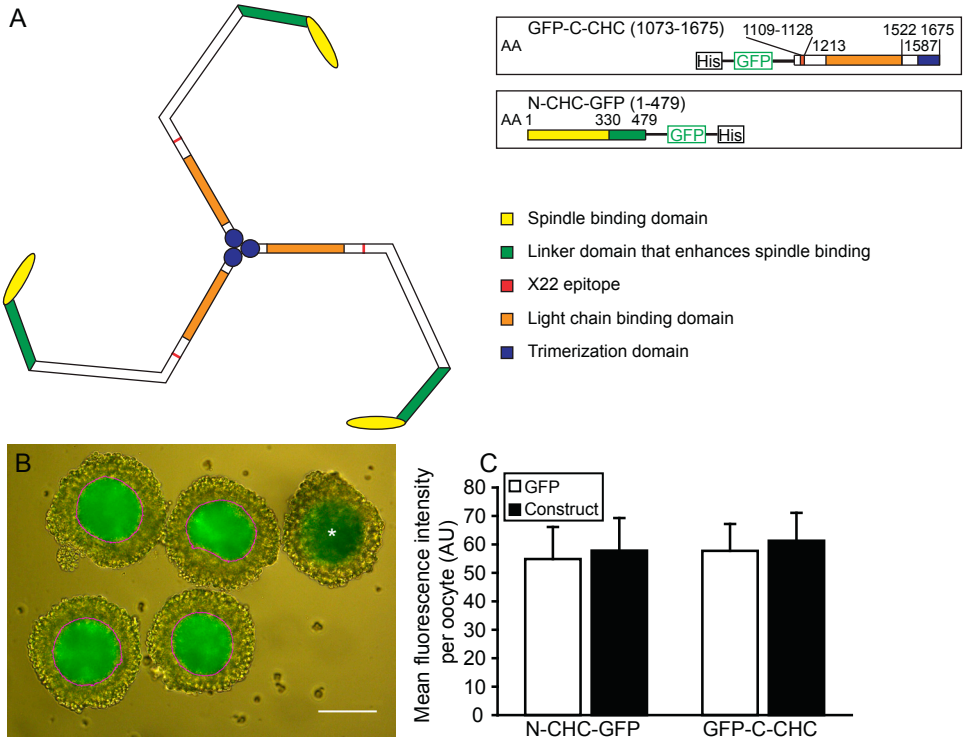

Figure 2 – Clathrin constructs

*(A) Schematic overview of the CHC constructs. The color-coded domains on the constructs are indicated in identical colors on the clathrin triskelion shown on the left and the location of the GFP-tag on each of the constructs is shown on the right. (B) Merged brightfield and fluorescent images showing five oocytes injected with GFP-C-CHC. As an example, the oocyte marked with * was removed from the experiment based on its relatively low fluorescence intensity. A region of interest (ROI; shown in magenta) was drawn around the remaining four oocytes by thresholding the fluorescent image (the same threshold was used for all injection experiments in this study). (C) Bar graph showing measured total fluorescence within threshold-generated ROIs for injected oocytes. Bars represent mean fluorescence intensity ± SD in arbitrary units (AU) of 45-63 oocytes from three independent experiments. No significant difference was found between oocytes injected with N-CHC-GFP (P = 0.24) or GFP-C-CHC (P = 0.09) and GFP-injected oocytes from the same experiments using a two-tailed homoscedastic Student's t-test.*

Clathrin constructs

To elucidate the role of clathrin during oocyte maturation, dominant negative GFP tagged truncated CHC protein constructs were generated using transfected HEK293E cells and isolated to homogeneity (see materials and methods section and Fig 2A). The C-terminal construct (GFP-C-CHC)

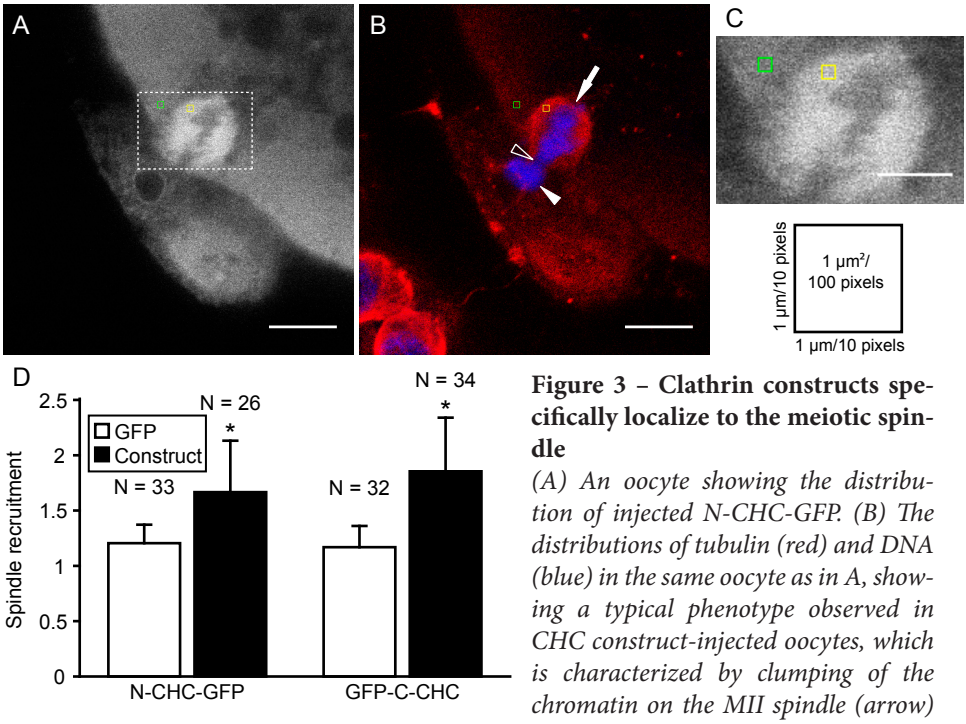

Figure 3 – Clathrin constructs specifically localize to the meiotic spindle

(A) An oocyte showing the distribution of injected N-CHC-GFP. (B) The distributions of tubulin (red) and DNA (blue) in the same oocyte as in A, showing a typical phenotype observed in CHC construct-injected oocytes, which is characterized by clumping of the chromatin on the MII spindle (arrow) and an extruded polar body (arrowhead) that remained attached to the spindle via a "DNA bridge" (open arrowhead). Scale bars, 20 µm. (C) Enlargement of the area indicated by the dashed rectangle in A. Scale bar, 5 µm. A schematic representation indicating the size of the regions of interest (ROIs) on the spindle (yellow square) and in the cortex (green square) is shown below the image. Spindle recruitment was calculated by dividing the mean GFP fluorescence intensity on the spindle by that in the cortex. For each oocyte two ROIs on the spindle (one on each side of the metaphase plate) and two ROIs in the cortex were analyzed for GFP fluorescence intensity to calculate spindle recruitment. To ensure objective measurements each spindle/cortex-pair of ROIs was created within a single confocal section showing only tubulin and DNA staining (as in B) and transposed onto the equivalent section showing GFP fluorescence (as in A). (D) Bar chart showing spindle recruitment in oocytes injected with control GFP or CHC constructs. Bars represent mean spindle recruitment ± SD from three independent experiments and the number of oocytes measured is shown above each bar. Both N-CHC-GFP ($P < 0.001$) and GFP-C-CHC ($P < 0.001$) revealed significantly higher recruitment to MII spindles (asterisks) compared to GFP in injected oocytes using a two-tailed heteroscedastic Student's t-test.

contains the CHC trimerization domain, the CLC binding domain, and GFP- and His-tags at its N-terminus. A similar construct was previously shown to trimerize with endogenous clathrin and inhibit clathrin-mediated endocytosis in HeLa cells [19]. The N-terminal construct (N-CHC-GFP) encompasses

a domain that was previously demonstrated to interfere with clathrin-mediated endocytosis and associate with mitotic spindles in somatic cells [4], and contains GFP- and His-tags at its C-terminus. We also tried to produce GFP tagged full length CHC. Unfortunately these constructs were not stably expressed by our producer cell line. Any way, GFP-tagged full length CHC cannot be expected to act as a negative control, given that bulky tags at either the N- or C-terminus will also interfere with the function of full length clathrin (Fig 2A). Instead, non-conjugated GFP was used as a negative control.

Isolated constructs were then microinjected into immature oocytes. To control for the amount injected, total GFP fluorescence in oocytes was measured by epifluorescence microscopy [20] directly after injection (Fig. 2B). Of the successfully injected oocytes, total fluorescence did not differ significantly between oocytes injected with GFP or either CHC construct (Fig. 2C). After injection, oocytes were matured for 44 h, fixed, immunolabeled for tubulin, and stained for DNA to determine the location of the metaphase spindle and the polar body (Fig. 3A). Consistent with the distribution of endogenous clathrin, both N-CHC-GFP and GFP-C-CHC were found to accumulate at the meiotic spindle and at the cortex (Fig. 3A,B). To quantify the recruitment of CHC constructs to the meiotic spindles [4], we determined relative GFP fluorescence intensities in representative areas on the spindle and at the oocyte cortex (Fig. 3C). Both N-CHC-GFP and GFP-C-CHC were significantly enriched on the spindle in comparison to non-conjugated GFP (Fig. 3D).

Figure 4 – Aberrant meiotic profiles generated in response to clathrin constructs
Oocytes were injected with GFP or GFP-CHC constructs (left column and green in the merged fourth column), matured for 44 h, fixed, and labeled for the presence of tubulin (second column and red in the merged fourth column) and DNA (third column and blue in the merged fourth column). (A-D) Control GFP-injected oocyte showing a normal MII spindle and polar body. (E-L) Examples of N-CHC-GFP-injected oocytes, showing patchy condensation of chromosomes on the MII spindle and a "DNA bridge" (open arrowheads) between the spindle and the polar body, which varied from long and thin (E-H) to short and thick (I-L). (M-T') Examples of GFP-C-CHC injected oocytes. Some of these oocytes showed a phenotype similar to (M-P). We also observed oocytes that displayed scattered chromosomes and satellite spindles, which were markedly distinct from N-CHC-GFP-injected oocytes (Q-T'). Open arrowheads indicate a long and thin DNA bridge (M-P) or the position of satellite spindles (Q-T'). Images shown in Q-T and Q'-T' are from the same oocyte and are composed of a total of 12 (2 x 6) consecutive confocal sections. Filled arrows and arrowheads indicate the position of the MII spindle and polar body, respectively. Scale bars, 10 μm.

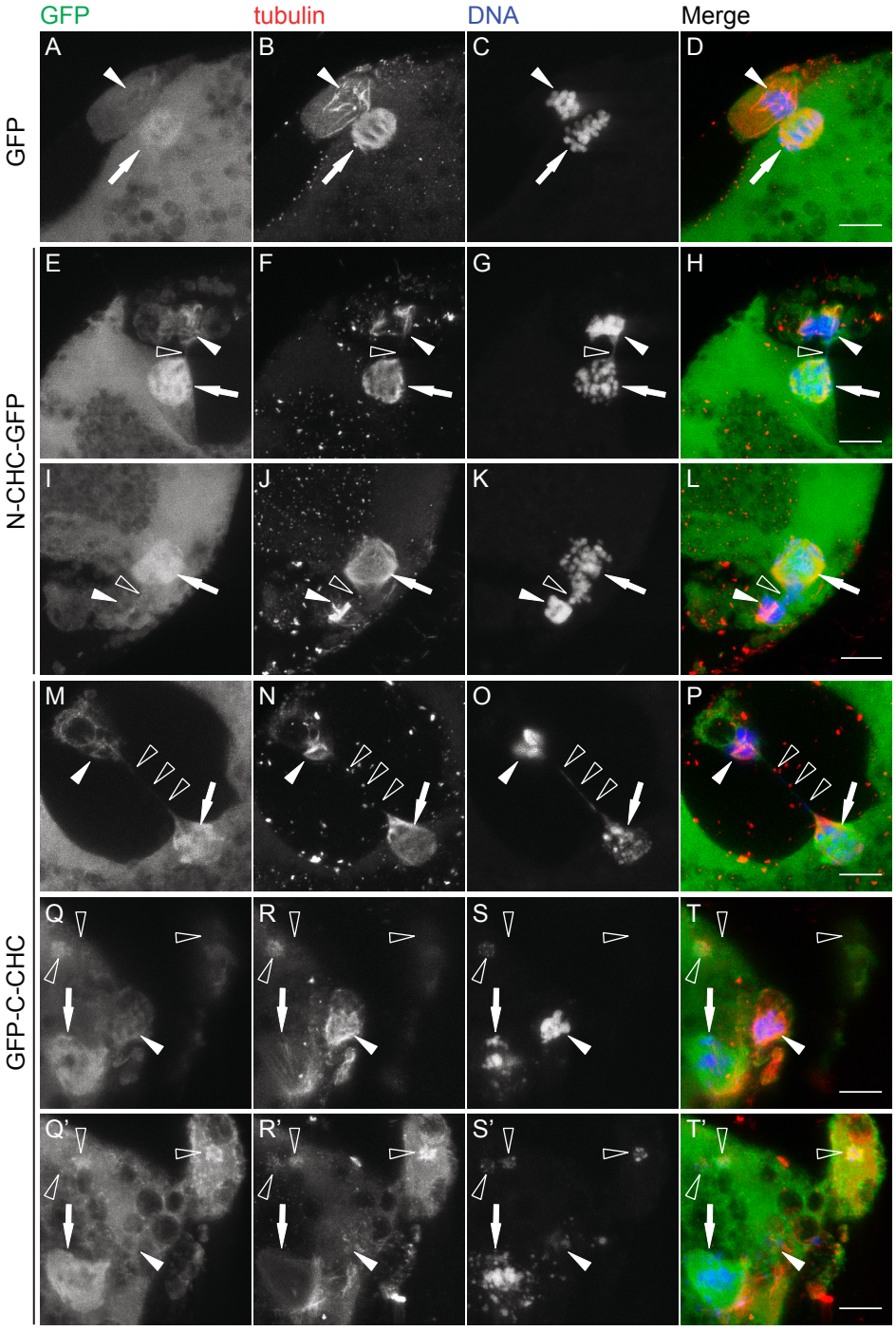
GFP
tubulin
DNA
Merge
GFP
N-CHC-GFP
GFP-C-CHC
A
B
C
D
E
F
G
H
I
J
K
L
M
N
O
P
Q
R
S
T
Q'
R'
S'
T'

Clathrin constructs disrupt meiotic divisions in oocytes

We next investigated the effects of injected N-CHC-GFP and GFP-C-CHC on oocyte maturation. A normal MII pattern was observed in the majority of oocytes that were injected with non-conjugated GFP (Figs. 4A-D and 5A,B). Severe defects were observed, however, in both N-CHC-GFP- and GFP-C-CHC-injected oocytes. Both CHC constructs caused misalignment of chromosomes on the metaphase plate and formation of large clumps of condensed chromatin interspersed with patches of less condensed chromatin (Fig. 4E-T'). In addition, chromosomes were regularly observed outside the metaphase spindle (e.g. Fig. 4I-L), and the polar body often remained con-

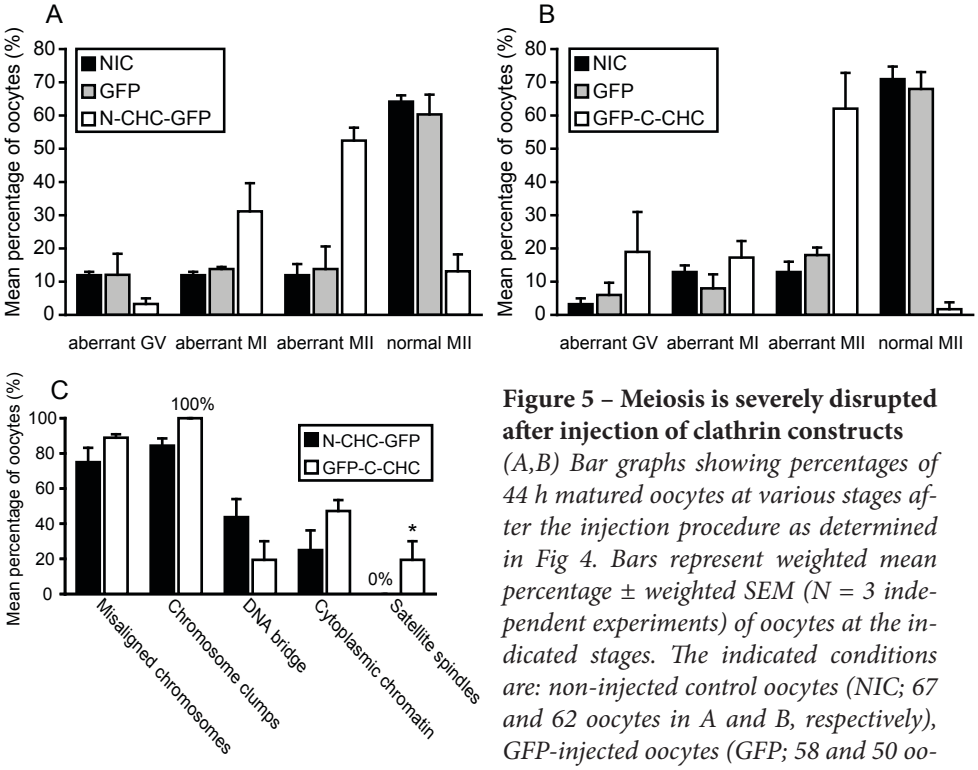

Figure 5 – Meiosis is severely disrupted after injection of clathrin constructs
(A,B) Bar graphs showing percentages of 44 h matured oocytes at various stages after the injection procedure as determined in Fig 4. Bars represent weighted mean percentage ± weighted SEM (N = 3 independent experiments) of oocytes at the indicated stages. The indicated conditions are: non-injected control oocytes (NIC; 67 and 62 oocytes in A and B, respectively), GFP-injected oocytes (GFP; 58 and 50 oocytes in A and B, respectively), N-CHC-GFP-injected oocytes (N-CHC-GFP; A; 61 oocytes), and GFP-C-CHC-injected oocytes (GFP-C-CHC; B; 58 oocytes). Significance of the results is indicated in the results section. (C) Oocytes that were scored as aberrant MII in (A) and (B) displayed the specified defects. The data were analyzed by chi-square tests and the asterisk indicates a significant difference at $P < 0.05$ (Bonferroni corrected).

nected to the oocyte via a "DNA bridge" (open arrowheads) that varied in thickness and length (long and thin in E-H and M-P, and short and thick in I-L). These bridges displayed labeling for GFP, but not for tubulin, indicating that the spindle midbody was no longer present. These phenotypes are illustrated more clearly in supplemental movies S1-S4, which show 360º rotations of 3D reconstructions of the same oocytes as shown in figure 4A-H. In a subset of GFP-C-CHC-injected oocytes, condensed chromosomes were scattered throughout the area around the metaphase spindle (Fig. 4Q-T'). These scattered chromosomes formed small clusters that also contained tubulin (open arrowheads in fig. 4Q-T') creating small spindle-like structures, which we refer to as "satellite spindles". In this example, one of these satellite spindles was observed in an additional polar body that was almost completely extruded from the oocyte (Fig. 4Q'-T', top right), suggesting that satellite spindles had at least some of the functionality of normal meiotic spindles.

To quantify the effects of the CHC constructs on oocyte maturation, 44 h matured oocytes were scored into four categories based on their tubulin and DNA staining patterns: aberrant GV (clearly visible nucleus), aberrant MI (meiosis I; includes oocytes from prometaphase I up to and including telophase I), aberrant MII (clearly visible metaphase spindle and polar body, showing abnormal structure), and normal MII (clearly visible metaphase spindle and polar body). Oocytes that showed a normal GV or MI pattern after maturation were also scored as aberrant, since these oocytes lacked competence to complete maturation. Oocytes that could not be scored into any of these categories (~ 4%) were excluded from analysis. Of the non-injected and GFP-injected oocytes, 60-70% showed normal morphology at MII (Fig. 5A,B). In contrast, of the N-CHC-GFP- and GFP-C-CHC-injected oocytes only 13% and 2% respectively reached normal MII, while most revealed an aberrant MII morphology. Statistical analysis of these data shows that oocytes injected with N-CHC-GFP or GFP-C-CHC were significantly inhibited in progressing through maturation as compared to GFP-injected oocytes. In both N-CHC-GFP and GFP-C-CHC conditions, the strongest significant effect was found for the comparison of their ratio of aberrant versus normal MII oocytes with that in the control group. The ratio of aberrant MI versus normal MII oocytes was, however, also significantly higher for both CHC constructs. Only GFP-C-CHC-injected oocytes differed significantly in comparison to the control group in the ratio of aberrant GV versus normal MII phenotypes.

To specify MII aberrancies further, we scored aberrant MII oocytes by phenotype using the following categories: misaligned chromosomes (chro-

matin outside the equator of the MII spindle), chromosome clumps (large clumps of condensed chromatin interspersed with patches of less condensed chromatin), DNA bridge (direct link between chromatin in the polar body and the oocyte), cytoplasmic chromatin (loose chromosomes present in the cytoplasm, including satellite spindles), and satellite spindles (clumps of chromosomes near the MII spindle that contain tubulin, thus forming spindle-like structures). Almost all oocytes injected with either one of the CHC constructs showed misaligned chromosomes and chromosome clumps. A DNA bridge was observed more frequently in N-CHC-GFP as compared to GFP-C-CHC injected oocytes, while the frequency of occurrence of cytoplasmic chromatin was higher in GFP-C-CHC compared to N-CHC-GFP injected oocytes. Finally, satellite spindles were observed in ~20% of GFP-C-CHC-injected oocytes, whereas this defect was not observed in N-CHC-GFP injected oocytes. Statistical analysis of these results using chi-square tests only showed a significant difference between N-CHC-GFP- and GFP-C-CHC-injected oocytes for the occurrence of satellite spindles (Fig. 5C). We conclude that clathrin plays a crucial role in both MI and MII and is required for proper chromosome segregation in maturing oocytes.

Discussion

In this study, we have demonstrated that clathrin is associated with meiotic spindles in porcine oocytes and that interference with clathrin function by injection of dominant negative CHC protein constructs disrupted meiosis progression. Moreover, we provide compelling evidence supporting involvement of clathrin in chromosome segregation during oocyte meiosis.

Clathrin is a cytosolic protein that was recently shown to stabilize the mitotic spindle in somatic cells [4;5]. The present study was undertaken to assess whether clathrin is of similar importance in the meiotic divisions of porcine oocytes. Consistent with previous observations for mouse MII oocytes [9], we demonstrate by immunofluorescence microscopy that both heavy and light chain components of CHC are associated with metaphase spindles in porcine oocytes (Fig. 1). The initial observations by Maro et al. [9] were thought to reflect association of clathrin-coated vesicles with spindle fibers. In somatic cells however, clathrin was shown to bind the mitotic spindle directly, while membranes did not associate with the spindle [4;5]. Using lipophylic dyes, we also could not detect association of any membranes with the meiotic spindle in oocytes (data not shown).

Unlike somatic cells, fully grown mammalian oocytes are characterized by repressed transcription [21-25], and oocytes thus cannot be manipulated by cDNA transfection. Given the ubiquitous and crucial functions of clathrin, clathrin knock-out animals have not been generated and conditional knock-out systems for oocytes are not available. Although exogenous proteins can be expressed by injection of mRNA in porcine oocytes, the efficiency of this injection procedure is low (~30% of injected oocytes show expression during maturation) and expression levels vary extensively between oocytes [26]. The method used here to microinject dominant-negative clathrin protein constructs was highly efficient (~75% of injected oocytes showed sustained fluorescence), and allowed instantaneous introduction of a reproducible amount of exogenous protein into each oocyte (Fig. 2). Microinjected GFP-tagged constructs, corresponding to the N- or C-terminal domains of CHC (Fig. 2), were both recruited to MII spindles (Fig. 3). N-CHC-GFP, which contains the previously determined spindle binding domain [4], was recruited to the meiotic spindle to the same extent as GFP-C-CHC (Fig. 3). These observations suggest that both constructs contain spindle recruitment domains, although it cannot be excluded that our constructs have been recruited to the spindle by endogenous full length CHC that may have been incorporated in 'mixed' triskelions. A recent study showed that formation of a complex, which consists of clathrin, B-Myb, and filamin, is required for recruitment of clathrin to the mitotic spindle in somatic cells, and the authors suggested that the C-terminal trimerization domain of clathrin could also be involved in the formation of this complex [10]. In another study, the N-terminal domain appeared to be indispensable for spindle localization, since a construct lacking this domain (331-1639) failed to be recruited to mitotic spindles [5]. It should be noted that these results were obtained in somatic cells that had been depleted of endogenous clathrin by RNAi, and as such did not allow formation of mixed triskelions containing both endogenous CHC and the truncated CHC construct. Unfortunately, application of RNAi knockdown of endogenous clathrin in oocytes is highly unlikely to succeed, since even in highly active mitotic cells CHC RNAi does not show an effect on the mitotic index until 48 h after transfection [4] and clathrin is known to have a very long half-life [27].

Oocytes injected with either one of our CHC constructs displayed severe defects in MII morphology (Figs. 4 and 5) while maturation rates and MII morphology of GFP-injected control oocytes did not differ from those of non-injected controls (Figs. 4A-D and 5A,B). Both CHC constructs caused misalignment of chromosomes and formation of chromosome clumps, which

could be explained by CHC construct-induced failure of the spindle checkpoint during meiosis I. When some homologous chromosomes separate normally and others remain attached to each other and are pulled either into the nascent polar body or into the oocyte, chromosome clumps would form on the second metaphase spindle. Moreover, the aberrant presence of homologous chromosome pairs on the second metaphase spindle may disrupt proper chromosome alignment. The relatively high percentage of oocytes that failed to complete the first metaphase (Fig. 5A,B) may thus represent oocytes in which chromosome alignment was not properly achieved. Although these inferences remain speculative, it is clear that future research on clathrin function in meiotic spindles should include investigation of checkpoint controls, particularly since clathrin adaptor proteins have been implicated in spindle function and checkpoint control in mitotic cells [28;29].

Aside from the commonly induced misaligned chromosomes and chromosome clumps, we also found several marked differences between the effects of GFP-C-CHC and N-CHC-GFP. In response to GFP-C-CHC, condensed chromatin was frequently observed in the cytoplasm, forming satellite spindles in some oocytes (Figs. 4M-T' and 5C), indicating that the capture and alignment of chromosomes by spindle fibers was disrupted. In contrast, N-CHC-GFP predominantly caused failure of polar body extrusion, although cytoplasmic chromatin was also observed in some of these oocytes (Fig. 4E-L and 5C). N-CHC-GFP lacks the trimerization domain (Fig. 2A) and triskelion formation is essential for clathrin-mediated stabilization of metaphase spindles in somatic cells [5], suggesting that N-CHC-GFP disrupts spindle function by competing with binding of endogenous clathrin to the spindle.

Clathrin-mediated endocytosis may also be affected by these CHC constructs. A possible effect of inhibition of endocytosis is failure of polar body cytokinesis, since it has been demonstrated that endocytosis at the cleavage furrow is important for cytokinesis in several types of mitotic cells [30-35]. We cannot exclude that endocytosis is also important for cytokinesis in oocytes. However, we observed that respectively 44% and 19% of N-CHC-GFP- or GFP-C-CHC-injected oocytes remained connected to their polar body via a DNA bridge (Figs. 4E-P and 5C), demonstrating that chromosome segregation is incomplete in these oocytes. These cytoplasmic connections between oocytes and their polar bodies did not contain tubulin, suggesting that the spindle midbody, which may be involved in abscission during cytokinesis [36], is no longer present. These results indicate destabilization of the first meiotic spindle, and since cytokinesis is normally preceded by chromosome

segregation, we conclude that interference with endocytosis dependent cytokinesis cannot explain our results.

Studies on Xenopus oocytes [37;38] have indicated that meiosis resumption involves endocytosis of a G protein coupled receptor. The G protein coupled receptor GPR3 appears to be required for maintenance of meiotic arrest in mouse, rat, and human oocytes [39-42], suggesting that endocytosis of this receptor may also be involved in resumption of oocyte meiosis in mammals. Since clathrin is required for endocytosis of specific receptors in somatic cells [6;8;43], these findings suggest an alternative role for clathrin in resumption of meiosis. Constructs similar to our CHC constructs have been demonstrated to interfere with membrane traffic in somatic cells [4;19]. In our study, however, meiosis progression beyond GVBD was not affected in the majority of CHC construct-injected oocytes (Fig. 5A,B). Therefore, inhibition of G protein coupled receptor endocytosis cannot explain our results.

Taken together, our findings in porcine oocytes are consistent with a role for clathrin in stabilizing metaphase spindles [4;5]. Disruption of clathrin function in maturing oocytes causes severe spindle-related defects, which may be due to spindle checkpoint failure and/or spindle destabilization during meiosis I. Although we have established that clathrin plays a pivotal role in meiosis progression during porcine oocyte maturation, further research will be required to untangle the contributions of its functions to meiotic spindle stability.

References

[1] Mehlmann LM. Stops and starts in mammalian oocytes: recent advances in understanding the regulation of meiotic arrest and oocyte maturation. Reproduction 2005; 130: 791-799.

[2] Richard FJ. Regulation of meiotic maturation. J Anim Sci 2007; 85: E4-E6.

[3] Martin RH. Meiotic errors in human oogenesis and spermatogenesis. Reprod Biomed Online 2008; 16: 523-531.

[4] Royle SJ, Bright NA, Lagnado L. Clathrin is required for the function of the mitotic spindle. Nature 2005; 434: 1152-1157.

[5] Royle SJ, Lagnado L. Trimerisation is important for the function of clathrin at the mitotic spindle. J Cell Sci 2006; 119: 4071-4078.

[6] Kirchhausen T. Clathrin. Annu Rev Biochem 2000; 69: 699-727.

[7] Okamoto CT, McKinney J, Jeng YY. Clathrin in mitotic spindles. Am J

Physiol Cell Physiol 2000; 279: C369-C374.
[8] Ungewickell EJ, Hinrichsen L. Endocytosis: clathrin-mediated membrane budding. Curr Opin Cell Biol 2007; 19: 417-425.
[9] Maro B, Johnson MH, Pickering SJ, Louvard D. Changes in the distribution of membranous organelles during mouse early development. J Embryol Exp Morphol 1985; 90: 287-309.
[10] Yamauchi T, Ishidao T, Nomura T, Shinagawa T, Tanaka Y, Yonemura S, Ishii S. A B-Myb complex containing clathrin and filamin is required for mitotic spindle function. EMBO J 2008; 27: 1852-1862.
[11] Amano T, Mori T, Watanabe T. Activation and development of porcine oocytes matured in vitro following injection of inositol 1,4,5-trisphosphate. Anim Reprod Sci 2004; 80: 101-112.
[12] Hölzenspies JJ, Stoorvogel W, Colenbrander B, Roelen BA, Gutknecht DR, van Haeften T. CDC2/SPDY transiently associates with endoplasmic reticulum exit sites during oocyte maturation. BMC Dev Biol 2009; 9: 8.
[13] Nathke IS, Heuser J, Lupas A, Stock J, Turck CW, Brodsky FM. Folding and trimerization of clathrin subunits at the triskelion hub. Cell 1992; 68: 899-910.
[14] Brodsky FM. Clathrin structure characterized with monoclonal antibodies. I. Analysis of multiple antigenic sites. J Cell Biol 1985; 101: 2047-2054.
[15] Liu SH, Wong ML, Craik CS, Brodsky FM. Regulation of clathrin assembly and trimerization defined using recombinant triskelion hubs. Cell 1995; 83: 257-267.
[16] Abramoff MD, Viergever MA. Computation and visualization of three-dimensional soft tissue motion in the orbit. IEEE Trans Med Imaging 2002; 21: 296-304.
[17] R Development Core Team. R: a language and environment for statistical computing. R Foundation for Statistical Computing, Vienna, Austria. ISBN 3-900051-07-0. 2008. Available at: http://www.R-project.org.
[18] Bates D, Maechler M, Dai B. lme4: Linear mixed-effects models using S4 classes. R package version 0.999375-28. 2008. Available at: http://lme4.r-forge.r-project.org.
[19] Liu SH, Marks MS, Brodsky FM. A dominant-negative clathrin mutant differentially affects trafficking of molecules with distinct sorting motifs in the class II major histocompatibility complex (MHC) pathway. J Cell Biol 1998; 140: 1023-1037.

[20] Lee GM. Measurement of volume injected into individual cells by quantitative fluorescence microscopy. J Cell Sci 1989; 94(Pt 3): 443-447.
[21] Fair T, Hyttel P, Greve T, Boland M. Nucleus structure and transcriptional activity in relation to oocyte diameter in cattle. Mol Reprod Dev 1996; 43: 503-512.
[22] Bouniol-Baly C, Hamraoui L, Guibert J, Beaujean N, Szollosi MS, Debey P. Differential transcriptional activity associated with chromatin configuration in fully grown mouse germinal vesicle oocytes. Biol Reprod 1999; 60: 580-587.
[23] Motlik J, Kopecny V, Travnik P, Pivko J. RNA synthesis in pig follicular oocytes. Autoradiographic and cytochemical study. Biol Cell 1984; 50: 229-235.
[24] Bjerregaard B, Maddox-Hyttel P. Regulation of ribosomal RNA gene expression in porcine oocytes. Anim Reprod Sci 2004; 82-83: 605-616.
[25] De La Fuente R, Eppig JJ. Transcriptional activity of the mouse oocyte genome: companion granulosa cells modulate transcription and chromatin remodeling. Dev Biol 2001; 229: 224-236.
[26] Ohashi S, Naito K, Liu J, Sheng Y, Yamanouchi K, Tojo H. Expression of Exogenous Proteins in Porcine Maturing Oocytes after mRNA Injection: Kinetic Analysis and Oocyte Selection Using EGFP mRNA. The Journal of Reproduction and Development 2001; 47: 351-357.
[27] Acton SL, Brodsky FM. Predominance of clathrin light chain LCb correlates with the presence of a regulated secretory pathway. J Cell Biol 1990; 111: 1419-1426.
[28] Cayrol C, Cougoule C, Wright M. The beta2-adaptin clathrin adaptor interacts with the mitotic checkpoint kinase BubR1. Biochem Biophys Res Commun 2002; 298: 720-730.
[29] Lehtonen S, Shah M, Nielsen R, Iino N, Ryan JJ, Zhou H, Farquhar MG. The endocytic adaptor protein ARH associates with motor and centrosomal proteins and is involved in centrosome assembly and cytokinesis. Mol Biol Cell 2008; 19: 2949-2961.
[30] Niswonger ML, O'Halloran TJ. A novel role for clathrin in cytokinesis. Proc Natl Acad Sci U S A 1997; 94: 8575-8578.
[31] Albertson R, Riggs B, Sullivan W. Membrane traffic: a driving force in cytokinesis. Trends Cell Biol 2005; 15: 92-101.
[32] Feng B, Schwarz H, Jesuthasan S. Furrow-specific endocytosis during cytokinesis of zebrafish blastomeres. Exp Cell Res 2002; 279: 14-20.
[33] Schweitzer JK, Burke EE, Goodson HV, Souza-Schorey C. Endocytosis

resumes during late mitosis and is required for cytokinesis. J Biol Chem 2005; 280: 41628-41635.
[34] Warner AK, Keen JH, Wang YL. Dynamics of membrane clathrin-coated structures during cytokinesis. Traffic 2006; 7: 205-215.
[35] Montagnac G, Echard A, Chavrier P. Endocytic traffic in animal cell cytokinesis. Curr Opin Cell Biol 2008; 20: 454-461.
[36] Montagnac G, Chavrier P. Endosome positioning during cytokinesis. Biochem Soc Trans 2008; 36: 442-443.
[37] Wang J, Liu XJ. A G protein-coupled receptor kinase induces Xenopus oocyte maturation. J Biol Chem 2003; 278: 15809-15814.
[38] El-Jouni W, Haun S, Hodeify R, Hosein WA, Machaca K. Vesicular traffic at the cell membrane regulates oocyte meiotic arrest. Development 2007; 134: 3307-3315.
[39] Mehlmann LM, Saeki Y, Tanaka S, Brennan TJ, Evsikov AV, Pendola FL, Knowles BB, Eppig JJ, Jaffe LA. The Gs-linked receptor GPR3 maintains meiotic arrest in mammalian oocytes. Science 2004; 306: 1947-1950.
[40] Mehlmann LM. Oocyte-specific expression of Gpr3 is required for the maintenance of meiotic arrest in mouse oocytes. Dev Biol 2005; 288: 397-404.
[41] Hinckley M, Vaccari S, Horner K, Chen R, Conti M. The G-protein-coupled receptors GPR3 and GPR12 are involved in cAMP signaling and maintenance of meiotic arrest in rodent oocytes. Dev Biol 2005; 287: 249-261.
[42] DiLuigi A, Weitzman VN, Pace MC, Siano LJ, Maier D, Mehlmann LM. Meiotic arrest in human oocytes is maintained by a Gs signaling pathway. Biol Reprod 2008; 78: 667-672.
[43] Moore CA, Milano SK, Benovic JL. Regulation of receptor trafficking by GRKs and arrestins. Annu Rev Physiol 2007; 69: 451-482.

Supplemental Data

Supplemental figure 1 – SDS-PAGE analysis of clathrin constructs

Coomassie staining of a 10 % polyacrylamide gel loaded with GFP or purified protein constructs. Lanes: 1 = 1 µg GFP; 2 = 3 µg GFP; 3 = Marker; 4 = 1 µg N-CHC-GFP; 5 = 3 µg N-CHC-GFP; 6 = Marker; 7 = 1 µg GFP-C-CHC; 8 = 3 µg GFP-C-CHC. Analysis of GFP and both protein constructs shows a clear band at the predicted molecular weights of ~27 kDa for GFP, ~80 kDa for N-CHC-GFP, and ~97 kDa for GFP-C-CHC (arrow). Additional bands in the GFP-C-CHC lanes are degradation products. Lane numbers are shown at the top of each lane, molecular weight (MW) indicators are shown to the left of the gel, and loaded purified proteins are indicated at the bottom of each pair of lanes containing approximately 1 (left) or 3 µg (right) of protein.

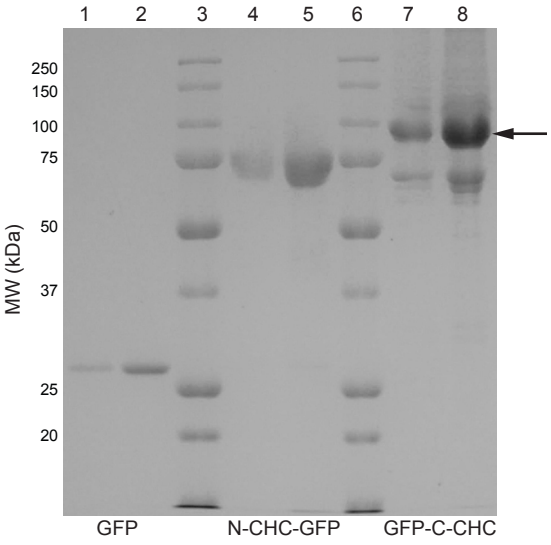

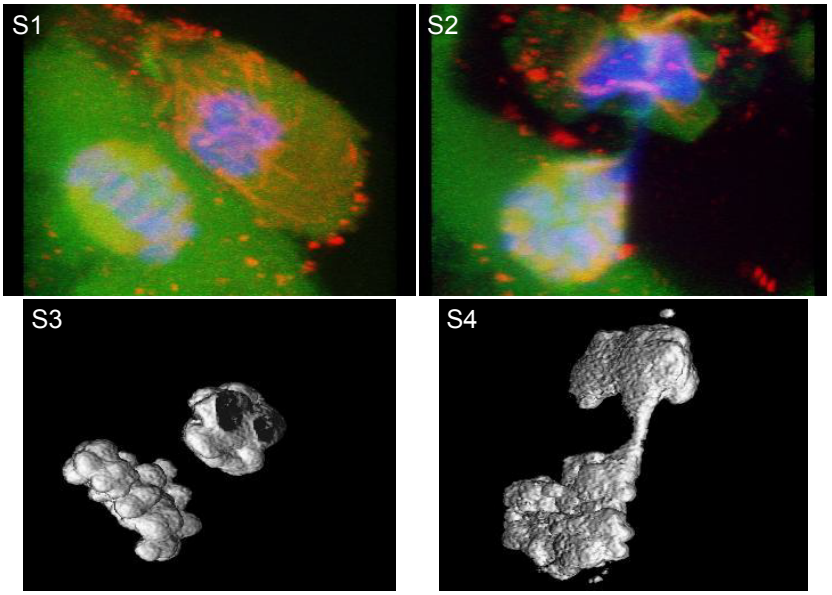

Supplemental Movie Stills

Stills of 360° rotational movies showing 3D reconstructions of stacks of ~50 confocal sections taken at 0.5 μm intervals of the same oocytes as shown in figure 4A-D and 4E-H. (S1-S2) The oocytes were injected with GFP (green in S1), or N-CHC-GFP (green in S2), subjected to 44 h of maturation, fixed, and labeled for tubulin (red) and DNA (blue). The oocyte injected with N-CHC-GFP shows chromosome clumps and a 'DNA bridge' (see results section for a description of these phenotypes). (S3-S4) To illustrate the concept of chromosome clumps and a DNA bridge more clearly, the DNA labeling of these oocytes was subjected to a smooth filter followed by isosurface rendering in the VolumeJ plugin. In the resulting 360° rotational movies, the GFP-injected oocyte shows clearly defined chromosomes, which are completely separated from the DNA in the polar body, on the metaphase plate (S3). The N-CHC-GFP-injected oocyte, however, shows variations in chromosome size and shape, and retains a connection with the polar body via a DNA bridge (S4). Movies were produced in ImageJ with identical enhancement, thresholding, and 3D reconstruction settings between stacks of images, which were recorded at identical confocal settings.

Chapter 5

General discussion:

Novel insights and future perspectives on oocyte maturation

Novel insights and future perspectives on oocyte maturation

Venturing beyond the superficial requires more detailed analysis

Mammalian oocyte maturation has traditionally been defined by extensive nuclear changes, but recent research has made it clear that in addition to this nuclear maturation process, cytoplasmic components are also drastically rearranged in a process known as cytoplasmic maturation [1-3]. Nuclear and cytoplasmic maturation are both essential for oocytes to obtain the competence to be fertilized and to undergo subsequent embryonic development. The term cytoplasmic maturation was coined when it was discovered that the overall distribution of cell organelles, cytoskeletal elements, and proteins changes dramatically as maturation progresses [1].

An important reason to investigate cytoplasmic maturation is to gain a better understanding of how cells become pluripotent, i.e. obtain the ability to differentiate into any cell type. After fertilization, the newly formed embryo undergoes several rounds of rapid cell divisions that eventually lead to the formation of a blastocyst. The blastocyst is composed of an inner cell mass, which will give rise to the embryo proper, adjacent to a fluid-filled cavity, the blastocoel, and surrounded by an outer layer of trophoblast cells that will develop into the embryonic part of the placenta. When the cells of the inner cell mass are isolated and cultured in vitro under the right conditions, these cells will self renew instead of differentiate and are then called embryonic stem cells. Embryonic stem cells are characterized by their capacity for unlimited self-renewal while maintaining their pluripotency and are thus prime candidates to combat degenerative diseases and repair damaged tissues [4;5]. Cloning experiments, in which the genomic DNA of the oocyte is replaced with a nucleus from a fully differentiated somatic cell, have shown that the cytoplasm of the oocyte is capable of reprogramming exogenous genetic material, producing an embryo with the same genomic DNA as the donor cell [5;6]. Despite the implications for regenerative medicine of patient-specific embryonic stem cells that can be produced in this manner, generation of human embryos for therapeutic purposes is riddled with ethical concerns [7]. Several recent studies have shown that it is indeed possible to reprogram differentiated cells to an undifferentiated state with stem cell-like properties by inducing expression of a limited number of transcription factors [8-10]. However, the efficiency of this reprogramming procedure is quite low and understand-

ing the underlying mechanisms by which the oocyte cytoplasm reprograms a differentiated nucleus may lead to the development of improved strategies of reprogramming cells to a pluripotent state without the ethical issues. Since cytoplasmic extracts from immature and mature oocytes have a differential ability to reprogram somatic cell nuclei [11], studies on cytoplasmic changes during oocyte maturation may contribute to unraveling the mechanisms whereby pluripotency is established.

During development, oocytes become exceptionally large by accumulating mRNA and protein in the cytoplasm. These cytoplasmic stores allow several 'cleavage divisions', which lack intermittent growth phases, to occur in quick succession after fertilization. The resulting rapid increase in cell number allows differentiation to occur within the early embryo, a process that is required for the embryo to implant in or become attached to the endometrium. Due to the size of oocytes, cytoplasmic changes have generally been investigated at low magnification to enable patterns to be observed throughout the oocyte. Several studies have indicated that oocytes contain specialized compartments in the cytoplasm [1;12;13], in which microenvironments with relatively high concentrations of enzymes and their targets can be maintained, thus allowing efficient catalysis of essential enzymatic reactions. This compartmentalization of oocytes prevents loss of storage space, since sustaining enzymatic reactions throughout the cytoplasm would require much larger amounts of the constituent proteins to be present. Oocyte maturation is a lengthy process that can take one or more days to complete and most studies focus on a few distinct time points to characterize the nuclear and cytoplasmic changes during maturation. As a result, potentially important processes that occur at a local level and within a limited time frame can be easily overlooked. Once a process of this kind is discovered, a further understanding is generally obtained using functional studies by analyzing the effects of manipulation of constituent components, such as signaling molecules or structural elements. Manipulating intracellular events in the oocyte, but not the surrounding cumulus, can be efficiently achieved using the microinjection method described in chapter 3.

It is clear that a more detailed spatial and temporal examination of structural and molecular events in maturing oocytes is warranted, yet analysis of these events becomes exceedingly difficult and time consuming with increased scrutiny. The work described in this thesis shows that these problems can at least in part be circumvented by limiting heterogeneity, using new ways of applying existing methodology (chapter 2), and development and applica-

tion of novel tools to manipulate and visualize the mechanics of oocyte maturation (chapter 3 and 4).

Heterogeneity of ovaries

This thesis deals with experimental research on oocytes isolated from sow ovaries that were obtained from a slaughterhouse. Biological material obtained from large numbers of animals is inherently heterogeneous due to variations in genetic composition, physiological condition, environmental factors, and age between individuals. Sophisticated statistical tools allow researchers to reach meaningful conclusions using such variable results. However, a general rule of thumb in the realm of statistics dictates that more data must be collected as the variability increases, and the heterogeneity of sow material is compounded by several factors beyond the control of the individual researcher. In this section several of these compounding factors are discussed.

Since pigs are mainly kept for meat production, the vast majority of slaughtered pigs are prepubertal gilts, as an optimum of quality and amount of meat produced versus cost is reached very early in life, generally before 6 months of age [14]. These animals are less than ideal for research on reproduction as in vivo fertility is not reached until puberty. Indeed, in vitro experiments using oocytes isolated from gilts and sows have shown that sow oocytes have significantly higher developmental potential [15]. Despite this major advantage of using sow instead of gilt oocytes for reproduction research, variability in the quality of slaughterhouse material can be a major problem. Although sows are often culled when their reproductive capacity is still fairly close to optimal, ovaries obtained from the slaughterhouse may also originate from relatively young sows with reproductive problems and relatively old sows that have been highly productive [16]. Unfortunately, these different groups cannot be distinguished by selection of ovaries in the laboratory, as ovarian morphology is not correlated with developmental competence of porcine oocytes [17]. Batches of sows that are taken to the slaughterhouse for culling are likely to originate from farms in the same area, thus introducing variation between batches in the type of feed, hormonal supplementation, or living conditions, which can all influence reproductive capacity [18;19]. The stability of average sow reproductive capacity is further compromised by seasonal variations [20].

Finally, variations in oocyte quality are introduced by fluctuations in temperature and time between slaughter and isolation of oocytes [21]. To

minimize the influence of these factors, batches of ovaries that reached a temperature below 26 ºC on arrival at the laboratory were discarded, and pickup of ovaries from the slaughterhouse was routinely timed to avoid rush hour traffic, yet variability between batches remained high. Therefore, experiments in which less than 60 % of oocytes in the control group had matured after 44 h of in vitro maturation were routinely excluded from analysis. Using this criterion, many batches had to be discarded, but variation was reduced considerably. Although this combination of measures ensured the viability of sow oocytes as a model system, batches of ovaries could only be obtained 2-3 times a week and the number of successful experiments that could be performed was thus rather limited. Nevertheless, the porcine oocyte has several exceptional characteristics, including a very long duration of maturation, in particular pre-germinal vesicle breakdown (GVBD) maturation, compared to other mammalian species, making it an ideal model to study temporally restricted events during oocyte maturation. In the studies presented in this thesis, the advantageous properties of the porcine model were maximally exploited, whereas experimental variation was kept to a minimum. Despite the multitude of obstacles discussed above, this work has produced several interesting novel insights into the inner workings of mammalian oocytes.

Local and temporal restrictions on cytoplasmic events

Mammalian oocytes mature spontaneously when removed from the inhibitory influence of the follicle and in most mammalian species GVBD occurs within hours after maturation is initiated. Although GVBD is generally used as a morphological marker for the onset of oocyte maturation, initiation of maturation is followed by distinct chromatin configuration changes that precede GVBD [22;23]. Since nuclear and cytoplasmic maturation are intricately interwoven processes, pre-GVBD cytoplasmic changes may accompany the chromatin configuration changes in the GV. Pigs are an ideal animal model to study the possibility of pre-GVBD cytoplasmic events during oocyte maturation, as porcine oocytes are maintained at the GV stage for approximately 22 hours when cultured in vitro [24]. The investigation into the distribution of CDC2 in combination with numerous organelle markers presented in chapter 2 demonstrates that reorganization of cell organelles and redistribution of essential (regulators of) protein kinases is involved in pre-GVBD maturation. The observed transient accumulation of CDC2 at endoplasmic reticulum exit sites (ERES), which were exclusively found within a single cluster in the cortex,

presumably functions to shut down vesicle transport at ERES during meiosis in oocytes as it does at the G2/M phase transition in mitotic cells [25].

In an attempt to confirm this hypothesis, several pilot experiments were conducted in which oocytes were incubated with inhibitors of CDC2 activity (purvalanol A) and intracellular vesicle transport (brefeldin A and H89). Inhibition of CDC2 activity using inhibitors that have a comparable or lower specificity than purvalanol A [26-28], is known to reversibly prevent meiosis resumption in porcine oocytes [29;30]. However, meiosis was not fully blocked in the presence of 1 μM purvalanol A (data not shown). Due to aspecificity of the inhibitor, higher concentrations could affect other potentially relevant kinases as well [26] and this avenue of investigation was therefore abandoned pending development of more specific methods of CDC2 inhibition. Brefeldin A (BFA) and high concentrations of H89 inhibit COPI- and COPII-mediated intracellular vesicle transport, respectively [31;32]. In somatic cells, BFA reversibly inhibits vesicle fusion at Golgi stacks and thereby causes redistribution of most Golgi proteins into the ER [33]. Golgi matrix proteins, including GM130, on the other hand, redistribute into small Golgi remnants that associate with ERES in response to BFA treatment [34;35]. Reversible BFA-induced Golgi collapse has also been observed in mouse oocytes [36] and BFA treatment of porcine oocytes could thus provide important insights into regulation of the secretory system during maturation. H89 is mainly known for selective inhibition of PKA [37]. Since the activity of PKA maintains prophase I arrest in oocytes [38-40], incubation with high concentrations of H89 was not expected to affect the progression of oocyte maturation, allowing the use of high concentrations to inhibit COPII-mediated membrane trafficking [32]. CDC2 causes disassembly of ERES in somatic cells [25] and premature cessation of vesiculation at ERES by treatment with H89 could affect CDC2 localization by removing its target proteins. These preliminary experiments using BFA and H89 focused on the protein that most frequently coincided with the cortical ERES cluster, CDC2, since the high frequency of P-GM130 association with ERES reported in chapter 2 had not been uncovered yet. Both BFA (20 μg/ml) and H89 (100 μM) did not affect the localization of CDC2 during short incubations (up to 1 h), whereas longer incubations (> 22 h) caused degeneration of almost all oocytes (data not shown).

Although manipulation of vesicle transport in oocytes did not affect CDC2 association with ERES, a different approach will likely prove more fruitful. First and foremost, the distribution of the transmembrane protein P-GM130 provides a better readout for these studies, since disassembly of ERES

is accompanied by redistribution of transmembrane proteins into the reticular ER [25] and P-GM130 associated with ERES much more frequently than CDC2 (see chapter 2 Fig. 5). In addition, BFA and H89 could produce unexpected side effects, such as the recently discovered disruption of asymmetric spindle positioning by BFA in mouse oocytes [41]. Therefore, although BFA and H89 can be very useful in determining whether secretion plays a role in oocyte maturation, a detailed understanding will require more specific methods of interference. One possible method of highly specific and direct interference with vesicle transport between ER and Golgi is provided by the microinjection technique described in chapter 3, which could be used to introduce exogenous mutant proteins into oocytes, such as mutant Sar1 to block ER export, or mutant Arf1 to block Golgi to ER vesicle transport [35].

The findings presented in chapter 2 have revealed that accumulation of organelles and highly dynamic compartmentalization of regulatory proteins within cytoplasmic subdomains constitute an integral part of oocyte maturation. Regulation of cellular processes at a local level may therefore play a much more prominent role in oocyte maturation than was previously thought.

Clathrin-mediated stabilization of metaphase spindles in oocytes

The meiotic divisions that prepare the mammalian oocyte for fertilization and ensure diversity in the genetic endowment of offspring are governed by a complex network of regulatory mechanisms. Since these mechanisms are not fail-safe, errors in oocyte meiosis are not uncommon and the mis-segregation of chromosomes that often ensues can lead to formation of an aneuploid embryo after fertilization. Although most forms of aneuploidy are embryonic lethal, some aneuploid embryos are carried to term, at which point the aneuploidy is manifested as severe physical and/or mental disorders in humans [42]. A major cause of aneuploidy is mis-segregation of chromosomes resulting from failure of the spindle checkpoint, a process that prevents the onset of anaphase when chromosome alignment on the metaphase plate is incomplete and is regulated by kinetochore-associated proteins [43]. Interference with the function of clathrin, a cytoplasmic protein that stabilizes the kinetochore fibers in metaphase spindles, was recently shown to cause mis-segregation of chromosomes in mitotic cells [44]. Although a role for clathrin in stabilization of meiotic spindles in oocytes has not been established, these findings suggest that clathrin could also be important to prevent chromosome mis-segregation in maturing oocytes.

An efficient way of investigating a role for clathrin in somatic cells has been to manipulate clathrin function by introducing dominant negative clathrin constructs [44;45]. With the continued development of novel tools to interfere with intracellular processes in somatic cells, microinjection has become the favored method to apply these tools to the manipulation of oocytes without affecting the surrounding support cells. However, current microinjection protocols often lack a means of selecting for successful injection, post-injection viability, and matched final concentrations of injected substances between oocytes. These selection methods could reduce the variability of results from microinjection experiments and thus increase their power. A novel microinjection protocol that employs these selection methods is introduced in chapter 3. This protocol was then applied to investigate the involvement of clathrin in progression through the meiotic cell cycle in porcine oocytes as described in chapter 4. Clathrin was found to associate with metaphase spindles and interference with clathrin function at the spindle using injection of dominant negative clathrin heavy chain (CLTC) protein constructs caused severe spindle-related defects in oocytes. These constructs constituted the N- or C-terminal domain of CLTC coupled to GFP and are respectively referred to as N-CLTC-GFP and GFP-C-CLTC. Overexpression of an N-terminal CLTC construct similar to N-CLTC-GFP in somatic cells caused a significant reduction in transferrin uptake, but showed no effect on the mitotic index of these cells [44], suggesting that this construct does not interfere with clathrin function at the mitotic spindle. These contradictory findings are difficult to interpret, but may reflect differences in the ratio of dominant negative CLTC constructs and endogenous CLTC and/or in the regulation of spindle stability between oocytes and mitotic cells.

The C-terminal domain of CLTC has been implicated in clathrin recruitment to mitotic spindles [46]. However, somatic cells expressing a construct that constituted either full length CLTC (1-1675) or CLTC lacking several C-terminal residues (1-1639) and represent two different isoforms of CLTC showed an identical level of spindle recruitment [47]. These cells had been depleted of endogenous clathrin using CLTC RNAi, and both isoforms contained the spindle binding domain, suggesting that equal levels of spindle recruitment could have resulted from a lack of competition for binding sites at the spindle. Consequently, these data do not prove that the C-terminal 46 AA of CLTC is not involved in spindle recruitment, and it is possible that these CLTC isoforms provide cells with separate clathrin populations performing separate functions. This interpretation will have to remain in the realm of

speculation however, until such time as a role for the C-terminal domain in spindle recruitment of clathrin can be either confirmed or disproven. Nevertheless, if the C-terminal domain is indeed required for spindle recruitment, this would produce counterintuitive effects in the experimental system described in chapter 4. If N-CLTC-GFP and GFP-C-CLTC are equally capable of disrupting clathrin function at the spindle, spindle recruitment of endogenous clathrin, but not N-CLTC-GFP, would reduce the availability of binding sites at the spindle. N-CLTC-GFP would therefore have a less pronounced effect on spindle stability than GFP-C-CLTC, which could explain the differences in observed phenotypes between these constructs.

Elucidating the precise role of clathrin and functionality of its domains will require further research, but this thesis has provided a solid backbone for further experimentation. Aside from using the same techniques to examine the effects of the many other clathrin constructs that have been described previously [44;45;47], future research using inhibitors of clathrin-mediated membrane trafficking could be used to completely separate spindle-related and membrane-related roles of clathrin during oocyte maturation.

References

[1] Brevini TA, Cillo F, Antonini S, Gandolfi F. Cytoplasmic remodelling and the acquisition of developmental competence in pig oocytes. Anim Reprod Sci 2006; 98: 23-38.

[2] Ferreira EM, Vireque AA, Adona PR, Meirelles FV, Ferriani RA, Navarro PA. Cytoplasmic maturation of bovine oocytes: Structural and biochemical modifications and acquisition of developmental competence. Theriogenology 2009; 71: 836-848.

[3] Inoue A, Nakajima R, Nagata M, Aoki F. Contribution of the oocyte nucleus and cytoplasm to the determination of meiotic and developmental competence in mice. Hum Reprod 2008; 23: 1377-1384.

[4] Thomson JA, Itskovitz-Eldor J, Shapiro SS, Waknitz MA, Swiergiel JJ, Marshall VS, Jones JM. Embryonic stem cell lines derived from human blastocysts. Science 1998; 282: 1145-1147.

[5] Hochedlinger K, Jaenisch R. Nuclear reprogramming and pluripotency. Nature 2006; 441: 1061-1067.

[6] Campbell KH, McWhir J, Ritchie WA, Wilmut I. Sheep cloned by nuclear transfer from a cultured cell line. Nature 1996; 380: 64-66.

[7] de WG, Mummery C. Human embryonic stem cells: research, ethics

and policy. Hum Reprod 2003; 18: 672-682.
[8] Takahashi K, Yamanaka S. Induction of pluripotent stem cells from mouse embryonic and adult fibroblast cultures by defined factors. Cell 2006; 126: 663-676.
[9] Wernig M, Meissner A, Foreman R, Brambrink T, Ku M, Hochedlinger K, Bernstein BE, Jaenisch R. In vitro reprogramming of fibroblasts into a pluripotent ES-cell-like state. Nature 2007; 448: 318-324.
[10] Okita K, Ichisaka T, Yamanaka S. Generation of germline-competent induced pluripotent stem cells. Nature 2007; 448: 313-317.
[11] Miyamoto K, Tsukiyama T, Yang Y, Li N, Minami N, Yamada M, Imai H. Cell-Free Extracts from Mammalian Oocytes Partially Induce Nuclear Reprogramming in Somatic Cells. Biol Reprod 2009.
[12] Beckhelling C, Chang P, Chevalier S, Ford C, Houliston E. Pre-M phase-promoting factor associates with annulate lamellae in Xenopus oocytes and egg extracts. Mol Biol Cell 2003; 14: 1125-1137.
[13] Miller DS, Horowitz SB. Intracellular compartmentalization of adenosine triphosphate. J Biol Chem 1986; 261: 13911-13915.
[14] Bee G, Calderini M, Biolley C, Guex G, Herzog W, Lindemann MD. Changes in the histochemical properties and meat quality traits of porcine muscles during the growing-finishing period as affected by feed restriction, slaughter age, or slaughter weight. J Anim Sci 2007; 85: 1030-1045.
[15] Hyun SH, Lee GS, Kim DY, Kim HS, Lee SH, Kim S, Lee ES, Lim JM, Kang SK, Lee BC, Hwang WS. Effect of maturation media and oocytes derived from sows or gilts on the development of cloned pig embryos. Theriogenology 2003; 59: 1641-1649.
[16] Le Cozler Y, Dagorn J, Lindberg JE, Aumaître A, Dourmad JY. Effect of age at first farrowing and herd management on long-term productivity of sows. Livestock Production Science 1998; 53: 135-142.
[17] Bagg MA, Vassena R, Papasso-Brambilla E, Grupen CG, Armstrong DT, Gandolfi F. Changes in ovarian, follicular, and oocyte morphology immediately after the onset of puberty are not accompanied by an increase in oocyte developmental competence in the pig. Theriogenology 2004; 62: 1003-1011.
[18] Foxcroft GR, Vinsky MD, Paradis F, Tse WY, Town SC, Putman CT, Dyck MK, Dixon WT. Macroenvironment effects on oocytes and embryos in swine. Theriogenology 2007; 68 Suppl 1: S30-S39.
[19] Hulten F, Wallenbeck A, Rydhmer L. Ovarian activity and oestrous signs

among group-housed, lactating sows: influence of behaviour, environment and production. Reprod Domest Anim 2006; 41: 448-454.
[20] Peltoniemi OA, Virolainen JV. Seasonality of reproduction in gilts and sows. Soc Reprod Fertil Suppl 2006; 62: 205-218.
[21] Hunter MG. Oocyte maturation and ovum quality in pigs. Reviews of Reproduction 2000; 5: 122-130.
[22] De La Fuente R. Chromatin modifications in the germinal vesicle (GV) of mammalian oocytes. Dev Biol 2006; 292: 1-12.
[23] Tan JH, Wang HL, Sun XS, Liu Y, Sui HS, Zhang J. Chromatin configurations in the germinal vesicle of mammalian oocytes. Mol Hum Reprod 2009; 15: 1-9.
[24] Schoevers EJ, Kidson A, Verheijden JH, Bevers MM. Effect of follicle-stimulating hormone on nuclear and cytoplasmic maturation of sow oocytes in vitro. Theriogenology 2003; 59: 2017-2028.
[25] Kano F, Tanaka AR, Yamauchi S, Kondo H, Murata M. Cdc2 kinase-dependent disassembly of endoplasmic reticulum (ER) exit sites inhibits ER-to-Golgi vesicular transport during mitosis. Mol Biol Cell 2004; 15: 4289-4298.
[26] Gray NS, Wodicka L, Thunnissen AM, Norman TC, Kwon S, Espinoza FH, Morgan DO, Barnes G, LeClerc S, Meijer L, Kim SH, Lockhart DJ, Schultz PG. Exploiting chemical libraries, structure, and genomics in the search for kinase inhibitors. Science 1998; 281: 533-538.
[27] Meijer L, Borgne A, Mulner O, Chong JP, Blow JJ, Inagaki N, Inagaki M, Delcros JG, Moulinoux JP. Biochemical and cellular effects of roscovitine, a potent and selective inhibitor of the cyclin-dependent kinases cdc2, cdk2 and cdk5. Eur J Biochem 1997; 243: 527-536.
[28] Kitagawa M, Okabe T, Ogino H, Matsumoto H, Suzuki-Takahashi I, Kokubo T, Higashi H, Saitoh S, Taya Y, Yasuda H, . Butyrolactone I, a selective inhibitor of cdk2 and cdc2 kinase. Oncogene 1993; 8: 2425-2432.
[29] Schoevers EJ, Bevers MM, Roelen BA, Colenbrander B. Nuclear and cytoplasmic maturation of sow oocytes are not synchronized by specific meiotic inhibition with roscovitine during in vitro maturation. Theriogenology 2005; 63: 1111-1130.
[30] Weng YC, Sha SW, Chiou CM, Tang PC, Yang JH, Ju JC. Butyrolactone I reversibly alters nuclear configuration, periooplasmic microtubules and development of porcine oocytes. Theriogenology 2007; 67: 509-519.
[31] Puri S, Linstedt AD. Capacity of the golgi apparatus for biogenesis from

the endoplasmic reticulum. Mol Biol Cell 2003; 14: 5011-5018.
[32] Lee TH, Linstedt AD. Potential role for protein kinases in regulation of bidirectional endoplasmic reticulum-to-Golgi transport revealed by protein kinase inhibitor H89. Mol Biol Cell 2000; 11: 2577-2590.
[33] Klausner RD, Donaldson JG, Lippincott-Schwartz J. Brefeldin A: insights into the control of membrane traffic and organelle structure. J Cell Biol 1992; 116: 1071-1080.
[34] Seemann J, Jokitalo E, Pypaert M, Warren G. Matrix proteins can generate the higher order architecture of the Golgi apparatus. Nature 2000; 407: 1022-1026.
[35] Ward TH, Polishchuk RS, Caplan S, Hirschberg K, Lippincott-Schwartz J. Maintenance of Golgi structure and function depends on the integrity of ER export. J Cell Biol 2001; 155: 557-570.
[36] Moreno RD, Schatten G, Ramalho-Santos J. Golgi apparatus dynamics during mouse oocyte in vitro maturation: effect of the membrane trafficking inhibitor brefeldin A. Biol Reprod 2002; 66: 1259-1266.
[37] Lochner A, Moolman JA. The many faces of H89: a review. Cardiovasc Drug Rev 2006; 24: 261-274.
[38] Kim JS, Cho YS, Song BS, Wee G, Park JS, Choo YK, Yu K, Lee KK, Han YM, Koo DB. Exogenous dibutyryl cAMP affects meiotic maturation via protein kinase A activation; it stimulates further embryonic development including blastocyst quality in pigs. Theriogenology 2008; 69: 290-301.
[39] Pirino G, Wescott MP, Donovan PJ. Protein kinase A regulates resumption of meiosis by phosphorylation of Cdc25B in mammalian oocytes. Cell Cycle 2009; 8: 665-670.
[40] Mehlmann LM. Stops and starts in mammalian oocytes: recent advances in understanding the regulation of meiotic arrest and oocyte maturation. Reproduction 2005; 130: 791-799.
[41] Wang L, Wang ZB, Zhang X, FitzHarris G, Baltz JM, Sun QY, Liu XJ. Brefeldin A disrupts asymmetric spindle positioning in mouse oocytes. Dev Biol 2008; 313: 155-166.
[42] Martin RH. Meiotic errors in human oogenesis and spermatogenesis. Reprod Biomed Online 2008; 16: 523-531.
[43] Steuerwald N. Meiotic spindle checkpoints for assessment of aneuploid oocytes. Cytogenet Genome Res 2005; 111: 256-259.
[44] Royle SJ, Bright NA, Lagnado L. Clathrin is required for the function of the mitotic spindle. Nature 2005; 434: 1152-1157.

[45] Liu SH, Marks MS, Brodsky FM. A dominant-negative clathrin mutant differentially affects trafficking of molecules with distinct sorting motifs in the class II major histocompatibility complex (MHC) pathway. J Cell Biol 1998; 140: 1023-1037.
[46] Yamauchi T, Ishidao T, Nomura T, Shinagawa T, Tanaka Y, Yonemura S, Ishii S. A B-Myb complex containing clathrin and filamin is required for mitotic spindle function. EMBO J 2008; 27: 1852-1862.
[47] Royle SJ, Lagnado L. Trimerisation is important for the function of clathrin at the mitotic spindle. J Cell Sci 2006; 119: 4071-4078.

Dutch Summary

Nederlandse Samenvatting

Hoofdstuk 1

Gedurende de embryonale ontwikkeling van vrouwelijke zoogdieren ontstaan in de ovaria (eierstokken) grote aantallen eicellen (oocyten), waarvan een gedeelte degenereert tijdens de foetale en postnatale ontwikkeling van het dier. Het overgebleven deel wordt rond de geboorte geïncorporeerd in zogenaamde primordiale follikels. De primordiale follikel bestaat uit een eicel in het profase stadium van de eerste meiotische deling die omgeven is door één enkele laag afgeplatte somatische cellen, de follikelepitheelcellen. Gedurende zowel de oestrische als menstruele cyclus worden diverse follikels onder invloed van hormonen gerekruteerd voor verdere ontwikkeling en groei. Nadat een follikel gerekruteerd is veranderen de follikelepitheelcellen in granulosacellen die kubisch van vorm zijn en zich actief vermenigvuldigen. Uiteindelijk resulteert deze groei en ontwikkeling in één (mens, koe) of meerdere (varken, muis) follikel(s) in het preovulatoire stadium. Deze pre-ovulatoire follikels bestaan uit een sterk in volume toegenomen eicel, omgeven door meerdere lagen cumuluscellen. Deze cumuluscellen zijn gemodificeerde granulosacellen die via 'gap junctions' in direct contact staan met de eicel. Het cumulus-eicel complex bevindt zich in een holte met follikelvloeistof, met daar omheen een wand van 'murale' granulosacellen.

De eicel in een pre-ovulatoire follikel is in staat de meiose te hervatten na een adequate hormonale stimulus, of zodra de eicel uit de follikel wordt verwijderd en in kweek wordt gebracht. Het daaropvolgende maturatieproces gaat gepaard met progressie van de meiotische celcyclus van profase I tot metafase II (nucleaire maturatie) en met veranderingen in de expressie en lokalisatie van cytoplasmatische eiwitten en structurele componenten van celorganellen (cytoplasmatische maturatie), zoals het Golgiapparaat en het endoplasmatisch reticulum (ER). Voortgang van de eicelmaturatie is sterk afhankelijk van de opeenvolgende activiteiten van verschillende celcyclus regulerende eiwitten. Een belangrijke celcyclus-regulerend eiwit is CDC2 (cell division cycle 2), een kinase die centraal staat in de regulatie van zowel de mitotische als de meiotische celcyclus. Tijdens de meiose is CDC2 onder meer betrokken bij de regulatie van membraantransport. Of CDC2 ook een dergelijke functie vervult tijdens de maturatie van eicellen is onbekend.

De meiotische deling van eicellen is asymmetrisch en heeft ondermeer als doel om opgeslagen eiwitten en mRNA voor de eicel te behouden door

overtollig genetisch materiaal in een relatief zeer kleine dochtercel, het poollichaampje, af te scheiden. Deze reductiedeling tijdens de meiose zorgt ervoor dat de eicel bij de bevruchting slechts één kopie van ieder chromosoom bevat, zodat de ontstane haploïde eicel kan worden bevrucht met een haploïde spermacel om een diploïde zygote te vormen. Deling van cellen is afhankelijk van correcte vorming van de spoelfiguur, een structuur bestaande uit spoeldraden die chromosomen binden en vervolgens verplaatsen naar het evenaarsvlak van de spoelfiguur. Recentelijk is ontdekt dat clathrine, een eiwit dat een belangrijke rol speelt in membraantransport, tijdens de mitotische celdeling de spoelfiguur stabiliseert. Een dergelijke functie voor clathrine tijdens de asymmetrische meiotische delingen van de eicel is momenteel nog niet aangetoond.

Hoofdstuk 2

De kinase CDC2 is belangrijk voor een optimaal verloop van diverse belangrijke processen tijdens de eicelmaturatie. CDC2-activiteit wordt gedeeltelijk gereguleerd door veranderingen in de subcellulaire distributie van CDC2. Hoewel we weten dat CDC2 betrokken is bij de initiatie van eicelmaturatie, is de lokalisatie van CDC2 aan het begin van de maturatie tot nog toe niet in detail onderzocht. In hoofdstuk 2 is de distributie van CDC2 en twee van zijn regulatoire eiwitten, cycline B en 'speedy' (SPDY), tijdens de eerste fase van de maturatie van varkenseicellen onderzocht. Om deze veranderingen in distributie te kunnen relateren aan veranderingen in hun specifieke functie is ook de lokalisatie van diverse celorganellen.bestudeerd. De resultaten van deze studie laten zien dat CDC2 zich gedurende korte tijd associeert met subdomeinen van het ER, die gespecialiseerd zijn in membraantransport en daarom ook wel 'ER exit sites' (ERES) genoemd worden. Deze ERES zorgen ervoor dat eiwitten, geproduceerd in het ER, naar het Golgi apparaat vervoerd worden waar ze in de juiste configuratie gevouwen worden om hun functie te kunnen vervullen. In eicellen bleken deze ERES te clusteren in een structuur in de cortex. Remming van eicelmaturatie met behulp van forskolinbehandeling verhinderde de verplaatsing van CDC2 naar deze geclusterde ERES. Gefosforyleerd GM130 (P-GM130), een eiwit dat in somatische cellen in gefragmenteerde Golgi gevonden wordt, werd in eicellen vrijwel exclusief in ERES aangetroffen. De lokalisatie van P-GM130 bleef onveranderd na forskolinbehandeling van eicellen. Na wegwassen van forskolin uit het maturatiemedium bleek de tijdelijke associatie van CDC2 met ERES samen te vallen met een tijdelijke

dispersie van P-GM130 in het ER, waardoor een mogelijke rol voor CDC2 in redistributie van Golgicomponenten van ERES naar het ER aannemelijk wordt. Van de CDC2-regulerende eiwitten bleek SPDY, in plaats van het meer bekende cycline B, te co-lokaliseren met CDC2 bij ERES. Deze observatie suggereert dat het CDC2/SPDY complex betrokken is bij de regulatie van secretie in maturerende eicellen.

Hoofdstuk 3

Zoogdiereicellen zijn moeilijk te manipuleren op moleculair niveau door hun lage transcriptionele activiteit en door de aanwezigheid van grote hoeveelheden in het cytoplasma opgeslagen mRNA en eiwit. Ondanks de ontwikkeling van microinjectietechnieken om intracellulaire processen in eicellen te kunnen manipuleren, is het succes van de injectie, de uiteindelijke concentratie in de eicel van geïnjecteerde stoffen en de levensvatbaarheid van eicellen na injectie moeilijk te beoordelen met de momenteel beschikbare technieken. Om deze experimentele beperkingen te overkomen wordt in hoofdstuk 3 een nieuwe methode beschreven, waarmee fluorescerende stoffen door middel van een hoge-druk injectiesysteem in de eicel worden gebracht en het succes van injectie met behulp van epifluorescentie microscopie eenvoudig en betrouwbaar kan worden vastgesteld. Gedurende de validatie bleek deze methode effectief in de succesvolle manipulatie van eicellen door injectie van reproduceerbare concentraties van stoffen, zonder dat dit resulteerde in negatieve effecten op de eicelmaturatie. Daarnaast bleek deze methode ook zeer geschikt om de snelheid, waarmee kleine moleculen zich door 'gap junctions' tussen de eicel en de daaraan grenzende cumuluscellen kunnen verplaatsen, te bepalen.

Hoofdstuk 4

Gedurende de maturatie ondergaat de eicel de eerste meiotische deling en vorming van de tweede metafase spoelfiguur. Clathrine is een groot cytosolisch eiwit dat betrokken is bij membraantransport. Recentelijk is een mogelijke andere belangrijke functie van clathrine tijdens de mitotische deling beschreven. Gedurende de mitose is membraantransport geremd en bindt clathrine de tubuline-spoeldraden die verbonden zijn aan kinetochoren van de chromosomen, waardoor stabilisatie van de spoelfiguur optreedt. Echter, of clathrine ook een vergelijkbare functie vervult tijdens de meiotische de-

lingen is niet bekend. Met behulp van de in hoofdstuk 3 beschreven microinjectietechniek zijn C- en N-terminale delen van clathrine, gemarkeerd met 'green fluorescent protein' (GFP), ingebracht in ongematureerde eicellen om de effecten van deze eiwitconstructen op de maturatie te bestuderen. Beide eiwitconstructen bleken op een vergelijkbare wijze als endogeen clathrine te associëren met de meiotische spoelfiguren. Injectie van deze constructen veroorzaakte opvallende defecten gedurende de eicelmaturatie, waaronder mislukte uitlijning van de chromosomen, klompvorming van chromatine op de metafase plaat, vorming van satelliet spoelfiguren en incomplete uitscheiding van het poollichaampje. Deze resultaten laten zien dat clathrine een cruciale rol speelt in de functie van de spoelfiguur in maturerende eicellen. Ondanks deze interessante bevinding is verder onderzoek noodzakelijk om de details van het functioneren van clathrine tijdens de meisose te analyseren.

Hoofdstuk 5

De nucleaire en cytoplasmatische veranderingen tijdens eicelmaturatie zijn essentieel voor zoogdiereicellen om competentie voor fertilisatie en vroeg embryonale ontwikkeling te verkrijgen. Onderzoek aan deze processen draagt bij aan begrip van het ontstaan van pluripotentie, een eigenschap van cellen waardoor deze zich kunnen differentiëren tot vrijwel ieder celtype. Uit kloneringsexperimenten, waarin het genomisch DNA van de eicel wordt vervangen door de kern van een volledig gedifferentieerde somatische cel, is gebleken dat het cytoplasma van de eicel in staat is om het genetisch materiaal uit somatische cellen te herprogrammeren tot een ongedifferentieerde staat. Een dergelijke eicel kan zich in kweek ontwikkelen tot een embryo in het blastocyststadium, waaruit vervolgens pluripotente embryonale stamcellen geïsoleerd kunnen worden. Dergelijke donorspecifieke embryonale stamcellen kunnen vervolgens zonder gevaar voor afstoting worden ingezet om beschadigde weefsels te repareren. Het gebruik van deze techniek voor therapeutische doeleinden brengt echter een scala aan ethische problemen met zich mee. Recentelijk is aangetoond dat gedifferentieerde cellen door inductie van expressie van enkele transcriptiefactoren, stamcelachtige eigenschappen kunnen gaan vertonen. Aangezien de efficiëntie van deze procedure erg laag is, kan een beter begrip van de mechanismen, waarmee het cytoplasma van de eicel het genomisch DNA uit een somatische cel herprogrammeert, leiden tot verbetering van de technieken om gedifferentieerde cellen pluripotent te maken. Deze techniek heeft grote potentie in de opwekking van donorspecifieke

pluripotente cellen, omdat de ethische overwegingen van kloneringsexperimenten hierbij niet van toepassing zijn.

Om veranderingen in cytoplasmatische processen die zich vaak op lokaal niveau in eicellen afspelen, te bestuderen is een gedetailleerde analyse absoluut noodzakelijk.. Door de enorme omvang van eicellen relatief tot somatische cellen en de lange duur van de eicelmaturatie wordt echter vaak alleen op lage vergroting en slechts op enkele tijdstippen van de maturatie naar dergelijke processen gekeken. Dit heeft als gevolg dat potentieel belangrijke processen, die van korte duur zijn of zich op een zeer lokaal niveau afspelen, eenvoudig over het hoofd gezien kunnen worden. Detectie van deze details wordt nog verder bemoeilijkt door de inherente heterogeniteit van varkenseicellen verkregen uit slachthuismateriaal, die voornamelijk wordt veroorzaakt door individuele verschillen in genetische samenstelling, fysiologische conditie, omgevingsfactoren en uiteraard leeftijd. Ondanks al deze tekortkomingen is de varkenseicel ideaal om kortdurende en lokaal voorkomende processen te bestuderen door zijn bijzondere eigenschappen, zoals de relatief grote omvang en de lange maturatieduur ten opzichte van veel andere zoogdieren. Het onderzoek in hoofdstuk 2 laat zien dat de eicel al voor de afbraak van de kern veranderingen in de distributie van organellen en kinases ondergaat. De in dit proefschrift aangetoonde kortstondige associatie van CDC2 met corticaal geclusterde ERES in eicellen zorgt er waarschijnlijk voor dat membraantransport vanaf ERES wordt stilgelegd. Diverse pogingen om deze hypothese te bevestigen met behulp van stoffen die de betrokken mechanismen remmen lieten helaas geen specifieke effecten zien.. Desondanks blijkt uit dit onderzoek wel dat lokale processen een veel prominentere rol innemen in de eicelmaturatie van zoogdieren dan voorheen werd verondersteld.

De meiotische delingen van de eicel, waardoor de nakomelingen uiteindelijk een zeer variabele genetische samenstelling krijgen, worden door een scala van zeer complexe systemen gereguleerd. Fouten in deze systemen leiden vaak tot incorrecte scheiding van de chromosomen in de metafaseplaat, waardoor bevruchting kan leiden tot de vorming van een embryo met een abnormaal aantal chromosomen (aneuploïdy). Aneuploïdy is meestal dodelijk voor het embryo, maar leidt soms ook tot een levensvatbaar embryo dat in staat is de zwangerschap te voltooien, maar door defecten in de ontwikkeling zware mentale danwel fysieke afwijkingen zal vertonen. In de mens kan dit bijvoorbeeld leiden tot trisomie van chromosoom 21, een afwijking die downsyndroom veroorzaakt. In mitotische cellen is het cytoplasmatische eiwit clathrine belangrijk voor de stabilisatie van de spoelfiguur en remming

van de functie van clathrine door dominant negatieve clathrine-constructen in deze cellen tot expressie te brengen, veroorzaakt foutieve chromosoom segregatie gedurende de mitose. In hoofdstuk 4 is de leemte in de huidige kennis over de functie van clathrine in eicellen verminderd door dominant-negatieve clathrine-constructen (N- en C-terminaal) tot expressie te brengen in somatische kweekcellen, de resulterende eiwitconstructen uit deze cellen te isoleren en met behulp van microinjectie in varkenseicellen te brengen. In eicellen veroorzaken zowel N- als C-terminale clathrine eiwitconstructen defecten in de metafase spoelfiguur, terwijl overexpressie van vergelijkbare constructen in somatische cellen veel grotere verschillen in effecten op de mitose laat zien. Hier moet wel bij vermeld worden dat de opzet van de experimenten op somatische cellen vaak in combinatie met clathrine 'knockdown' door middel van RNAi uitgevoerd zijn wat de diverse verschillen zou kunnen verklaren. De gevonden tegenstrijdigheden kunnen echter ook veroorzaakt worden door verschillen in de ratio endogeen clathrine versus geïntroduceerde dominant-negatieve constructen en/of in regulatie van de stabiliteit van de spoelfiguur tussen eicellen en somatische cellen. Om de precieze functie van clathrine in eicellen en de rol van de verschillende clathrine-domeinen daarin te begrijpen is meer onderzoek nodig. Desalniettemin levert het in dit proefschrift gepresenteerde onderzoek een solide basis voor verdere experimentatie.

Acknowledgements

Dankwoord

Het werk dat ten grondslag ligt aan de totstandkoming van dit proefschrift was onmogelijk geweest zonder de hulp en morele ondersteuning van veel collega's, vrienden en familie. In het nu volgende wil ik deze mensen graag mijn dank betuigen.

Allereerst Theo van Haeften; je bent gedurende dit promotietraject mijn steun en toeverlaat geweest, zelfs in tijden van mindere gezondheid stond je altijd voor me klaar en dat waardeer ik enorm. Zowel op wetenschappelijk als persoonlijk vlak heb ik genoten van onze samenwerking, waarbij ik immens veel van je geleerd heb.

Zo ook Bernard Roelen; naast je grenzeloze bereidheid om tijd en moeite in het bediscussiëren van mijn onderzoek te steken, bleek al snel dat je ook in muziek en humor mijn taal sprak. Dit alles leidde vrijwel altijd tot zeer interessante en vermakelijke gedachtewisselingen, waar ik me ongetwijfeld nog menigmaal om zal verkneukelen.

Mijn promotoren: Willem Stoorvogel en Ben Colenbrander. Willem, hartelijk dank voor je vele inzichten in experimentele opzet en in wetenschappelijk schrijven. Ben, je interesse in mijn onderzoek was telkens weer een bron voor leuke gesprekken.

Carla Zijlstra, mijn kamergenote bij Celbiologie, je hebt deze periode voor mij aanzienlijk veraangenaamd. Waar ik ieder ander al lang in het harnas had gejaagd, bleek jij uitzonderlijk weerbarstig ten overstaan van mijn grillen en je was zelfs nog bereid om mijn paranimf te worden! Ik voel me bevoorrecht dat ik met jou een kamer heb mogen delen.

Esther van 't Veld, je inzet en bereidheid om later door te gaan dan redelijkerwijs van je verwacht kon worden, zelfs wanneer dit niet altijd leidde tot de resultaten waar we op hoopten, waren gedurende de laatste twee jaar een stevige steun in de rug voor me. Bedankt voor de zeer prettige samenwerking!

Dagmar Gutknecht, aan je betrokkenheid en input gedurende de eerste helft van mijn promotietraject als copromotor hecht ik veel waarde en het was dan ook erg jammer dat je door omstandigheden mijn begeleiding in de capabele handen van Bernard en Theo moest achterlaten. Desalniettemin is je impact op dit proefschrift verre van gering, zonder de adviezen en instructies van jou en Anneke de Vreeden was de microinjectietechniek niet van de grond gekomen en daar ben ik jullie beiden erg dankbaar

voor.

Richard Wubbolts en Anko de Graaff van het Centrum voor Cellulaire Beeldvorming, bedankt voor de uitzonderlijke hulp en vele leermomenten. Richard, dankzij onze onderonsjes op het CCB waren de vele uren in de microscoop turen een stuk draaglijker. Anko, je diepgaande kennis van de apparatuur, geduld met het uitleggen ervan en je bijzondere trouble-shooting talent hebben me vele uren werk bespaard.

Roland Romijn en Wieger Hemrika van U-Protein Express BV, hartelijk dank voor het vele werk dat jullie hebben verricht om clathrine eiwit constructen tot expressie te brengen en te isoleren. Zonder jullie vergaande inzet en kennis was het onderzoek gepresenteerd in hoofdstuk 4 niet mogelijk geweest.

Verder wil ik graag de volgende mensen nog bedanken:

Mijn collega's bij Landbouwhuisdieren; Ewart Kuijk voor de vele discussies over ons beider data, experimenten en muziek, waarbij ik veel van je heb opgestoken en het was me dan ook een waar genoegen om met je samen te werken; Leni van Tol voor hulp met bestellingen en PCR, en natuurlijk het leuke en gezellige contact; Eric Schoevers voor het inspringen wanneer nodig en je hulp met vele praktische overwegingen; Arend Rijneveld voor hulp bij diverse bestellingen en prettige samenwerking; Karlijn Wilschut en Leonie du Puy voor jullie interesse en de boeiende conversaties, veel succes met de laatste loodjes! Hilde Aardema voor de uitwisseling van ideeën over je data en het gebruik van imageJ; Jason Tsai for interesting discussions, I thoroughly enjoyed working with you; Bart Gadella voor je interesse in mijn onderzoek en erg vermakelijke en interessante discussies; Frans van Kooij, Jamal Afkir, Nourdine Aharram en Maurits Schippers voor het regelen en ophalen van slachthuismateriaal; Christine Oei, Omran Algriany, Elly Zeinstra, Karianne Peterson en Peter Ursem voor de altijd prettige werksfeer. Verder eenieder die geholpen heeft bij het aanprikken van ovaria om materiaal te verzamelen (waaronder diverse mensen die ik hierboven al genoemd heb).

Hans Vernooij voor adviezen op het gebied van de statistiek; Dr. Martin Lowe for his generosity in providing P-GM130 antibody; Ger Arkesteijn en Els van der Vlist voor de hulp bij uitvoering van FACS experimenten; Hedwig Kruitwagen voor het verstrekken van samples en primers voor PCR; Louis Penning voor zijn hulp met het ontwikkelen van primers voor

sequencing en PCR; Frank van Steenbeek voor zijn hulp met sequencing; Peter van Kooten voor de productie van clathrine antilichamen; Erwin van Heiningen van VWR Nederland voor het regelwerk omtrend de verkrijging van de microinjectieopstelling en de prettige samenwerking daarin; master studenten Vasiliki Magoula, Nathalie Brabers en Linda Thijssen voor jullie praktische bijdragen en inzet; Mieke de Boer-Brouwer voor uitvoering van en hulp bij diverse experimenten. Ruud Eerland voor ondersteuning met van alles en nog wat; Chris van de Lest voor de bijstand in computer gerelateerde zaken; Judith van Kronenburg en Petra Boon voor assistentie bij administratieve rompslomp; en alle andere collega's bij de departementen Biochemie & Celbiologie en Landbouwhuisdieren voor de prettige samenwerking.

Dit proefschrift was niet tot stand gekomen zonder de ondersteuning van mijn ouders waar ik altijd van op aan kon. Daarnaast hebben velen uit mijn omgeving interesse getoond danwel voor de nodige verzetjes gezorgd, waaronder mijn broer Philip en mijn vrienden, John en Anette (respectievelijk paranimf en kaft-ontwerpster; ik zaage, kom mar deur oor!), Rutger en Elske, Paul, Thomas, Martijn, Menno, Sergio en Marc. Allemaal hartelijk dank voor jullie steun en jullie vriendschap!

Curriculum Vitae

Curriculum Vitae

Jurriaan Jochem Hölzenspies werd geboren op 25 november 1978 te Utrecht. In 1996 behaalde hij zijn VWO-diploma aan de RSG Goeree-Overflakkee te Middelharnis. Vervolgens studeerde hij Biologie aan de Universiteit Utrecht met als specialisatie de ontwikkelingsbiologie, waarbij hij twee onderzoeksstages heeft afgerond. Gedurende zijn eerste stage bij de vakgroep Neuroethologie van de Universiteit Utrecht onderzocht hij de membraaneigenschappen van electroreceptorcellen in de glasmeerval (Kryptopterus bicirrhis) met behulp van microchirurgie en patch-clamp technieken onder begeleiding van Dr. M.L. Struik. Tijdens zijn tweede stage bij de groep van Dr. A.J. Durston aan het Hubrecht Laboratorium onderzocht hij de rol van mesodermale expressie van Hox genen in het vastleggen van posteriore identiteit in het neuroectoderm van de Afrikaanse klauwpad (Xenopus laevis) met behulp van weefseltransplantatie, injectie van morpholino-antisense oligonucleotiden en in situ hybridisatie onder begeleiding van Dr. S. Wacker. Ook schreef hij een scriptie over de rol van Gli eiwitten in de Sonic Hedgehog signaleringsroute tijdens ledemaat-ontwikkeling onder begeleiding van A.A. Thomas van de vakgroep Ontwikkelingsbiologie aan de Universiteit Utrecht. Na afronding van zijn studie in 2002 maakte hij gedurende zes maanden een wereldreis, gevolgd door een oriëntatieperiode waarin hij onder andere als analist bij GenMab te Utrecht en als assistent account manager bij uitzendbureau Lab Support werkte. In 2004 begon hij aan het in dit proefschrift beschreven promotieonderzoek bij de afdelingen Landbouwhuisdieren en Biochemie & Celbiologie van de Faculteit Diergeneeskunde aan de Universiteit Utrecht onder begeleiding van dr.ir. T. van Haeften, dr. B.A.J. Roelen, prof.dr. W. Stoorvogel en prof.dr. B. Colenbrander.

Publications

Hölzenspies JJ, Stoorvogel W, Colenbrander B, Roelen BA, Gutknecht DR, van Haeften T. CDC2/SPDY transiently associates with endoplasmic reticulum exit sites during oocyte maturation. BMC Dev Biol 2009; 9: 8.

Hölzenspies JJ, Stoorvogel W, Colenbrander B, Roelen BA, van Haeften T. A method for (co-)injection of quantifiable amounts of fluorescent molecules into mammalian oocytes. In preparation.

Hölzenspies JJ, Roelen BA, Colenbrander B, Romijn RA, Hemrika W, Stoorvogel W, van Haeften T. Clathrin is essential for meiotic spindle function in porcine oocytes. Submitted, 2009.